Oxidative Medicine and Cellular Longevity

Molecular Basis of the Inflammation Related to Obesity

Lead Guest Editor: Pedro González-Muniesa
Guest Editors: Paul Cordero, Ana B. Crujeiras, Diego F. García-Díaz, and Ewa Stachowska

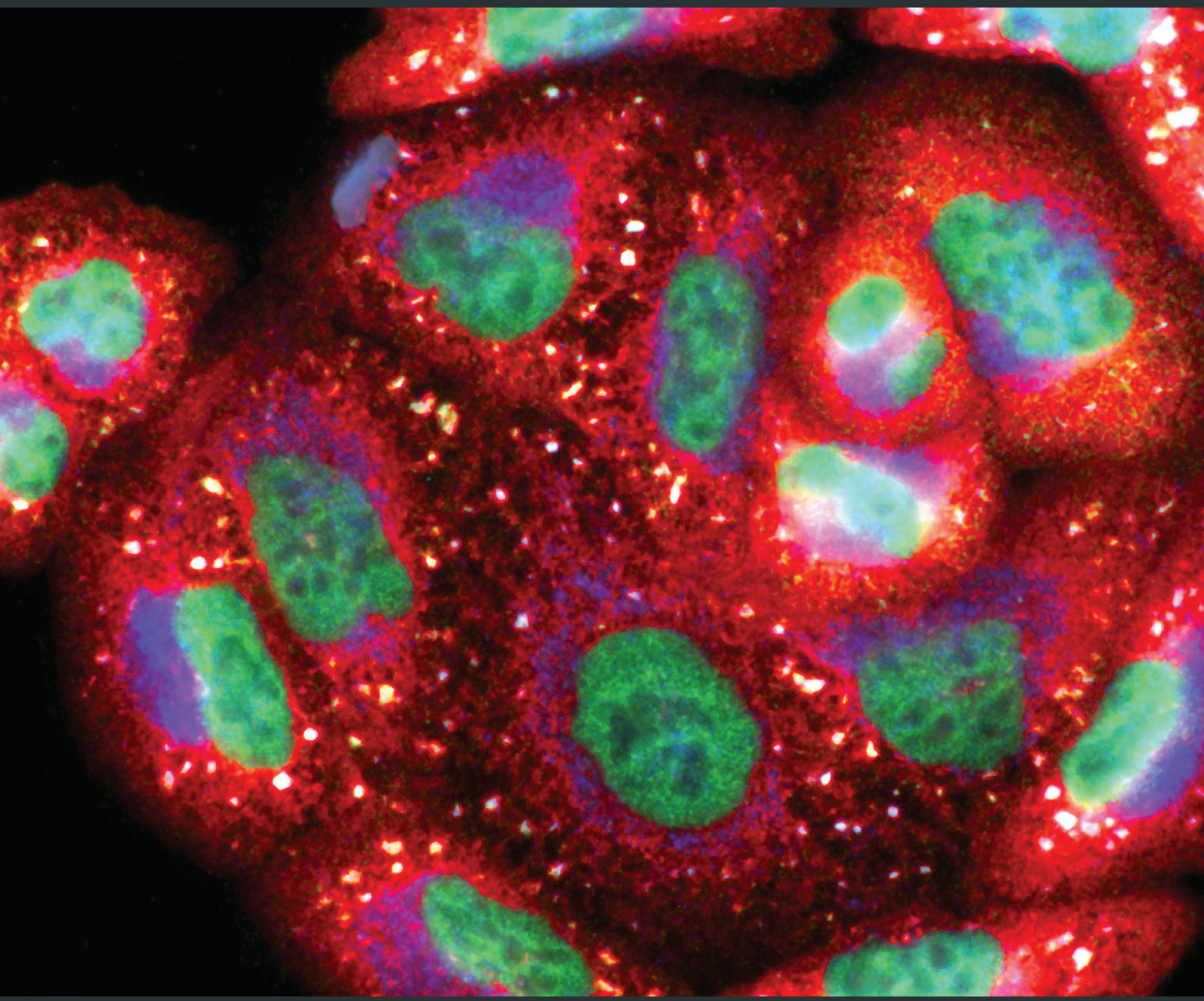

Molecular Basis of the Inflammation Related to Obesity

Oxidative Medicine and Cellular Longevity

Molecular Basis of the Inflammation Related to Obesity

Lead Guest Editor: Pedro González-Muniesa
Guest Editors: Paul Cordero, Ana B. Crujeiras, Diego F. García-Díaz, and Ewa Stachowska

Editorial Board

Contents

Hindawi
Oxidative Medicine and Cellular Longevity
Volume 2019, Article ID 5250816, 2 pages
https://doi.org/10.1155/2019/5250816

Editorial

Molecular Basis of the Inflammation Related to Obesity

Ana B. Crujeiras[1,2] **Paul Cordero**[3] **Diego F. Garcia-Diaz**[4] **Ewa Stachowska**[5] **and Pedro González-Muniesa**[2,6,7,8]

[1]*Epigenomics in Endocrinology and Nutrition Group, Epigenomics Unit, Instituto de Investigacion Sanitaria de Santiago (IDIS), Complejo Hospitalario Universitario de Santiago (CHUS/SERGAS), Santiago de Compostela, Spain*
[2]*CIBERobn Physiopathology of Obesity and Nutrition, Centre of Biomedical Research Network, ISCIII, Madrid, Spain*
[3]*Institute for Liver and Digestive Health, University College London, Royal Free Hospital, Rowland Hill Street, London, UK*
[4]*Laboratorio de Nutrigenomica, Departamento de Nutricion, Facultad de Medicina, Universidad de Chile, Chile*
[5]*Department of Biochemistry and Human Nutrition, Pomeranian Medical University, Szczecin, Poland*
[6]*University of Navarra, Department of Nutrition, Food Science and Physiology, School of Pharmacy and Nutrition, Pamplona, Spain*
[7]*University of Navarra, Centre for Nutrition Research, School of Pharmacy and Nutrition, Pamplona, Spain*
[8]*IDISNA, Navarra's Health Research Institute, Pamplona, Spain*

Correspondence should be addressed to Pedro González-Muniesa; pgonmun@unav.es

Received 30 January 2019; Accepted 30 January 2019; Published 17 February 2019

Almost two thousand millions of adults suffer from overweight or obesity in the world [1]. After decades of research, we understand that the solution to this problem is not easy, as the pernicious trend is still increasing [2].

This disease is defined as an excessive fat accumulation together with a moderate but chronic inflammation [3]. This accompanying proinflammatory status is considered the link between obesity and the development of its related comorbidities such as insulin resistance and type 2 diabetes, cardiovascular diseases, cancer, and nonalcoholic fatty liver disease [4].

The main triggers for this inflammation have been traditionally considered oxygen tension, oxidative stress, and endoplasmic reticulum stress [5]. This special issue contains articles analyzing oxidative stress, adipokine secretory pattern, methylation, or nanomedicine to further untangle the processes involved in this disease and to offer promising/possible alternative therapeutical tools.

In this sense, D. Stygar and collaborators measured in rats the levels of selected adipokines and other proteins, such as FABP4, leptin, chemerin, and CRP, to show the proinflammatory effect of a high-fat diet. Interestingly, this effect was reversed by the treatment of obesity with metabolic surgery. As mentioned earlier, it seems clear the relation of an abnormally enlarged adipose tissue and oxidative stress as it has been analyzed in the article of Y. Gramlich and coworkers. These authors suggest that obese patients undergoing coronary artery bypass grafting showed altered myocardial redox patterns, indicating an increased oxidative stress with inadequate antioxidant compensation. This might explain why patients with high BMI suffering from coronary artery disease are more susceptible to cardiomyopathy and possible damage by ischemia and reperfusion, for example, during cardiac surgery. On the other hand, oxidative stress seems to be related with diabetic retinopathy, one of the multiple accompanying side-effects of obesity [6]. In this sense, A. Maugeri and collaborators stated that hyperglycemia increased ROS production and alters the DNA methylation process, therefore altering the expression of certain genes. They also found in their study that curcumin seems to reduce oxidative stress and improves methylation activities, considering this compound an effective antioxidant to counteract this condition. In the same area, another potent antioxidant with self-regenerative properties, nanoparticles of cerium oxide, was tested by A. Lopez-Pascual and coworkers in three types of cells (adipocytes, macrophages, and myotubes) under

proinflammatory conditions. These nanoparticles showed a mild insulin-sensitizing effect on murine adipocytes and myotubes that needs to be further studied. Finally, in another manuscript, M. Carreira et al. stated that *Sirt6* expression could be a potential therapeutic target to counteract obesity-related liver diseases because it is downregulated by the chronic low-grade inflammation and oxidative stress induced by excess adiposity.

In conclusion, it is recognized worldwide that the main predisposing factors to develop obesity are overconsumption of calories and sedentary lifestyle, although the reality is quite more complex [7]. These two options either together or individually will lead to an abnormal enlarged adipose tissue, accompanied by a proinflammatory status [8]. We have known this for many years but without being able to tackle the epidemy of obesity. Therefore, we need to understand the molecular pathways involved in this pathological condition to provide new therapeutic tools, being the reason for this special issue.

Conflicts of Interest

The authors declare that there is no conflict of interest regarding the publication of this editorial.

Ana B. Crujeiras
Paul Cordero
Diego F. Garcia-Diaz
Ewa Stachowska
Pedro González-Muniesa

References

[1] World Health Organization, *Obesity and Overweight*, WHO, 2018, https://www.who.int/mediacentre/factsheets/fs311/en/.

[2] NCD Risk Factor Collaboration (NCD-RisC), "Trends in adult body-mass index in 200 countries from 1975 to 2014: a pooled analysis of 1698 population-based measurement studies with 19·2 million participants," *The Lancet*, vol. 387, no. 10026, pp. 1377–1396, 2016.

[3] N. Ouchi, J. L. Parker, J. J. Lugus, and K. Walsh, "Adipokines in inflammation and metabolic disease," *Nature Reviews Immunology*, vol. 11, no. 2, pp. 85–97, 2011.

[4] P. González-Muniesa, M. A. Mártinez-González, F. B. Hu et al., "Obesity," *Nature Reviews Disease Primers*, vol. 3, article 17034, 2017.

[5] P. González-Muniesa, L. Garcia-Gerique, P. Quintero, S. Arriaza, A. Lopez-Pascual, and J. A. Martinez, "Effects of hyperoxia on oxygen-related inflammation with a focus on obesity," *Oxidative Medicine and Cellular Longevity*, vol. 2016, Article ID 8957827, 11 pages, 2016.

[6] J. M. Santos, G. Mohammad, Q. Zhong, and R. A. Kowluru, "Diabetic retinopathy, superoxide damage and antioxidants," *Current Pharmaceutical Biotechnology*, vol. 12, no. 3, pp. 352–361, 2011.

[7] D. Sellayah, F. R. Cagampang, and R. D. Cox, "On the evolutionary origins of obesity: a new hypothesis," *Endocrinology*, vol. 155, no. 5, pp. 1573–1588, 2014.

[8] E. P. Williams, M. Mesidor, K. Winters, P. M. Dubbert, and S. B. Wyatt, "Overweight and obesity: prevalence, consequences, and causes of a growing public health problem," *Current Obesity Reports*, vol. 4, no. 3, pp. 363–370, 2015.

Hindawi
Oxidative Medicine and Cellular Longevity
Volume 2019, Article ID 2695289, 10 pages
https://doi.org/10.1155/2019/2695289

Research Article

Cerium Oxide Nanoparticles Regulate Insulin Sensitivity and Oxidative Markers in 3T3-L1 Adipocytes and C2C12 Myotubes

Amaya Lopez-Pascual,[1,2] **Andoni Urrutia-Sarratea**,[1] **Silvia Lorente-Cebrián**,[1,2,3] **J. Alfredo Martinez**,[1,2,3,4] **and Pedro González-Muniesa**[1,2,3,4]

[1]*University of Navarra, Department of Nutrition, Food Science and Physiology, School of Pharmacy and Nutrition, Pamplona, Spain*
[2]*University of Navarra, Centre for Nutrition Research, School of Pharmacy and Nutrition, Pamplona, Spain*
[3]*IdiSNA Navarra's Health Research Institute, Pamplona, Spain*
[4]*CIBERobn Physiopathology of Obesity and Nutrition, Centre of Biomedical Research Network, ISCIII, Madrid, Spain*

Correspondence should be addressed to Pedro González-Muniesa; pgonmun@unav.es

Received 21 June 2018; Revised 5 October 2018; Accepted 12 December 2018; Published 4 February 2019

Academic Editor: Giulio Ceolotto

Insulin resistance is associated with oxidative stress, mitochondrial dysfunction, and a chronic low-grade inflammatory status. In this sense, cerium oxide nanoparticles (CeO_2 NPs) are promising nanomaterials with antioxidant and anti-inflammatory properties. Thus, we aimed to evaluate the effect of CeO_2 NPs in mouse 3T3-L1 adipocytes, RAW 264.7 macrophages, and C2C12 myotubes under control or proinflammatory conditions. Macrophages were treated with LPS, and both adipocytes and myotubes with conditioned medium (25% LPS-activated macrophages medium) to promote inflammation. CeO_2 NPs showed a mean size of ≤25.3 nm (96.7%) and a zeta potential of 30.57 ± 0.58 mV, suitable for cell internalization. CeO_2 NPs reduced extracellular reactive oxygen species (ROS) in adipocytes with inflammation while increased in myotubes with control medium. The CeO_2 NPs increased mitochondrial content was observed in adipocytes under proinflammatory conditions. Furthermore, the expression of *Adipoq* and *Il10* increased in adipocytes treated with CeO_2 NPs. In myotubes, both *Il1b* and *Adipoq* were downregulated while *Irs1* was upregulated. Overall, our results suggest that CeO_2 NPs could potentially have an insulin-sensitizing effect specifically on adipose tissue and skeletal muscle. However, further research is needed to confirm these findings.

1. Introduction

The metabolic syndrome is a complex interplay of comorbidities including central adiposity, dyslipidemia, hyperglycemia, and hypertension [1]. Over the last decades, this clustering of factors has been widely implicated in the pathogenesis of type 2 diabetes and cardiovascular disease [2, 3]. In the normal course of metabolism, the pancreatic β-cells release insulin which stimulates glucose, amino acid, and fatty acid uptake. However, when insulin resistance is present, as often happens in obese subjects, β-cells increase insulin secretion to maintain normal glucose tolerance [4]. Concerning insulin signaling, the phosphorylation of insulin substrate receptor 1 and 2 (IRS-1 and IRS-2) is a key cellular response for glucose uptake [5, 6]. Insulin resistance is related to many physiopathological features of metabolic syndrome such as the oxidative stress, mitochondrial dysfunction, and a chronic low-grade inflammatory status [5–8].

In this context, type 2 diabetes is a major public health problem, which has been extensively studied for prevention and therapy development [3], as the complex pathophysiology and the heterogeneous drug responses hamper the proper treatment of the disease [4, 9, 10]. New therapeutic approaches should identify additional targets [11], offering a more directed and therefore effective treatment for type 2 diabetes [6]. As novel strategies, antioxidant treatment has been proposed to combat oxidative stress in diabetic patients [5] as well as anti-inflammatory approaches to immunomodulate towards a more balanced insulin response [12]. In this sense, nanomedicine is being used in noninvasive approaches

to treat metabolic-related diseases as type 2 diabetes [9]. The administration of nanostructured particles has shown a therapeutic potential due to a better distribution and cellular uptake than other drugs, as well as the transexcitation reactions that make them able to take part in redox reactions [13–15]. The cerium oxide nanoparticles (CeO_2 NPs) are one of the most promising nanomaterials for antioxidant and anti-inflammatory pharmacological applications [13, 16, 17]. Hence, CeO_2 NPs have been proposed for diverse biological purposes such as therapy for neurodegenerative disorders, oxidative stress-related diseases, diabetes, chronic inflammation, and cancer among others [13, 16, 18]. Moreover, cerium exists in two oxidative states: Ce^{+3} and Ce^{+4} [16]. The therapeutic benefit is attributed to its ability to mimic superoxide dismutase, behaving as efficient reactive oxygen species (ROS) scavengers (Ce^{+3} to Ce^{+4}) and changing the oxidation state to mimic catalase activity that reduces hydrogen peroxide releasing protons and O_2 (Ce^{+4} to the initial Ce^{+3}). Therefore, this self-regenerative property renders the nanoparticles a very valuable tool for pharmacological treatment of oxidative-related disorders [13, 16]. Previous studies have evidenced useful properties of CeO_2 NPs related to redox status modulation in many conditions such as macular degeneration [19], lung damage [20], liver toxicity [21], cardiac dysfunction [22], smoke-related cardiomyopathy [23], adipogenesis [24], and weight-gain reduction [25]. On the other hand, some authors described DNA damage and inflammation in the lung, heart, liver, kidney, spleen, and brain [26], inability to counteract monocyte inflammation [27], lung-cell apoptosis [28], and monocyte cell death through apoptosis and autophagy [29]. Consequently, the hypothesis of this study was that a treatment with nanoparticles could potentially attenuate type 2 diabetes features and metabolic syndrome markers in 3T3-L1 adipocytes and C2C12 myotubes. As aforementioned, the literature gives insight into the specific cell-type effect of this potential treatment. Thus, the objective of the present study was to evaluate the effect of CeO_2 NPs on markers of oxidative stress, mitochondrial dysfunction, and inflammation in mouse adipocyte, macrophage, and myotube cell cultures under control or proinflammatory conditions.

2. Material and Methods

2.1. Cell Cultures. The cell lines were obtained from the American Type Culture Collection (ATCC®) and cultured according to the accompanying specifications. Concretely, mouse 3T3-L1 preadipocytes, C2C12 myoblasts, and RAW 264.7 macrophages (ATCC® CL-173™, CRL-1772™ and TIB-71™, respectively) were cultured in growth medium composed by DMEM (Gibco, NZ) with 25 mM glucose and 100 U/ml penicillin-streptomycin (Invitrogen, NZ), supplemented with 10% (*v*/*v*) heat-inactivated serum following the protocols recommended by the supplier. Thus, bovine serum was used for preadipocytes while fetal bovine serum was for myoblasts and macrophages (Invitrogen, NZ). Cells were seeded in 12-well plates and maintained in a humidified atmosphere of 5% CO_2 at 37°C in a standard incubator.

When preadipocytes reached confluence, they were differentiated for 48 hours (h) in complete medium (DMEM containing 25 mM glucose, 10% fetal bovine serum, and antibiotics) and supplemented with dexamethasone (1 mM; Sigma-Aldrich, MO, US), isobutylmethylxantine (0.5 mM; Sigma-Aldrich, MO, US), and insulin (10 μg/ml; Sigma-Aldrich, MO, US). The media were replaced with complete medium and insulin for 48 h. Four days post differentiation cocktail, cell media were replaced with complete medium and changed every 2 days until day 9 post differentiation. On the other hand, myoblasts were differentiated for 48 h with complete medium (DMEM containing 25 mM glucose, 2% horse serum and antibiotics) and supplemented with insulin (10 μg/ml). RAW 264.7 macrophages were grown in complete medium (DMEM containing 25 mM glucose, 10% fetal bovine serum, and antibiotics) until they reached confluence, when they are ready to be treated.

2.2. Treatments. Macrophages were activated with LPS (500 ng/ml from *Escherichia coli* K12, InvivoGen, CA, US) for 24 h after cells had reached confluence. To generate a proinflammatory environment in vitro, conditioned medium (CM) was used as previously described [30] to simulate the macrophage infiltration in adipocytes and myotubes for 24 h. This proinflammatory medium was generated using 25% of the medium from activated macrophages with LPS (500 ng/ml for 24 h) and 75% complete medium.

CeO_2 NPs used for this study (544841; Sigma-Aldrich, MO, US) were previously characterized as reported elsewhere [31]. Nanoparticles were diluted in ultrapure MilliQ water at a concentration of 10 mg/ml. The CeO_2 NPs were first characterized in terms of size, dispersion, and surface charge. For this purpose, CeO_2 NPs were diluted in MilliQ water in order to ensure that the light scattering intensity was within the sensitivity range of the instrument. Particle surface charge was determined by Z-potential, based on the study of the surface charge through particle mobility in an electric field. The average particle diameter size and polydispersity index were analyzed by photon correlation spectroscopy. All these data were measured by laser Doppler velocimetry (Zetasizer Nano, Malvern Instruments, UK) using a quartz cell at 25°C with a detection angle of 90°. At least three different batches were analyzed to give an average value and standard deviation for the particle diameter, PDI, and zeta potential. Dilutions to 100 μg/ml, 50 μg/ml, 20 μg/ml, and 10 μg/ml were performed just before the experiments with cell culture medium. The proinflammatory media and CeO_2 NPs were added simultaneously to cell cultures. The complete medium without proinflammatory conditions (LPS/CM) was used as a control medium. The complete medium without nanoparticles nor proinflammatory stimulation (CM) was used as nontreated control (hereinafter the NTC). The supernatants, intracellular (total cell lysate) proteins, and total RNA were collected with their appropriate reagent and stored at −20°C for subsequent analysis.

2.3. Cell Metabolic Assays. The metabolic activity of cells was determined by the 3-(4,5-dimethyl-thiazol-2-yl)-2,5-diphenyl tetrazolium bromide (MTT; Sigma-Aldrich, MO, US)

reduction assay in 96-well plates. The treatments were performed as described in the section above. Cells were incubated for 2 h with 0.45 mg/ml MTT dye to allow the formation of the dark blue formazan crystals generated by living cells. Then, the medium was removed and 100 μl of solubilization solution was added to dissolve the crystals as described in the manufacturer's instructions. Absorbance was read with Multiskan Spectrum (Thermo Scientific, MA, US) at 570/630 nm wavelength.

The effect of the treatment on cellular metabolism was also evaluated through biochemical markers. Thus, glucose uptake (Hk-CP; Horiba, FR), lactate release (A11A01721; ABX Diagnostic, FR), and glycerol release (GLY 105; Randox Laboratories, UK) were measured from supernatants after the 24 h treatment with a PENTRA C200 autoanalyzer (Horiba, FR). Glucose uptake was calculated by the difference between glucose amount (present in the culture media) before and after the incubation period.

Additionally, secreted adiponectin (ADIPOQ), interle ukin-6 (IL-6), monocyte chemoattractant pProtein-1 (MCP-1), and tumor necrosis factor alpha (TNF-α) were measured in the supernatants using commercial ELISA kits (DY1065, DY406, DY479 and DY410, respectively; R&D, ES). Intracellular levels of the transcription factors hypoxia-inducible factor-1 alpha (HIF-1α) were also determined with ELISA kits (DYC1935; R&D, ES), following the manufacturer's instructions. The results were normalized to total protein content as determined by Pierce BCA assay (Thermo Scientific, IL, US).

2.4. ROS Production. To determine extra- and intracellular ROS concentration, 2,7-dichlorofluorescein diacetate (DCF H-DA) was used following the guidelines of the supplier. Briefly, cells and supernatants were incubated with 1 μM DCFH-DA for 40 min in a standard incubator (5% CO_2 at 37°C), then supernatants were loaded on a 96-well plate and fluorescence measured using a POLARstar spectrofluorometer (BMG Labtech, DE) at 485/530 nm. Whereas cells were lysed by freeze-thaw method at -80°C for 2 h and then resuspended in 500 μl phosphate-buffered saline, then the lysates were loaded on a 96-well plate following the same protocol used for supernatants.

2.5. Mitochondrial Content. Mitochondria were labelled using MitoTracker Green FM (Molecular Probes, Life Technologies Ltd., Paisley, UK), which reacts with the free thiol groups of cysteine residues belonging to mitochondrial proteins. Cells were incubated with this mitochondria-specific dye according to the manufacturer's protocol at a final concentration of 25 nM for 30 min prior to visualization. For fluorescence intensity quantification, a POLARstar Galaxy spectrofluorometer plate reader (BMG Labtech, DE) was used, set up to 554 nm excitation and 576 nm emission wavelengths. Fluorescent microscopy was performed on living cells with ZOE Fluorescent Cell Imager (Bio-Rad Laboratories, DE).

2.6. Analysis of Gene Expression. Total RNA was extracted from treated cells using QIAzol reagent (Qiagen, NL) according to the manufacturer's instructions. A total amount of 2 μg of RNA were transcribed to cDNA using MultiScribe™ MuLV and random primers (High-Capacity cDNA Reverse Transcription Kit; Applied Biosystems, CA, US). Real-time PCR was performed in an ABI Prism 7900HT Fast System Sequence Detection System (Applied Biosystems, CA, US) equipped with the SDS software (version 2.4.1) using SYBR Green (iQ™ SYBR® Green supermix, Bio-Rad Laboratories, DE) and primers designed with Primer-BLAST software (National Center for Biotechnology Information, MD, USA; https://www.ncbi.nlm.nih.gov/tools/primer-blast/), according to published cDNA [30] or genomic sequences (Table S1) and with melting temperatures ranging from 58 to 60°C. A 2-fold dilution series was prepared from pooled cDNA samples to evaluate primer efficiency ($E = 10^{[-1/\text{slope}]}$) and specificity as described elsewhere [32]. The relative expression was determined by the $E^{-\Delta\Delta Ct}$ method after internal normalization to *Ppia* as housekeeping gene.

2.7. Statistical Analysis. Data are presented as mean and SEM. Statistical significance and interaction were analyzed by two-way ANOVA followed by Dunnet post hoc test for multiple comparisons when comparing the effect of CeO_2 NPs at different doses in control or proinflammatory conditions (LPS/CM). One-way ANOVA followed by Dunnet and Kruskal-Wallis test followed by Dunn test for the nonparametric statistics were used to compare the effect of CeO_2 NPs on gene expression in proinflammatory conditions (LPS/CM). The comparison between the gene expression of two groups (control vs. inflammation) was analyzed by unpaired Student's *t*-test for parametric, and Mann-Whitney *U* test for nonparametric statistics. Statistical analyses and graphs were performed using Prism 5.0 software (GraphPad Software Inc., CA, US). Values of $p < 0.05$ were considered statistically significant.

3. Results

3.1. Nanoparticle Characterization. Z-potential was measured to analyze the changes on surface charge and, therefore, to estimate the adherence of CeO_2 NPs to the cells. Negative or positive values are characteristic of stable colloidal systems. However, positive charges might provoke a certain degree of toxicity *in vitro* [33]. Z-potential mean formulation of CeO_2 NPs was 30.57 ± 0.58 mV. Formulation polydispersity index average was 0.36 ± 0.01. This value is an indicator of the homogeneity of the formulation since nanoparticles with values ranging between 0 and 0.3 are considered acceptable according to dynamic light scattering specifications, while values higher than 0.7 indicate a wide range of distribution. Tested nanoparticles presented a mean size distribution as manufacturer reported (96.7% is ≤25.3 nm in MilliQ water).

3.2. Cell Metabolism. The potential influence of CeO_2 NPs in cell metabolic activity was tested using MTT assay which mainly measures the cell mitochondrial activity through NAD(P)H-dependent cellular oxidoreductase enzymes. Figure 1 shows the cell viability of the three different cell

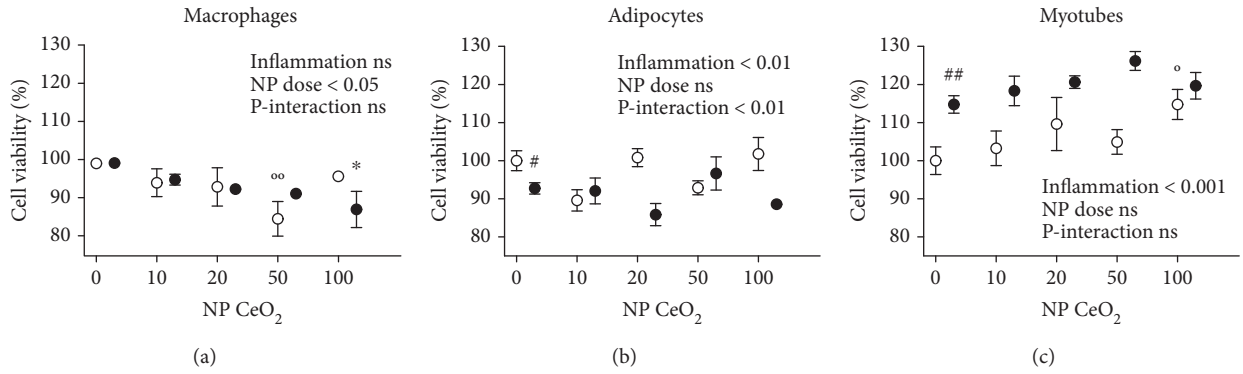

Figure 1: Cell metabolic activity in RAW 264.7 macrophages (a), 3T3-L1 adipocytes (b), and C2C12 myotubes (c) measured with MTT assay at 24 h after CeO_2 NP treatment at 10, 20, 50, and 100 μg/ml doses in percentage compared to nontreated control (NTC). White shapes: control medium; black shapes: inflammation in macrophages activated with lipopolysaccharide (LPS), adipocytes, and myotubes treated with conditioned medium (CM); $^{\#}p < 0.05$, $^{\#\#}p < 0.01$ control vs. inflammation; $^{\circ}p < 0.05$, $^{\circ\circ}p < 0.01$ CeO_2 NPs vs. control; $^{*}p < 0.05$ CeO_2 NPs vs. inflammation; data ($n = 6$/group) are expressed as mean (SEM).

types after exposure to CeO_2 NPs at increasing doses ranging from 10, 20, 50, to 100 μg/ml. First, the inflammatory stimuli (CM vs. NTC) decreased metabolic activity in adipocytes (Figure 1(b)) while increased in myotubes (Figure 1(c)). Moreover, the interaction between the treatment with CeO_2 NPs and inflammatory status was only statistically significant in adipocytes (Figure 1(b)). The nanoparticles were considered noncytotoxic since the metabolic activity was higher than 80% as compared to each cell type control. However, macrophages showed a statistically significant reduction in the cell metabolic activity at dose 50 μg/ml of CeO_2 NPs in control medium and 100 μg/ml of CeO_2 NPs in proinflammatory conditions (LPS) (Figure 1(a)). Conversely, the effect on myotubes was the opposite, increasing the metabolism at the dose of 100 μg/ml CeO_2 NPs in control medium (Figure 1(c)).

To further analyze if the CeO_2 NP treatment affects cellular metabolism, glucose uptake, lactate release, and glycerol release were determined in supernatants after 24 h of CeO_2 NP treatment. Inflammation (LPS/CM vs. NTC) increased glucose uptake in all cell types analyzed (Figure S1(a-c)), while lactate release and glycerol release were higher only in macrophages and adipocytes, respectively (Figure S1(d, g)). There was no significant interaction between the treatment with CeO_2 NPs and inflammatory status in glucose uptake, lactate release, and glycerol release in any cell type. Glucose uptake and lactate release showed a statistically significant increase in macrophages in proinflammatory conditions (LPS) treated with 10 and 50 μg/ml CeO_2 NPs, respectively (Figure S1(a, d)). Beyond that, neither macrophages, adipocytes, nor myotubes showed an alteration in the levels of the metabolic markers determined. In addition, anaerobic metabolism (calculated through the lactate generated over glucose consumption) remained unchanged in all cell types (data not shown).

Moreover, to test the effect of CeO_2 NPs on inflammation, the secretion of several metabolic-related cytokines was measured in supernatants after 24 h of treatment. The secretion of IL-6, MCP-1, and TNF-α was increased in both macrophages (Figure S2(a, d, g)) and adipocytes (Figure S2(b, e, h)) in proinflammatory conditions (LPS/CM vs. NTC). IL-6 and TNF-α release was induced in myotubes in proinflammatory conditions (CM vs. NTC) (Figure S2(c, i)). Moreover, ADIPOQ secretion was lower in adipocytes and myotubes under proinflammatory conditions (CM vs. NTC) (Figure S2(j, k)). An interaction effect between the treatment inflammation was found in the secretion of IL-6 in myotubes (Figure S2(c)), as well as in TNF-α in macrophages (Figure S2(g)). The treatment with CeO_2 NPs in control medium does not affect the release of the cytokines selected as metabolic-related markers in any cell type. On the other hand, a statistically significant increase of IL-6 was observed in myotubes under proinflammatory conditions (CM) at dose 10 and 50 μg/ml of CeO_2 NPs (Figure S2(c)). MCP-1 levels were lower in macrophages under proinflammatory conditions (LPS) at dose 20 μg/ml of CeO_2 NPs (Figure S2(d)). TNF-α increased in macrophages at dose 20 and 50 μg/ml of CeO_2 NPs (Figure S2(g)). ADIPOQ release did not change in adipocytes and myotubes under proinflammatory conditions (CM) after the CeO_2 NP treatment (Figure S2(j, k)). Furthermore, HIF-1α was measured to explore the potential effects of CeO_2 NPs on inflammation-derived activation of this master regulator of the hypoxic cascade. The results showed a lack of effect of these CeO_2 NPs concerning the hypoxic cascade in both adipocytes (Figure S3(b)) and myotubes (Figure S3(c)). However, macrophages under proinflammatory conditions (LPS vs. NTC) increased the levels of HIF-1α after the treatment with CeO_2 NPs at dose 10 μg/ml while decreased at dose 50 μg/ml (Figure S3(a)).

3.3. Antioxidant Activity. Intra- and extracellular antioxidant activity of CeO_2 NPs was evaluated with the fluorophore DCFH-DA. Inflammation (LPS/CM vs. NTC) increased intracellular ROS levels in macrophages and adipocytes (Figures 2(a) and 2(b)), as well as induced extracellular ROS production in adipocytes and myotubes (Figures 2(e) and 2(f)). An interaction effect was detected between the treatment with CeO_2 NPs and inflammatory status in the intracellular ROS production in myotubes (Figure 2(c)), as

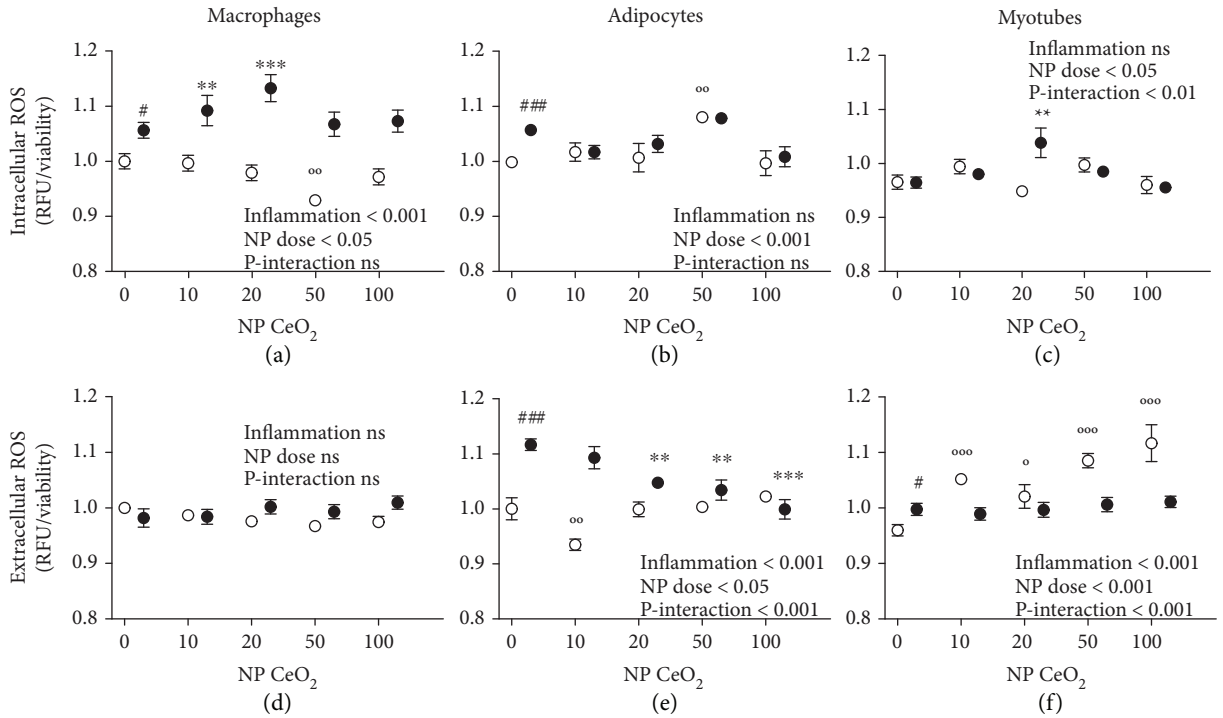

Figure 2: Intra- and extracellular ROS production in RAW 264.7 macrophages (a, d), 3T3-L1 adipocytes (b, e), and C2C12 myotubes (c, f) measured with DCFH-DA assay at 24 h after CeO_2 NP treatment at 10, 20, 50, and 100 μg/ml doses in percentage compared to nontreated control (NTC). White shapes: control medium; black shapes: inflammation in macrophages activated with lipopolysaccharide (LPS), adipocytes, and myotubes treated with conditioned medium (CM); $^{\#}p < 0.05$, $^{\#\#\#}p < 0.001$ control vs. inflammation; $^{\circ}p < 0.05$, $^{\circ\circ}p < 0.01$, $^{\circ\circ\circ}p < 0.001$ CeO_2 NPs vs. control; $^{**}p < 0.01$, $^{***}p < 0.001$ CeO_2 NPs vs. inflammation; data ($n = 6$/group) are expressed as mean (SEM).

well as in the extracellular ROS levels in adipocytes and myotubes (Figures 2(e) and 2(f)). Intracellular ROS levels were significantly increased in macrophages and myotubes (Figures 2(a) and 2(c)) at a dose 20 μg/ml of CeO_2 NPs with inflammation (LPS and CM, respectively) and in adipocytes at 50 μg/ml of CeO_2 NPs in control medium (Figure 2(b)). Furthermore, a statistically significant reduction was found on intracellular ROS in macrophages at a dose 50 μg/ml of CeO_2 NPs in control medium (Figure 2(a)). On the other hand, the extracellular ROS levels were reduced in adipocytes at 20, 50, and 100 μg/ml of CeO_2 NPs in proinflammatory conditions (CM), thus in a dose-dependent manner, as well as at dose 10 μg/ml of CeO_2 NPs in control medium (Figure 2(e)). Finally, ROS levels were increased extracellularly in myotubes at any dose of CeO_2 NPs with control medium (Figure 2(f)). No statistically significant scavenging effects of CeO_2 NPs were seen (intra- and extracellularly) in macrophages (Figures 2(a) and 2(d)) either in control medium or proinflammatory conditions (LPS).

3.4. Mitochondria Quantification. To assess the potential effects of CeO_2 NPs on mitochondrial content, MitoTracker Green fluorescent probe was used. No statistically significant effects on mitochondrial quantification were found when comparing the proinflammatory conditions with NTC in any of the cell types (Figure 3). Additionally, adipocytes showed a treatment-inflammation interaction in mitochondria number (Figure 3(b)). A statistically significant increase in the mitochondrial content was observed in both adipocytes at 20 μg/ml of CeO_2 NPs in proinflammatory conditions (CM) and myotubes at 10 μg/ml of CeO_2 NPs in control medium, while a decrease was detected in adipocytes at dose 100 μg/ml of CeO_2 NPs in control medium and myotubes at the same dose but in proinflammatory conditions (CM) (Figures 3(b) and 3(c)).

3.5. Gene Expression Patterns. The most representative genes for metabolism-related comorbidities that changed at least in one cell type under proinflammatory stimuli compared to their controls were further analyzed by real-time PCR (Figure S4). To determine whether CeO_2 NPs could attenuate the proinflammatory stimulation (LPS/CM), the expression of candidate genes was measured as a screening of the pathways that potentially could be involved in the effects observed in the assays. No statistically significant differences were found in mRNA expression of selected genes in macrophages incubated with CeO_2 NPs (Figure 4(a)). The expression of *Adipoq* significantly increased in adipocytes at doses of 10 and 50 μg/ml of CeO_2 NPs and *Il10* at 50 μg/ml (Figure 4(b)). Furthermore, in myotubes, both *Il1b* at 20 μg/ml and *Adipoq* at 10 and 50 μg/ml of CeO_2 NPs were downregulated, while *Irs1* showed a statistically significant increase at 20 and 50 μg/ml of CeO_2 NPs (Figure 4(c)).

4. Discussion

In this study, we have shown that murine macrophages, adipocytes, and myotubes treated with CeO_2 NPs could

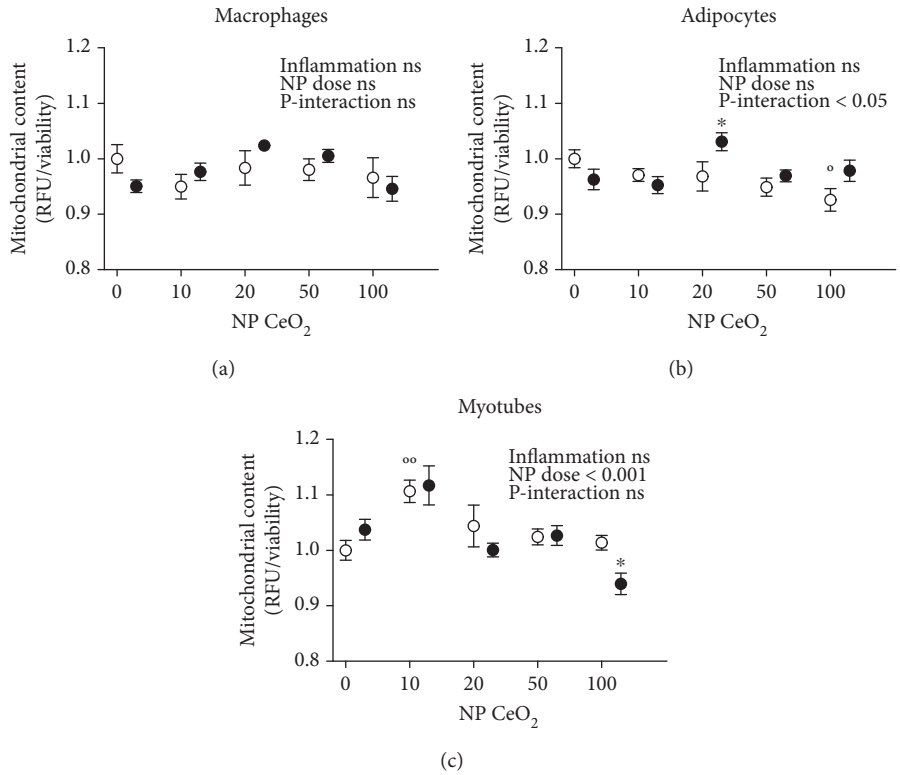

Figure 3: Mitochondrial content in RAW 264.7 macrophages (a), 3T3-L1 adipocytes (b), and C2C12 myotubes (c) analyzed with MitoTracker Green assay at 24 h after CeO_2 NP treatment at 10, 20, 50, and 100 μg/ml doses in fold change compared to nontreated control (NTC). White shapes: control medium; black shapes: inflammation in macrophages activated with lipopolysaccharide (LPS), adipocytes, and myotubes treated with conditioned medium (CM); $^{\circ}p < 0.05$, $^{\circ\circ}p < 0.01$ CeO_2 NPs vs. control; $^{*}p < 0.05$ CeO_2 NPs vs. inflammation; data ($n = 6$/group) are expressed as mean (SEM).

improve insulin sensitivity-related features at cellular level, after being exposed to proinflammatory stimuli. This research suggests that an in vitro treatment with CeO_2 NPs (without inflammatory stimuli) does not clearly improve the response of the oxidative and inflammatory pathways. On the other hand, a potential effect on insulin resistance was found in metabolic syndrome-related cell lines (myotubes and adipocytes) under proinflammatory stimuli by means of modulating the oxidative status, mitochondrial content, and gene expression. The effect of some insulin-sensitizing molecules could be related to the increased mitochondrial content, as type 2 diabetes features are related to lower mitochondria presence [7].

Oxidative stress and inflammation activate the gene transcription of many inflammatory factors, some of them are subsequently translated into secreted cytokines, which are proteins that are released and act to nearby (paracrine) or distant (endocrine) cells. The increased levels of proinflammatory cytokines (TNF-α, IL-6, and IL-1β) have been found to be important contributors to the underlying processes of the development of metabolic syndrome [5]. Although the implication of IL-6 has tended to be on proinflammatory signaling activation, recent studies suggested a dual role in the homeostatic control of metabolism, for instance, mice lacking *Il6* gene develop insulin resistance and liver inflammation, while patients receiving IL-6R blocking drug therapy increased body weight and developed dyslipidemia [34]. Moreover, the skeletal muscle-derived IL-6 has been suggested to have beneficial effects, modulating glucose and fatty acid metabolism during exercise but also contributing to the development of insulin resistance when chronically elevated [35]. In our experiments, CeO_2 NP treatment increased IL-6 release in myotubes under proinflammatory conditions, which could influence insulin sensitivity. However, no significant differences were observed in metabolic markers (glucose, lactate, and glycerol) in any of the cell types assayed in our study but an increase in glucose uptake and lactate release in macrophages under proinflammatory conditions treated with CeO_2 NPs, which suggests that the potential benefit on insulin resistance upon CeO_2 NP treatment might rely on other (*in vivo*) mechanisms which could not be considered in our experimental setting.

The research on the beneficial effects of nanoceria is still inconclusive, as several studies obtained contradictory findings about their biological activity. Several authors reported anti-inflammatory and antioxidant properties of CeO_2 NPs on cell cultures of murine macrophages [17], cardiomyocytes [23], mesenchymal stem cells, and β-cells [36] as well as neuronal-like cells [31]. *In vivo* animal studies showed beneficial effects of CeO_2 NPs on preventing weight gain accompanied by a decrease in plasma insulin, leptin, glucose, and triglycerides [25], reducing retinal neurodegenerative disease [19] and cardiac dysfunction [22], attenuating hypoxia-

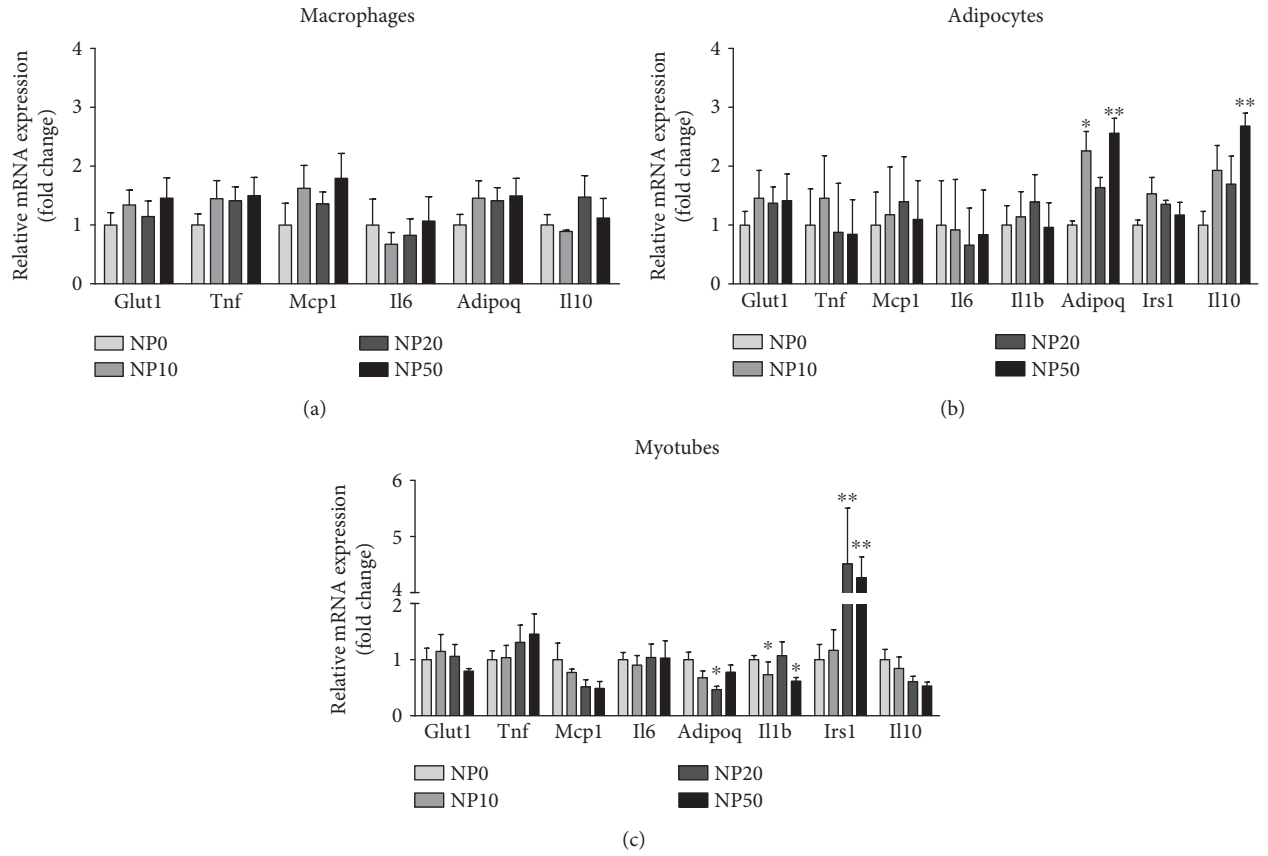

Figure 4: Relative mRNA expression levels in RAW 264.7 macrophages with LPS (a), 3T3-L1 adipocytes with CM (b), and C2C12 myotubes with CM (c) at 24 h after CeO_2 NP treatment at 10, 20, and 50 μg/ml doses. Normalized to *Ppia* housekeeping gene in fold change compared to nontreated control (NTC). $^{*}p < 0.05$, $^{**}p < 0.01$; data ($n = 6$/group) are expressed as mean (SEM). CM: conditioned medium; LPS: lipopolysaccharide.

derived lung damage [20], and alleviating liver ROS toxicity [21] among others. Conversely, other studies evidenced a lack of effectiveness on human monocytes [27, 37] or even deleterious effects on this cell type [29] and oxidative stress and inflammation in the lung, liver, kidney, heart, spleen, and brain of mice [26]. Moreover, these nanoparticles were used to induce cytotoxicity and oxidative damage in tumor cells [15, 28] at the same time protecting nonmalignant cells from chemotherapy [15]. The differences in biological targets (cell types and species), experimental designs (exposure to inflammation/oxidants for treatment or with the nanoparticles for prevention), nanoparticles (synthesis method, size, shape, and chemical characteristics), and objectives of the studies could lead to these variations, being the outcome interpretation and comparison highly complex. The dose of CeO_2 NPs used in the present study has been selected from previous studies involving 3T3-L1 adipocytes and rat mesenchymal stem cells which assessed the impact of these nanoparticles on adipogenesis and obesity-related parameters in rodents [24, 25]. As reported in our experimental assay, none of the doses used in this study seem to induce cell damage regarding to MTT assay data. However, the higher concentration of CeO_2 NPs (100 μg/ml) decreased the mitochondrial content and increased extracellular ROS levels in myotubes, and therefore it was not analyzed in functional assays.

The beneficial effect of nanoparticles in cell cultures could differ due to diverse biochemical characteristics, for instance a lower pH could drive them to act as oxidants and thus generating ROS [24]. The relative proportion of charges varies with the different methods used to prepare the nanoparticles [13]. These findings are of particular interest as the surface oxidation state of the CeO_2 NPs has been demonstrated to alter its enzyme-mimetic activity, thereby the ability of the nanoparticles to scavenge superoxide is directly related to Ce^{+3} concentrations at its surface [38]. In this sense, lower Ce^{+3}/Ce^{+4} ratios were found to be less efficient [16].

The novelty of the present findings is that CeO_2 NPs were tested in cell cultures under proinflammatory conditions, which are likely to be present in the event of therapeutic application of CeO_2 NPs in metabolic syndrome-related organs, thus representing a more physiological approach for evaluating their therapeutic properties [30]. Besides the oxidative stress pathways, we also tested the protective effect of the nanoparticles on the inflammatory response albeit with inconclusive results. The interactions found in the present study between inflammation and the treatment with

CeO_2 NPs in a large number of assays evidenced the differential effects of this potential therapy depending on the inflammatory status. Indeed, some authors recommended the evaluation of the nanomaterial therapeutic potential in the presence of immunomodulators [27], similar to the use of LPS and CM as proinflammatory stimuli in the present work. On the other hand, we found little beneficial effect of CeO_2 NPs on lipopolysaccharide-induced cytokine release from macrophages, suggesting that the previously reported effects in this cell type may be limited in their scope of action and do not extend to a general downregulation of the inflammatory response. Furthermore, we found a reduction in the viability of macrophages that could be explained by the lower cytoplasmic volume where the nanoparticles could be more concentrated and thus more toxic as previously described [37].

5. Conclusion

Overall, our results suggest that CeO_2 NPs could have a potential insulin-sensitizing effect specifically on adipose tissue and skeletal muscle as related to mitochondrial function. Nevertheless, the treatment does not seem to alter, in a physiologically relevant manner, the response of the oxidative and inflammatory pathways. Our results emphasize the need to evaluate the effects of nanoparticles in the presence of stimulators (LPS or CM) which are expected to occur *in vivo* under metabolic syndrome and its related conditions. Additional studies on primary human cells focusing on susceptible populations (with preexisting diseases), investigating the time, dose, and mechanism of action are necessary for the identification of the real benefits and hazards of CeO_2 NPs.

Data Availability

The data used to support the findings of this study are available from the corresponding author upon request.

Conflicts of Interest

The authors declare that there is no conflict of interest regarding the publication of this paper.

Acknowledgments

We would like to thank Asunción Redín and María Zabala (Centre for Nutrition Research, CIN) for their valuable technical support on this project. AL-P is acknowledged for the fellowships to Asociación de Amigos de la Universidad de Navarra (ADA) and the FPU from the Spanish Ministry of Education, Culture and Sport (MECD). This project has received funding from the Spanish Government Carlos III Health Institute Centre of Biomedical Research Network: CIBERobn Physiopathology of Obesity and Nutrition (CB1 2/03/30002) and the University of Navarra.

Supplementary Materials

Table S1: primer sequences for the quantitative PCR for the mouse genes analyzed. The gene identification number (ID) is the unique identifier number from the Entrez Global Query Cross-Database Search System at the National Center for Biotechnology Information. Figure S1: glucose uptake, lactate release, and glycerol release in RAW 264.7 macrophages (a, d), 3T3-L1 adipocytes (b, e, g), and C2C12 myotubes (c, f) at 24 h after CeO_2 NP treatment at 10, 20, and 50 μg/ml doses in fold change compared to nontreated control (NTC). White shapes: control medium; black shapes: inflammation in macrophages activated with lipopolysaccharide (LPS), adipocytes, and myotubes treated with conditioned medium (CM); $^{\#}p < 0.05$, $^{\#\#\#}p < 0.001$ control vs. inflammation; $^{**}p < 0.01$ CeO_2 NPs vs. inflammation; data ($n = 6$/group) are expressed as mean (SEM). Figure S2: secretion of IL-6, MCP-1, TNF-α, and ADIPOQ in RAW 264.7 macrophages (a, d, g), 3T3-L1 adipocytes (b, e, h, j), and C2C12 myotubes (c, f, i, k) at 24 h after CeO_2 NP treatment at 10, 20, and 50 μg/ml doses in ρg/mg total protein compared to nontreated control (NTC). C: control medium; LPS or CM: inflammation in macrophages activated with lipopolysaccharide (LPS), adipocytes, and myotubes treated with conditioned medium (CM); $^{\#\#}p < 0.01$, $^{\#\#\#}p < 0.001$ control vs. inflammation; $^{*}p < 0.05$, $^{**}p < 0.01$, $^{**}p < 0.001$ CeO_2 NPs vs. inflammation; data ($n = 6$/group) are expressed as mean (SEM). Figure S3: HIF-1α total protein in RAW 264.7 macrophages (a), 3T3-L1 adipocytes (b), and C2C12 myotubes (c) at 24 h after CeO_2 NP treatment at 10, 20, and 50 μg/ml doses in ρg/total protein compared to nontreated control (NTC). C: control medium; LPS or CM: inflammation in macrophages activated with lipopolysaccharide (LPS), adipocytes, and myotubes treated with conditioned medium (CM); $^{\#}p < 0.05$ control vs. inflammation; $^{*}p < 0.05$ NPs vs. inflammation; data ($n = 6$/group) are expressed as mean (SEM). Figure S4: relative mRNA analysis of metabolism-related markers in RAW 264.7 macrophages activated with LPS (a), 3T3-L1 adipocytes (b), and C2C12 myocytes (c) treated with conditioned medium (CM). Results normalized to Ppia housekeeping gene. $^{*}p < 0.05$, $^{**}p < 0.01$, $^{***}p < 0.001$ control vs. inflammation (LPS or CM); data ($n = 6$/group) are expressed as mean (SEM). *(Supplementary Materials)*

References

[1] K. G. M. M. Alberti, R. H. Eckel, S. M. Grundy et al., "Harmonizing the metabolic syndrome: a joint interim statement of the International Diabetes Federation Task Force on Epidemiology and Prevention; National Heart, Lung, and Blood Institute; American Heart Association; World Heart Federation; International Atherosclerosis Society; and International Association for the Study of Obesity," *Circulation*, vol. 120, no. 16, pp. 1640–1645, 2009.

[2] A. Lopez-Pascual, M. Bes-Rastrollo, C. Sayón-Orea et al., "Living at a geographically higher elevation is associated with lower risk of metabolic syndrome: prospective analysis of the SUN cohort," *Frontiers in Physiology*, vol. 7, pp. 1–9, 2017.

[3] L. Chen, D. J. Magliano, and P. Z. Zimmet, "The worldwide epidemiology of type 2 diabetes mellitus—present and future perspectives," *Nature Reviews Endocrinology*, vol. 8, no. 4, pp. 228–236, 2012.

[4] S. E. Kahn, R. L. Hull, and K. M. Utzschneider, "Mechanisms linking obesity to insulin resistance and type 2 diabetes," *Nature*, vol. 444, no. 7121, pp. 840–846, 2006.

[5] J. L. Rains and S. K. Jain, "Oxidative stress, insulin signaling, and diabetes," *Free Radical Biology & Medicine*, vol. 50, no. 5, pp. 567–575, 2011.

[6] K. F. Petersen and G. I. Shulman, "Etiology of insulin resistance," *The American Journal of Medicine*, vol. 119, no. 5, pp. S10–S16, 2006.

[7] M.-E. Patti and S. Corvera, "The role of mitochondria in the pathogenesis of type 2 diabetes," *Endocrine Reviews*, vol. 31, no. 3, pp. 364–395, 2010.

[8] J. L. Evans, I. D. Goldfine, B. A. Maddux, and G. M. Grodsky, "Are oxidative stress–activated signaling pathways mediators of insulin resistance and β-cell dysfunction?," *Diabetes*, vol. 52, no. 1, pp. 1–8, 2003.

[9] O. Veiseh, B. C. Tang, K. A. Whitehead, D. G. Anderson, and R. Langer, "Managing diabetes with nanomedicine: challenges and opportunities," *Nature Reviews Drug Discovery*, vol. 14, no. 1, pp. 45–57, 2015.

[10] D. M. Nathan, "Diabetes: advances in diagnosis and treatment," *JAMA*, vol. 314, no. 10, pp. 1052–1062, 2015.

[11] S. E. Kahn, M. E. Cooper, and S. Del Prato, "Pathophysiology and treatment of type 2 diabetes: perspectives on the past, present, and future," *The Lancet*, vol. 383, no. 9922, pp. 1068–1083, 2014.

[12] M. Y. Donath and S. E. Shoelson, "Type 2 diabetes as an inflammatory disease," *Nature Reviews Immunology*, vol. 11, no. 2, pp. 98–107, 2011.

[13] F. Caputo, M. De Nicola, and L. Ghibelli, "Pharmacological potential of bioactive engineered nanomaterials," *Biochemical Pharmacology*, vol. 92, no. 1, pp. 112–130, 2014.

[14] R. A. Yokel, T. C. Au, R. MacPhail et al., "Distribution, elimination, and biopersistence to 90 days of a systemically introduced 30 nm ceria-engineered nanomaterial in rats," *Toxicological Sciences*, vol. 127, no. 1, pp. 256–268, 2012.

[15] M. Sack, L. Alili, E. Karaman et al., "Combination of conventional chemotherapeutics with redox-active cerium oxide nanoparticles—a novel aspect in cancer therapy," *Molecular Cancer Therapeutics*, vol. 13, no. 7, pp. 1740–1749, 2014.

[16] C. Xu and X. Qu, "Cerium oxide nanoparticle: a remarkably versatile rare earth nanomaterial for biological applications," *NPG Asia Materials*, vol. 6, no. 3, article e90, 2014.

[17] S. M. Hirst, A. S. Karakoti, R. D. Tyler, N. Sriranganathan, S. Seal, and C. M. Reilly, "Anti-inflammatory properties of cerium oxide nanoparticles," *Small*, vol. 5, no. 24, pp. 2848–2856, 2009.

[18] F. Charbgoo, M. Ahmad, and M. Darroudi, "Cerium oxide nanoparticles: green synthesis and biological applications," *International Journal of Nanomedicine*, vol. 12, pp. 1401–1413, 2017.

[19] S. V. Kyosseva, L. Chen, S. Seal, and J. F. McGinnis, "Nanoceria inhibit expression of genes associated with inflammation and angiogenesis in the retina of Vldlr null mice," *Experimental Eye Research*, vol. 116, pp. 63–74, 2013.

[20] A. Arya, N. K. Sethy, S. K. Singh, M. Das, and K. Bhargava, "Cerium oxide nanoparticles protect rodent lungs from hypobaric hypoxia-induced oxidative stress and inflammation," *International Journal of Nanomedicine*, vol. 8, pp. 4507–4520, 2013.

[21] S. M. Hirst, A. Karakoti, S. Singh et al., "Bio-distribution and in vivo antioxidant effects of cerium oxide nanoparticles in mice," *Environmental Toxicology*, vol. 28, no. 2, pp. 107–118, 2013.

[22] J. Niu, A. Azfer, L. Rogers, X. Wang, and P. Kolattukudy, "Cardioprotective effects of cerium oxide nanoparticles in a transgenic murine model of cardiomyopathy," *Cardiovascular Research*, vol. 73, no. 3, pp. 549–559, 2007.

[23] J. Niu, K. Wang, and P. E. Kolattukudy, "Cerium oxide nanoparticles inhibits oxidative stress and nuclear factor-κB activation in H9c2 cardiomyocytes exposed to cigarette smoke extract," *Journal of Pharmacology and Experimental Therapeutics*, vol. 338, no. 1, pp. 53–61, 2011.

[24] A. Rocca, V. Mattoli, B. Mazzolai, and G. Ciofani, "Cerium oxide nanoparticles inhibit adipogenesis in rat mesenchymal stem cells: potential therapeutic implications," *Pharmaceutical Research*, vol. 31, no. 11, pp. 2952–2962, 2014.

[25] A. Rocca, S. Moscato, F. Ronca et al., "Pilot in vivo investigation of cerium oxide nanoparticles as a novel anti-obesity pharmaceutical formulation," *Nanomedicine: Nanotechnology, Biology and Medicine*, vol. 11, no. 7, pp. 1725–1734, 2015.

[26] A. Nemmar, P. Yuvaraju, S. Beegam, M. A. Fahim, and B. H. Ali, "Cerium oxide nanoparticles in lung acutely induce oxidative stress, inflammation, and DNA damage in various organs of mice," *Oxidative Medicine and Cellular Longevity*, vol. 2017, Article ID 9639035, 12 pages, 2017.

[27] S. Hussain, F. Al-Nsour, A. B. Rice et al., "Cerium dioxide nanoparticles do not modulate the lipopolysaccharide-induced inflammatory response in human monocytes," *International Journal of Nanomedicine*, vol. 7, p. 1387, 2012.

[28] S. Mittal and A. K. Pandey, "Cerium oxide nanoparticles induced toxicity in human lung cells: role of ROS mediated DNA damage and apoptosis," *BioMed Research International*, vol. 2014, Article ID 891934, 14 pages, 2014.

[29] S. Hussain, F. Al-Nsour, A. B. Rice et al., "Cerium dioxide nanoparticles induce apoptosis and autophagy in human peripheral blood monocytes," *ACS Nano*, vol. 6, no. 7, pp. 5820–5829, 2012.

[30] A. Lopez-Pascual, S. Lorente-Cebrián, M. J. Moreno-Aliaga, J. A. Martinez, and P. González-Muniesa, "Inflammation stimulates hypoxia-inducible factor-1α regulatory activity in 3T3-L1 adipocytes with conditioned medium from lipopolysaccharide-activated RAW 264.7 macrophages," *Journal of Cellular Physiology*, vol. 234, no. 1, pp. 550–560, 2018.

[31] G. Ciofani, G. G. Genchi, I. Liakos et al., "Effects of cerium oxide nanoparticles on PC12 neuronal-like cells: proliferation, differentiation, and dopamine secretion," *Pharmaceutical Research*, vol. 30, no. 8, pp. 2133–2145, 2013.

[32] M. W. Pfaffl, "A new mathematical model for relative quantification in real-time RT–PCR," *Nucleic Acids Research*, vol. 29, no. 9, article e45, 2001.

[33] X.-R. Shao, X.-Q. Wei, X. Song et al., "Independent effect of polymeric nanoparticle zeta potential/surface charge, on their cytotoxicity and affinity to cells," *Cell Proliferation*, vol. 48, no. 4, pp. 465–474, 2015.

[34] J. Scheller, A. Chalaris, D. Schmidt-Arras, and S. Rose-John, "The pro- and anti-inflammatory properties of the cytokine

interleukin-6," *Biochimica et Biophysica Acta (BBA) - Molecular Cell Research*, vol. 1813, no. 5, pp. 878–888, 2011.

[35] L. J. El-Kadre and A. C. A. Tinoco, "Interleukin-6 and obesity: the crosstalk between intestine, pancreas and liver," *Current Opinion in Clinical Nutrition & Metabolic Care*, vol. 16, no. 5, 2013.

[36] J. Zhai, Y. Wu, X. Wang et al., "Antioxidation of cerium oxide nanoparticles to several series of oxidative damage related to type II diabetes mellitus in vitro," *Medical Science Monitor*, vol. 22, pp. 3792–3797, 2016.

[37] S. Hussain, P. P. Kodavanti, J. D. Marshburn et al., "Decreased uptake and enhanced mitochondrial protection underlie reduced toxicity of nSanoceria in human monocyte-derived macrophages," *Journal of Biomedical Nanotechnology*, vol. 12, no. 12, pp. 2139–2150, 2016.

[38] E. G. Heckert, A. S. Karakoti, S. Seal, and W. T. Self, "The role of cerium redox state in the SOD mimetic activity of nanoceria," *Biomaterials*, vol. 29, no. 18, pp. 2705–2709, 2008.

Hindawi
Oxidative Medicine and Cellular Longevity
Volume 2018, Article ID 6256052, 7 pages
https://doi.org/10.1155/2018/6256052

Research Article

Oxidative Stress Induced by Excess of Adiposity Is Related to a Downregulation of Hepatic SIRT6 Expression in Obese Individuals

Marcos C. Carreira,[1,2] **Andrea G. Izquierdo**,[2,3] **Maria Amil**,[1,2] **Felipe F. Casanueva**,[1,2,4] **and Ana B. Crujeiras**[2,3]

[1]*Laboratory of Molecular and Cellular Endocrinology, Instituto de Investigacion Sanitaria de Santiago (IDIS), Complejo Hospitalario Universitario de Santiago (CHUS), Santiago de Compostela, Spain*
[2]*CIBER de Fisiopatologia de la Obesidad y Nutricion (CIBERobn), Instituto Salud Carlos III, Madrid, Spain*
[3]*Laboratory of Epigenomics in Endocrinology and Nutrition, Epigenomics Unit, Instituto de Investigacion Sanitaria de Santiago (IDIS), Complejo Hospitalario Universitario de Santiago (CHUS/SERGAS), Santiago de Compostela, Spain*
[4]*Universidad de Santiago de Compostela (USC), Santiago de Compostela, Spain*

Correspondence should be addressed to Felipe F. Casanueva; endocrine@usc.es
and Ana B. Crujeiras; anabelencrujeiras@hotmail.com

Received 29 May 2018; Revised 11 October 2018; Accepted 16 October 2018; Published 23 December 2018

Academic Editor: Giulio Ceolotto

Sirt6 is a member of the sirtuin family involved in physiological and pathological processes including aging, cancer, obesity, diabetes, and energy metabolism. This study is aimed at evaluating the relationship between liver *SIRT6* gene expression and the oxidative stress network depending on adiposity levels in Zucker rats, an animal model of metabolic syndrome. We observed that liver-specific *SIRT6* expression is reduced in an in vivo model of spontaneous obesity and metabolic syndrome. We also observed that *SIRT6* expression in the liver is positively associated with *SIRT1* and *GST-M2* expressions, two proteins involved in antioxidant protection pathways and inversely related to body weight and plasmatic oxidative status. Interestingly, the *SIRT6* expression is upregulated after energy restriction-induced weight loss concomitantly with an improvement in oxidative stress markers. These results suggest that *SIRT6* may be a potential therapeutic target for the treatment of obesity and associated metabolic disorders, such as liver disease.

1. Introduction

During the last years, numerous evidences suggested the oxidative stress as a key factor involved in the development of obesity and its comorbidities [1]. The oxidative stress in obesity is induced by an excessive generation and accumulation of reactive oxygen species (ROS) in different cellular structures due to the expansion of the adipose tissue and inefficiency in the energy metabolism leading to cellular damage [2, 3]. The metabolic syndrome associated with obesity identifies subjects who have an increase in morbidity and mortality and is correlated with the development of several pathologies that affect different organs such as the liver and the progression from steatosis to nonalcoholic steatohepatitis and hepatocarcinogenesis in which oxidative stress appears to be involved [4].

Sirtuins are a family of NAD^+-dependent protein deacetylases and ADP-ribosyltransferases with an important role in regulating the life span, aging, and cancer as well as energy metabolism and obesity and its metabolic associated disorders [5] and have therefore been proposed as a possible target for future therapies against these diseases.

Seven highly conserved family members of sirtuins have been identified (Sirt1-Sirt7) in mammals [6]. A number of studies revealed that Sirt1 has several beneficial effects on metabolic cell control and enhances the ability of cells to cope

with oxidative stress [7, 8]. However, relatively little is known about the other sirtuins Sirt2 to Sirt7 being suggested that seven sirtuins may have redundant or similar cellular functions with Sirt1 [9]. In this regard, the nucleus-specific Sirt6 level is involved in obesity and diabetes [10, 11]. Aging and overnutrition lead to decreased Sirt6 level resulting in alterations of glucose and lipid metabolism [10]. Deletion of Sirt6 in mice resulted in lethal hypoglycemia [9, 12, 13]. On the other hand, overexpression of Sirt6 improves blood lipid profiles in animals fed with high-fat diets [12]. Liver expression of Sirt6 is induced by caloric restriction and suppressed in diseases associated with lipid accumulation in the liver [12]. Hepatic-specific deletion of sirt6 resulted to triglyceride accumulation and liver steatosis [14]. In addition, adipose tissue-specific ablation of Sirt6 resulted in increased blood glucose, hepatic steatosis, and diet-induced obesity [10, 13]. Sirt6 levels are reduced in the adipose tissue of murine models of obesity and increased in the adipose tissue of humans with weight loss [15, 16].

Therefore, the aim of this study was to evaluate the hepatic gene expression of *SIRT6* and its relationship with the oxidative stress network depending on adiposity levels in Zucker rats, an animal model of metabolic syndrome.

2. Experimental Procedures

2.1. Animals. Male lean (Fa/fa; $n = 10$) and obese (fa/fa; $n = 10$) rats of the Zucker strain, 8 weeks old purchased from Charles River Laboratories (Barcelona, Spain), were maintained in controlled conditions of temperature, humidity, and illumination (12 h controlled photoperiod). They were allowed to acclimatize for 1 week on arrival. All rats had free access to water and standard laboratory diet (SAFE; Panlab, Spain), with 5.5% lipid, 23% protein, and 70% carbohydrate content. Body weight and food and water intake were measured during the experimental period. Finally (22 weeks), animals were euthanized and decapitated, and the livers and blood were obtained, immediately frozen on dry ice, and kept at −80°C until analysis. All animal experiments and procedures involved in this study were approved by the Ethical Committee at the University of Santiago de Compostela, in accordance with the European Union Normative for the use of experimental animals.

In the experimental weight loss protocol, fatty rats ($n = 30$) were randomly divided into three subgroups: an energy-restriction group (ER; $n = 10$), an exercise group (EX; $n = 10$), and an energy restriction plus exercise group (EREX; $n = 10$). These fatty rats were individually housed for 1 week, and their individual food intake was weighed and recorded. Then, the rats in the ER and the EREX groups were fed a diet 30% less in quantity than their individual food intake during 4 weeks (based on the weight of food).

Animals from the EX and the EREX groups were placed on a monitored rodent treadmill (Treadmill system 303401-R-04/C, TSE-Systems, Inc., Chesterfield, MO, USA) for 10 min/day and increased progressively in intensity from 10 m/min to 20 m/min during 1 week for familiarization. After that, animals were placed on the treadmill for 30 min/day at 20 m/min, 7 days per week for 4 weeks.

2.2. Body Composition. Body composition studies were performed every 2 weeks using a nuclear magnetic resonance imaging (MRI) system (Whole Body Composition Analyser, EchoMRI, Echo Medical Systems, USA).

2.3. RNA Extraction and Quantitative RT-PCR. Total RNA extraction from the liver was performed using Trizol (Invitrogen) according to the manufacturer's recommendations. The RNA (500 ng) was retrotranscribed into cDNA using the High Capacity cDNA Reverse Transcription Kit (Applied Biosystems, USA). The expression of the genes of interest was studied using TaqMan real-time PCR in Step One Plus system (Applied Biosystems, USA) using specific primers and probes obtained from inventoried TaqMan Gene Expression Assays (Applied Biosystems, USA) for SIRT6, SIRT1, and GST-M2 genes. All reactions were performed using the following cycling parameters: 50°C for 2 min, 95°C for 10 min, followed by 40 cycles of 95°C for 15 s, 60°C for 1 minute. For data analysis, the RNA level of the gene of interest was normalized using the β-actin values, according to the $2^{-\Delta\Delta Ct}$ method.

2.4. Oxidative Stress Blood Analysis. Plasmatic malondialdehyde (MDA) and total antioxidant capacity (TAC) were evaluated using commercially available colorimetric assay kits (OXIS International, Portland, OR, USA).

2.5. Statistical Analysis. The normal distribution was explored with the Kolmogorov-Smirnov test and the Shapiro-Wilk test. Because oxidative stress markers and gene expression levels were not normally distributed, the Mann–Whitney U test was applied to study the differences between obese and lean rats. The fold change in gene expression was calculated using the $2^{-\Delta\Delta Ct}$ relative quantitation method according to the manufacturer's guidelines (Applied Biosystems, USA) and reporting the data as the geometric mean (standard error of the mean, SEM). A p value < 0.05 was considered to be statistically significant, and a p value ≤ 0.1 was considered to be a trend for significance. The potential association between oxidative stress biomarkers and gene expression levels was evaluated using the Spearman rank correlation coefficient. Statistical analysis was performed by SPSS 15.0 software (SPSS Inc., USA) for Windows XP (Microsoft, USA) and GraphPad Prism 6.01 software (GraphPad Software Inc., USA).

3. Results

3.1. Characteristics of the Experimental Animal at 22 Weeks Old. We fed rats a standard diet while monitoring body weight gain and body composition. At the end of the experiment, the obese rats (fa/fa) showed higher body weight and consequently higher fat mass (9×) as well as lower free fat mass than their lean littermates (Fa/fa) (Table 1). In addition, plasma levels of oxidative stress biomarkers as MDA and TAC at the end of the experimental period were lower in lean than in obese phenotype (Table 1).

3.2. Hepatic Gene Expression of SIRT6, SIRT1, and GST-M2. Obese rats showed a marked decrease in the hepatic gene

Table 1: Characteristics of the experimental animal at 22 weeks old.

	Obese ($n = 10$)	Lean ($n = 10$)	p value
Body weight (g)	559 ± 28	410 ± 30	<0.001
Fat mass (g)	213 ± 11	24 ± 6	<0.001
Free fat mass (g)	261 ± 49	303 ± 19	0.021
MDA (μM)	1.75 ± 0.64	0.61 ± 0.19	0.001
TAC (mM Trolox)	436 ± 191	265 ± 40	0.020

Data are represented as the mean ± standard error of the mean (SEM). P value shows statistically significant differences compared with the control-lean group. MDA: malondialdehyde; TAC: total antioxidant capacity.

expression of *SIRT6* (30%) and *SIRT1* (50%). These results in *SIRT6* and *SIRT1* gene expressions were also observed in an animal model of diet-induced obesity (DIO; Supplementary Figure 1). In addition, the hepatic gene expression of *GST-M2*, the antioxidant enzyme glutathione-S-transferase Mu2, was also reduced (30%) (Figure 1(a)).

Because *SIRT1* and *GST-M2* are two proteins with proven involvement in the antioxidant protection pathway, we performed an association study between *SIRT6* expression and *SIRT1* and *GST-M2* expression in livers from all rats taken together. Interestingly, the hepatic *SIRT6* mRNA levels were positively associated with the gene expression of *SIRT 1* ($r = 0.59$; $p = 0.007$) and *GST-M2* ($r = 0.70$; $p = 0.037$) (Figure 1(b)).

3.3. Association of SIRT6 Gene Expression with Body Weight, MDA, and TAC. In accordance with the involvement of *SIRT6* in the regulation of oxidative stress process [10] and its association with *SIRT1* and *GST-M2* expression levels, we reasoned that the gene expression of *SIRT6* at the hepatic level should be correlated with body weight as well as with systemic markers of oxidative stress. In fact, increased hepatic *SIRT6* expression was associated with lower body weight (Figure 2(a)), lower plasma MDA levels (Figure 2(b)), and lower plasma TAC (Figure 2(c)).

3.4. Weight Loss, Systemic Oxidative Stress, and Hepatic Gene Expression. After the 4 weeks of weight loss treatments, the ER and EREX groups exhibited 26% less body weight (Figure 3(a)) than the Ad-L control group and similar to the lean control animals. No differences were observed between both groups or between the EX and the Ad-L group in body weight. According to the body weight loss data, the ER and EREX groups showed a significant reduction in the circulating levels of MDA and TAC (Figure 3(b)). Interestingly, in the EX group, despite not producing a reduction in body weight, it showed a reduction in the circulating levels of MAD and TAC similar to the effects observed for the EREX group (Figure 3(b)). Then, we investigated the effect of the weight loss interventions on hepatic gene expression of sirtuins and GST-M2. According to the body weight loss data, the ER and EREX groups but not the EX group showed a significant increase in SIRT6 and SIRT1 gene expressions (Figure 3(c)). However, the expression of GST-M2 showed no significant variations after the interventions (Figure 3(c)).

4. Discussion

This work shows that the oxidative stress induced by excess of adiposity is related to a downregulation of hepatic *SIRT6* expression in obese individuals. After weight loss induced by energy restriction, the hepatic *SIRT6* expression increases, concomitantly with an improvement in oxidative stress markers. Therefore, these results suggest that the potential role of SIRT6 in the protection against oxidative stress damage could be a therapeutic target to treat the damage caused by the association between obesity and oxidative stress.

Sirtuins play an important regulatory role in energy metabolism and they may be a potential therapeutic target for obesity and associated pathologies [5]. Among the sirtuin family members, sirt1 is the most well-studied sirtuin and it has been implicated in the protection against cellular oxidative stress, and it plays an important role in metabolic pathway regulation, specifically acting in adipocytes as an inhibitor of adipogenesis. Additionally, the expression of *SIRT1* is modulated by energy restriction in association with improvements in oxidative stress [7]. In this line, *SIRT6* was recently discovered as a relevant player in the predisposition to age-associated diseases [17]. The activity of *SIRT6* is reduced in obesity and diabetes and its hepatic-specific ablation increases liver steatosis onset [10]. However, the study of *SIRT6* is still very fresh [10]. In this work, we showed a downregulation of *SIRT6* in the liver of obese rats compared with their lean littermates.

The liver is a key metabolic organ controlling the overall lipid metabolism in response to hormonal and nutritional stimuli received and one of the organs most affected by excessive intake of carbohydrates or fat leading to metabolic pathologies associated with obesity. Several studies highlighted that obesity strongly contributes to the transition of nonalcoholic fatty liver disease (NAFLD) to nonalcoholic steatohepatitis (NASH) and hepatocellular carcinoma (HCC) [18, 19]. The absence of *SIRT6* increases the expression of genes responsible for hepatic long-chain fatty acid uptake and reduced expression of genes for β-oxidation leading to accumulation of triglycerides and fatty liver disease and hepatic steatosis [10]. Additionally, the participation of ROS in liver disease has been suggested [20]. Moreover, it was observed that genes related to oxidative stress regulation are overexpressed in early stages of HCC [21]. In this regard, obesity produces various metabolic alterations that contribute very actively to the general oxidative balance, creating the basis for the development of diseases such as diabetes, hypertension, cardiovascular disease, and cancer, among others. According to the literature, the major contributors to systemic oxidative stress in obesity are hyperglycemia, increased muscle activity to support weight gain, high lipid levels in different tissues, chronic inflammation, low antioxidant defenses, endothelial ROS production, and hyperleptinemia [1]. Oxidative stress in obesity is a systematic problem that can be reduced by improving antioxidant defenses through fat reduction, physical activity or exercise,

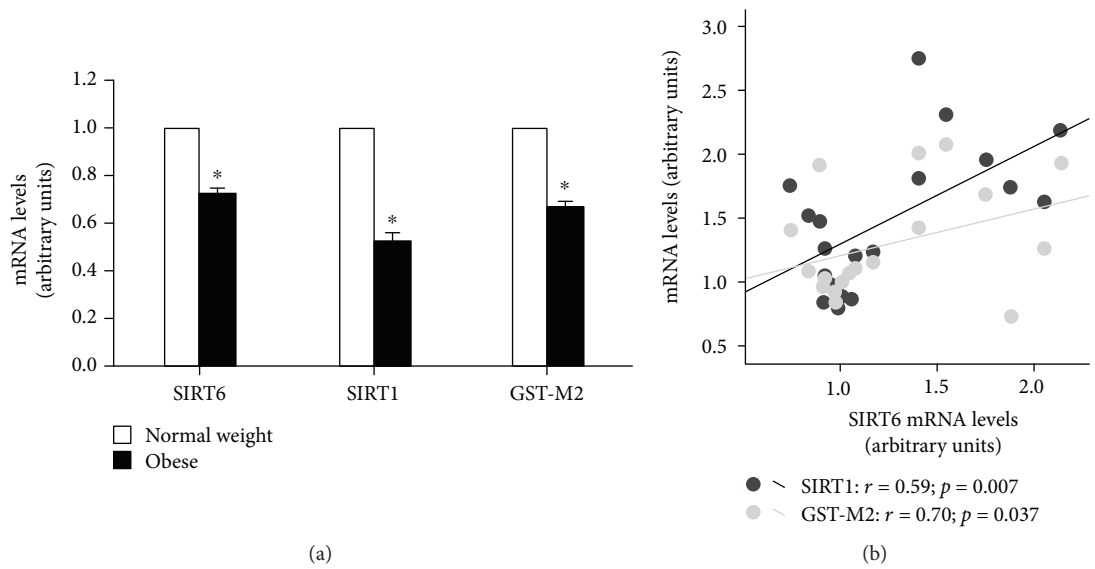

Figure 1: Liver expression of SIRT6, SIRT1, and GST-M2 genes in lean or obese rats (a). Data are represented as the mean ± standard error of the mean (SEM). Statistically significant differences compared with control-lean counterparts $^{*}p < 0.05$ vs. normal weight group. Association between SIRT6 mRNA levels with SIRT1 or GST-M2 genes in all animal taking together (b). SIRT1 ($r = 0.59$; $p = 0.007$), GST-M2 ($r = 0.70$; $p = 0.037$).

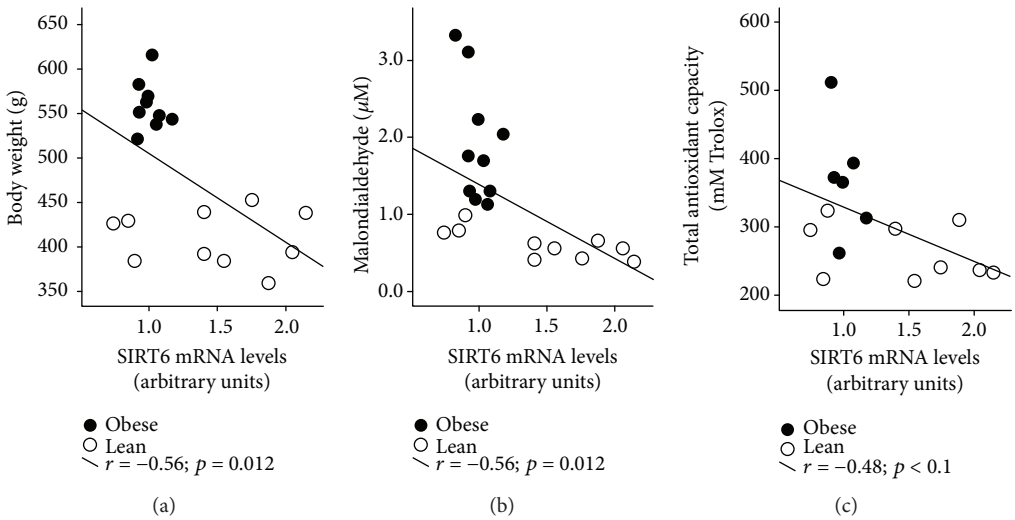

Figure 2: Association of SIRT6 gene expression with body weight (a), MDA (b), and TAC (c).

dietary restriction, surgical intervention, or antioxidant therapies which, based on the results showed in this work, may include *SIRT6*.

In accordance with a potential association between the expression of *SIRT6* with oxidative stress, we observed a correlation between *SIRT1* and *GST-M2*, both genes that codify proteins involved in the protection against oxidative stress [7, 22], which were also downregulated in the liver of obese fa/fa rats. These results suggest a dysregulation in the antioxidant defenses that promote the oxidative stress characteristic of obesity [23] which was confirmed by the high circulating levels of MDA and TAC.

The connection between oxidative stress, energy restriction, and sirtuin activity has been shown in the literature. The energy restriction reduces the cellular levels of NADH by increasing the NAD+/NADH ratio and causing an increase in Sirt2 activity [24]. As in the case of Sirt2, Sirt6 activity is also influenced by energy restriction. Prolonged restriction results in increased activity of Sirt6 at the brain, muscle, white adipose tissue, and liver levels [12, 13]. In addition, Sirt6 is also a mediator of the effects induced by energy restriction. *SIRT6* suppression decreases life extension activated by energy restriction, and *SIRT6* overexpression shows reduced body weight, increased metabolism, and reduced serum levels of insulin, glucose, cholesterol, and several adipokines [13, 25].

In this sense, the data obtained in this study show that body weight loss is associated with an increase in hepatic *SIRT6* expression and a reduction in systematic oxidative stress biomarkers in a similar way to the well-studied *SIRT1*.

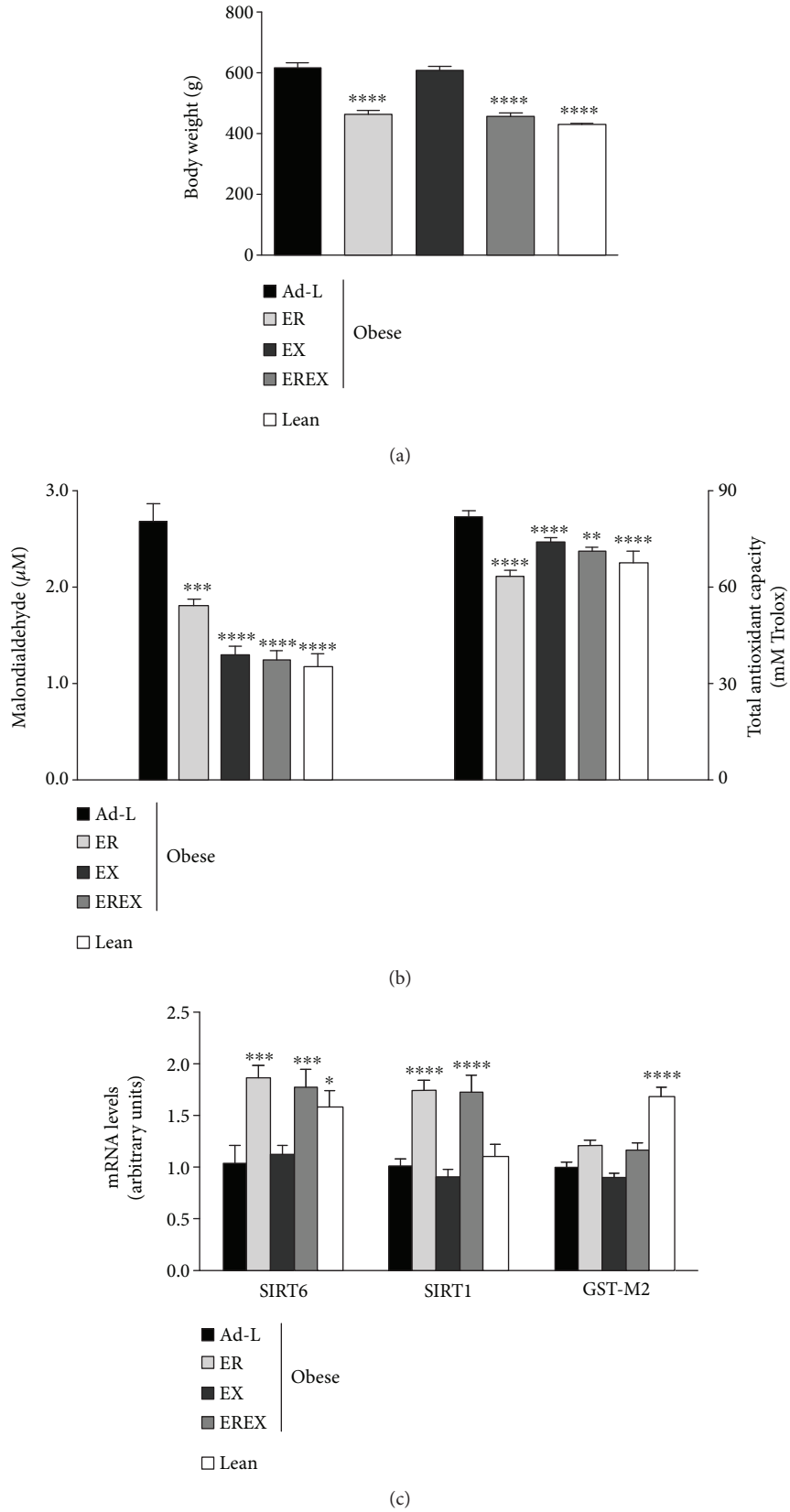

Figure 3: Effect of 4 weeks of weight loss interventions on body weight (a), serum oxidative stress biomarkers (b), and hepatic gene expression (c). Data are represented as mean and SEM, $n = 6 - 10$ animals/group. $^{*}p < 0.05$ vs. the Ad-L group, $^{**}p < 0.01$ vs. the Ad-L group, $^{***}p < 0.001$ vs. the Ad-L group, $^{****}p < 0.0001$ vs. the Ad-L group. Ad-L: ad libitum group; ER: energy-restriction group; EX: exercise group; EREX: energy restriction plus exercise group.

According to the important role of Sirt6 in the liver related to lipidic and glucose metabolism [10], these effects are observed in models of caloric restriction; however, physical exercise does not seem to have any influence on hepatic SIRT6 expression, although exercise has a potent reducing effect of oxidative stress at the systemic level. This suggests that the exercise model produces a decrease in systemic oxidative stress similar to the energy restriction model but probably through a different mechanism in which the skeletal muscle may be involved. All these data suggest that *SIRT6* acts similarly to *SIRT1* and may play a key role in regulating energy metabolism and defense against oxidative stress.

In conclusion, the results of the current work evidenced that *SIRT6* gene expression shows similar pattern of *SIRT1* gene expression, the most-studied sirtuin member, in the context of relationship with excess body weight and the regulation of oxidative stress. It supports the idea of a prominent role for *SIRT6* as a potential therapeutic target for the treatment of obesity and associated disease, particularly liver disease.

Abbreviations

ANOVA: Analysis of variance
HCC: Hepatocellular carcinoma
HFD: High-fat diet
GST-M2: Glutathione-S-transferase Mu2
MDA: Plasmatic malondialdehyde
MRI: Magnetic resonance imaging
NAFLD: Nonalcoholic fatty liver disease
NASH: Nonalcoholic steatohepatitis
ROS: Reactive oxygen species
SIRT: Sirtuin
TAC: Total antioxidant capacity.

Data Availability

The data used to support the findings of this study are available from the corresponding author upon request.

Conflicts of Interest

The authors declare no conflict of interest.

Authors' Contributions

MCC and AGI designed and performed experiments and wrote the manuscript; MA helped with experiments and contributed to the discussion; ABC and FFC obtained funding, designed experiments, and wrote the manuscript. MCC, AGI, ABC, and FFC are the guarantors of this work and, as such, had full access to all the data in the study and take responsibility for the integrity of the data and accuracy of the data analysis. All authors have reviewed and approved the article and have read the journal's authorship agreement. Marcos C Carreira and Andrea G Izquierdo contributed equally to this work and should be considered co-first authors. Felipe F Casanueva and Ana B. Crujeiras contributed equally to this work and should be considered co-main authors.

Acknowledgments

Authors thank Maribel Rendo from the Department of Molecular and Cellular Endocrinology of Instituto de Investigacion Sanitaria de Santiago (IDIS) for her support of research data management. This study was supported by Centro de Investigacion Biomedica en Red de Fisiopatologia de la Obesidad y Nutricion (CIBERobn) and grants from the Instituto de Salud Carlos III (PI17/01287) cofinanced by the European Regional Development Fund (FEDER). Andrea G. Izquierdo is funded by CIBERobn and Ana B. Crujeiras is funded by a research contract "Miguel Servet" (CP17/00088) from the Instituto de Salud Carlos III, cofinanced by the European Regional Development Fund (FEDER).

Supplementary Materials

Supplementary Figure 1: liver expression of SIRT6 and SIRT1 in lean or diet-induced obesity (DIO) Sprague Dawley rats (A). Data are represented as the mean ± standard error of the mean (SEM). Statistically significant differences compared with control-lean counterparts $^{*}p < 0.05$ vs. lean group. *(Supplementary Materials)*

References

[1] H. K. Vincent, K. E. Innes, and K. R. Vincent, "Oxidative stress and potential interventions to reduce oxidative stress in overweight and obesity," *Diabetes, Obesity & Metabolism*, vol. 9, no. 6, pp. 813–839, 2007.

[2] A. B. Crujeiras, D. Parra, E. Goyenechea, I. Abete, P. González-Muniesa, and J. A. Martínez, "Energy restriction in obese subjects impact differently two mitochondrial function markers," *Journal of Physiology and Biochemistry*, vol. 64, no. 3, pp. 211–219, 2008.

[3] O. Dizdar and E. Alyamac, "Obesity: an endocrine tumor?," *Medical Hypotheses*, vol. 63, no. 5, pp. 790–792, 2004.

[4] L. A. Streba, C. C. Vere, I. Rogoveanu, and C. T. Streba, "Nonalcoholic fatty liver disease, metabolic risk factors, and hepatocellular carcinoma: an open question," *World Journal of Gastroenterology*, vol. 21, no. 14, pp. 4103–4110, 2015.

[5] S. Michan and D. Sinclair, "Sirtuins in mammals: insights into their biological function," *The Biochemical Journal*, vol. 404, no. 1, pp. 1–13, 2007.

[6] R. A. Frye, "Characterization of five human cDNAs with homology to the yeast SIR2 gene: Sir2-like proteins (sirtuins) metabolize NAD and may have protein ADP-ribosyltransferase activity," *Biochemical and Biophysical Research Communications*, vol. 260, no. 1, pp. 273–279, 1999.

[7] A. B. Crujeiras, D. Parra, E. Goyenechea, and J. A. Martínez, "Sirtuin gene expression in human mononuclear cells is modulated by caloric restriction," *European Journal of Clinical Investigation*, vol. 38, no. 9, pp. 672–678, 2008.

[8] C. S. Lim, "Is SIRT6 a new biomarker for oxidative stress and longevity assurance gene?," *Medical Hypotheses*, vol. 69, no. 1, p. 231, 2007.

[9] Y. Kanfi, V. Peshti, R. Gil et al., "SIRT6 protects against pathological damage caused by diet-induced obesity," *Aging Cell*, vol. 9, no. 2, pp. 162–173, 2010.

[10] J. Kuang, L. Chen, Q. Tang, J. Zhang, Y. Li, and J. He, "The role of Sirt6 in obesity and diabetes," *Frontiers in Physiology*, vol. 9, p. 135, 2018.

[11] E. Michishita, J. Y. Park, J. M. Burneskis, J. C. Barrett, and I. Horikawa, "Evolutionarily conserved and nonconserved cellular localizations and functions of human SIRT proteins," *Molecular Biology of the Cell*, vol. 16, no. 10, pp. 4623–4635, 2005.

[12] Y. Kanfi, R. Shalman, V. Peshti et al., "Regulation of SIRT6 protein levels by nutrient availability," *FEBS Letters*, vol. 582, no. 5, pp. 543–548, 2008.

[13] J. Kuang, Y. Zhang, Q. Liu et al., "Fat-specific Sirt6 ablation sensitizes mice to high-fat diet-induced obesity and insulin resistance by inhibiting lipolysis," *Diabetes*, vol. 66, no. 5, pp. 1159–1171, 2017.

[14] H. S. Kim, C. Xiao, R. H. Wang et al., "Hepatic-specific disruption of SIRT6 in mice results in fatty liver formation due to enhanced glycolysis and triglyceride synthesis," *Cell Metabolism*, vol. 12, no. 3, pp. 224–236, 2010.

[15] J. E. Dominy Jr., Y. Lee, M. P. Jedrychowski et al., "The deacetylase Sirt6 activates the acetyltransferase GCN5 and suppresses hepatic gluconeogenesis," *Molecular Cell*, vol. 48, no. 6, pp. 900–913, 2012.

[16] A. R. Moschen, V. Wieser, R. R. Gerner et al., "Adipose tissue and liver expression of SIRT1, 3, and 6 increase after extensive weight loss in morbid obesity," *Journal of hepatology*, vol. 59, no. 6, pp. 1315–1322, 2013.

[17] P. Zhang, B. Tu, H. Wang et al., "Tumor suppressor p53 cooperates with SIRT6 to regulate gluconeogenesis by promoting FoxO1 nuclear exclusion," *Proceedings of the National Academy of Sciences of the United States of America*, vol. 111, no. 29, pp. 10684–10689, 2014.

[18] A. Marengo, C. Rosso, and E. Bugianesi, "Liver cancer: connections with obesity, fatty liver, and cirrhosis," *Annual Review of Medicine*, vol. 67, no. 1, pp. 103–117, 2016.

[19] J. A. Marrero, R. J. Fontana, G. L. Su, H. S. Conjeevaram, D. M. Emick, and A. S. Lok, "NAFLD may be a common underlying liver disease in patients with hepatocellular carcinoma in the United States," *Hepatology*, vol. 36, no. 6, pp. 1349–1354, 2002.

[20] Y. Sánchez-Pérez, C. Carrasco-Legleu, C. García-Cuellar et al., "Oxidative stress in carcinogenesis. Correlation between lipid peroxidation and induction of preneoplastic lesions in rat hepatocarcinogenesis," *Cancer Letters*, vol. 217, no. 1, pp. 25–32, 2005.

[21] O. Beltrán-Ramírez, S. Sokol, V. le-Berre, J. M. François, and S. Villa-Treviño, "An approach to the study of gene expression in hepatocarcinogenesis initiation," *Translational Oncology*, vol. 3, no. 2, pp. 142–148, 2010.

[22] A. B. Crujeiras, D. Parra, E. Goyenechea, I. Abete, and J. A. Martínez, "Tachyphylaxis effects on postprandial oxidative stress and mitochondrial-related gene expression in overweight subjects after a period of energy restriction," *European Journal of Nutrition*, vol. 48, no. 6, pp. 341–347, 2009.

[23] H. K. Vincent and A. G. Taylor, "Biomarkers and potential mechanisms of obesity-induced oxidant stress in humans," *International Journal of Obesity*, vol. 30, no. 3, pp. 400–418, 2006.

[24] L. Tasselli, Y. Xi, W. Zheng et al., "SIRT6 deacetylates H3K18ac at pericentric chromatin to prevent mitotic errors and cellular senescence," *Nature Structural & Molecular Biology*, vol. 23, no. 5, pp. 434–440, 2016.

[25] Y. Kanfi, S. Naiman, G. Amir et al., "The sirtuin SIRT6 regulates lifespan in male mice," *Nature*, vol. 483, no. 7388, pp. 218–221, 2012.

Hindawi
Oxidative Medicine and Cellular Longevity
Volume 2018, Article ID 6598326, 13 pages
https://doi.org/10.1155/2018/6598326

Research Article

Oxidative Stress in Cardiac Tissue of Patients Undergoing Coronary Artery Bypass Graft Surgery: The Effects of Overweight and Obesity

Yves Gramlich,[1] **Andreas Daiber**,[1] **Katja Buschmann**,[2] **Matthias Oelze**,[1] **Christian-Friedrich Vahl**,[2] **Thomas Münzel**,[1] **and Ulrich Hink**[1]

[1]*Center for Cardiology/Cardiology 1, Laboratory of Molecular Cardiology of the Johannes Gutenberg University, Mainz, Germany*
[2]*Department of Heart, Thoracic and Vascular Surgery of the Johannes Gutenberg University, Mainz, Germany*

Correspondence should be addressed to Andreas Daiber; daiber@uni-mainz.de

Received 9 April 2018; Accepted 14 October 2018; Published 17 December 2018

Guest Editor: Paul Cordero

Background. Obesity is one of the major cardiovascular risk factors and is associated with oxidative stress and myocardial dysfunction. We hypothesized that obesity affects cardiac function and morbidity by causing alterations in enzymatic redox patterns. *Methods*. Sixty-one patients undergoing coronary artery bypass grafting (CABG) were included in the study. Excessive right atrial myocardial tissue emerging from the operative connection to the extracorporeal circulation was harvested. Patients were assigned to control ($n = 19$, body mass index (BMI): <25 kg/m^2), overweight ($n = 25$, 25 kg/m^2 < BMI < 30 kg/m^2), or obese ($n = 17$, BMI: >30 kg/m^2) groups. Oxidative enzyme systems were studied directly in the cardiac muscles of patients undergoing CABG who were grouped according to BMI. Molecular biological methods and high-performance liquid chromatography were used to detect the expression and activity of oxidative enzymes and the formation of reactive oxygen species (ROS). *Results*. We found increased levels of ROS and increased expression of ROS-producing enzymes (i.e., p47phox, xanthine oxidase) and decreased antioxidant defense mechanisms (mitochondrial aldehyde dehydrogenase, heme oxygenase-1, and eNOS) in line with elevated inflammatory markers (vascular cell adhesion molecule-1) in the right atrial myocardial tissue and by trend also in serum (sVCAM-1 and CCL5/RANTES). *Conclusion*. Increasing BMI in patients undergoing CABG is related to altered myocardial redox patterns, which indicates increased oxidative stress with inadequate antioxidant compensation. These changes suggest that the myocardium of obese patients suffering from coronary artery disease is more susceptible to cardiomyopathy and possible damage by ischemia and reperfusion, for example, during cardiac surgery.

1. Introduction

Acute or chronic cardiovascular diseases, especially of myocardial origin, rank among the leading causes of death in Germany [1]. One of the most important risk factors for cardiovascular disease, in addition to smoking and diabetes mellitus, is obesity—a growing worldwide health problem that is associated with reduced life span [2, 3]. It is estimated that by 2020, three out of four Americans will be overweight [4]. Accordingly, obesity and disorders of the myocardium are considered important targets in therapy and research in order to lower the cardiovascular mortality and morbidity of the western population and preserve the quality of life of the elderly. An increased body mass index (BMI) is associated with an increased cardiovascular risk [5], increased left ventricular myocardial mass, and systolic and diastolic dysfunction [6–10]. While, in overweight individuals (BMI: 25–30 kg/m^2), an increase in left ventricular myocardial mass contributes to a reasonable compensation mechanism, overcompensation is seen in obese individuals (BMI: >30 kg/m^2) that may lead to left ventricular hypertrophy and reduced left ventricular function [11]. Accordingly, it has been shown that the cardiac muscle fibers of patients undergoing cardiac surgery show a negative correlation

between the force amplitude of the contractile apparatus and BMI [12]. Although elevated BMI is known to correlate with a higher cardiovascular morbidity [13], the mechanisms responsible for the contractile dysfunction shown in overweight individuals are largely unknown. It is thought that hypoxia-induced hypertrophy, inflammation, and oxidative stress may play a prominent role in this phenomenon. Other possible triggers are adipocyte-secreted adipokines that lead to reduced NO bioavailability and increased oxidative stress [14]. Elevated BMI correlates with the extent of oxidative stress-mediated endothelial dysfunction [15]. Macrophages in adipose tissue induce inflammation and can also lead to impaired vascular contractility [16, 17]. Increased release of reactive oxygen species (ROS), for example, by NADPH oxidases and mitochondrial enzymes, results in cardiomyocyte hypertrophy, fibrosis, and metalloproteinase activation, potentially leading to progression of heart disease [18]. The majority of these findings relate to animal studies and lack of confirmation in humans. There are only few data on whether overweight patients with coronary artery disease (CAD) have significantly elevated levels of oxidative stress in cardiac tissue. Accordingly, sources of ROS production and enzymatic function pertaining to inotropic and ischemic tolerance have not been adequately elucidated, particularly with respect to normal-weight patients.

2. Material and Methods

2.1. Patient Cohort. Sixty-one patients undergoing coronary artery bypass graft surgery (CABG) were included in our study. We harvested excess right atrial myocardial tissue resulting from operative connection to the extracorporeal circulation. Patients were categorized into the following three groups: control ($n = 19$, BMI: $<25\,kg/m^2$), overweight ($n = 25$, $25\,kg/m^2 < BMI < 30\,kg/m^2$), or obese ($n = 17$, BMI: $>30\,kg/m^2$) group. Patients with atrial arrhythmias or valvular heart disease and patients on dialysis were excluded from the study. Handling of all human materials and treatment of patients were in accordance with the Declaration of Helsinki. Informed consent was obtained from each patient after the study was explained to them. The local institutional ethics committee approved the study (number: 837.104.08 (6100)).

See supplemental Table S1 for the inclusion and exclusion criteria and supplemental Table S2 for the patient characteristics.

2.2. Isolation of Cardiac Mitochondria. Isolated mitochondria were prepared from excess right atrial myocardial tissue of the patients according to a previously published protocol for isolation of rat heart mitochondria [19]. Briefly, human myocardial tissue was glass-homogenized in HEPES buffer and subjected to cold centrifugation at 1500g at 4°C for 10 min and 2000g for 5 min. The resulting supernatant was centrifuged at 20,000g for 20 min, and the resulting pellet was resuspended in 1 mL of Tris buffer. The last centrifugation step was repeated, and the pellet was finally resuspended in 1 mL of Tris buffer. The protein content was determined by the Lowry method.

2.3. Detection of Oxidative Stress (Chemiluminescence) in Isolated Cardiac Mitochondria by High-Performance Liquid Chromatography- (HPLC-) Based Measurement of 2-Hydroxyethidium. Superoxide was measured by a modified HPLC-based method to quantify ethidium and 2-hydroxyethidium levels, as previously described [20]. Briefly, myocardial mitochondria (0.2 mg/mL) were incubated with 50 μM dihydroethidium (DHE) for 30 min at 37°C in PBS buffer and stored at −80°C. Upon thawing, DHE oxidation products were extracted by the addition of 50% acetonitrile and 50% PBS, incubated (10 min), centrifuged (20 min at 20,000g), and filtered (30 kDa Millipore Filter, 45 min at 16,000g). A 50 μL sample of this supernatant was subjected to HPLC analysis and measured, based on a previously described method [21, 22]. The system consisted of a control unit, two pumps, a mixer, detectors, a column oven, a degasser, and an autosampler from Jasco (Groß-Umstadt, Germany) and a C18-Nucleosil 100-3 (125 × 4) column from Macherey & Nagel (Düren, Germany). A high-pressure gradient was employed with acetonitrile, and 25 mM citrate buffer (pH 2.2) was used as the mobile phase with the following percentages of organic solvent: 0 min, 36%; 7 min, 40%; 8–12 min, 95%; and 13 min, 36%. The flow rate was 1 mL/min, and DHE was detected by its absorption at 355 nm, whereas 2-hydroxyethidium and ethidium were detected by their fluorescence (excitation: 480 nm; emission: 580 nm). The signal was normalized to the protein content of the mitochondrial preparations. Data on 2-hydroxyethidium were calibrated with respect to the superoxide formation rate by different xanthine oxidase concentrations for which the superoxide formation rate was determined by the cytochrome c assay [21].

2.4. Measurement of Mitochondrial Aldehyde Dehydrogenase (ALDH-2) Activity. ALDH-2 activity was assessed by HPLC using the mitochondrial fraction and 6-methoxy-2-naphthaldehyde (Monal-62) as a fluorescent substrate. A mitochondrial fraction (0.2 mg/mL) equivalent to the protein concentration (determined by "Lowry's method") was incubated at 37°C for 30 min with Monal-62, and the reaction was terminated by the addition of benomyl (20 μM)—an unspecific aldehyde dehydrogenase inhibitor. The oxidation of Monal-62 to the fluorescent naphthoic acid product [23] was traced by HPLC analysis as previously described [24].

2.5. Protein Expression. Protein expression and modification were assessed by a standard western and dot blot analysis using established protocols [25–27]. Isolated cardiac tissue was frozen and homogenized in liquid nitrogen. Proteins were separated by SDS-PAGE and blotted onto nitrocellulose membranes. After blocking, immunoblotting was performed with the following antibodies as described in supplemental Table S3. Detection and quantification were performed by enhanced chemiluminescence (ECL) with peroxidase-conjugated anti-rabbit/mouse (1 : 10,000, Vector Lab., Burlingame, CA) and anti-goat (1 : 5000, Santa Cruz Biotechnology, USA) secondary antibodies. Densitometric quantification of antibody-specific bands was performed with a ChemiLux

Imager (CsX-1400M, Intas, Göttingen, Germany) and Gel-Pro Analyzer software (Media Cybernetics, Bethesda, MD).

2.6. Fluorescence-Based ROS Detection in Cardiac Tissue. ROS formation was detected by oxidative fluorescence microtopography using DHE as a fluorescent probe in cardiac cryosections (ethidium plus 2-hydroxyethdium). The method was based on a previously published protocol [27, 28]. Briefly, cardiac tissue was embedded in Tissue-Tek O.C.T.™ resin and frozen in liquid nitrogen. The embedded tissue pieces were coded anonymously and stored at −80°C until further processing. The coding allowed a blinded, independent examination of the tissue samples. Before staining with DHE (1 μM) for 30 min at room temperature, frozen samples were cryosectioned. ROS detection was carried out by detecting 2-hydroxyethidium (2-HE; EOH—specific for superoxide anion radical) and ethidium (E+—unspecific oxidation product, e.g., by hydroxyl radicals or peroxidase-mediated reactions), both DHE oxidation products. ROS-derived red fluorescence was detected using a Zeiss Axiovert 40 CFL microscope, Zeiss lenses, and Axiocam MRm camera (Jena, Germany). Intensities of the DHE oxidation products' fluorescence were evaluated by densitometry.

2.7. Statistical Analysis. The statistical analysis was performed using SPSS (version 17, IBM). The Mann–Whitney U test was used to compare differences among the three study groups (control, overweight, and obese patients) [29]. Multiple significance level was set at $\alpha = 0.05$. To control the "family-wise error rate" (FWER), we carried out Bonferroni's correction for comparison of multiple means [30]. The linear regressions were tested for statistical significance using ANOVA. All data are presented as mean ± SEM.

3. Results

3.1. Impact of Body Weight on Cardiac Oxidative Stress Levels. To determine whether BMI directly affects the cardiac ROS levels, we evaluated ROS formation by different methods. The determination of 2-hydroxyethidium (2-HE) and ethidium (E+) by an HPLC-based assay provided evidence that the levels of ROS are somewhat elevated in isolated cardiac mitochondria of both overweight and obese patients, although not significantly (Figure 1(a)). While 2-HE is more specific for superoxide formation, ethidium is formed by a number of different oxidants (e.g., hydroxyl radicals, peroxynitrite, peroxides such as H_2O_2, and peroxidases). 2-HE was numerically elevated in overweight individuals by 22.5% ($p > 0.05$) and in obese patients by 20.3% ($p > 0.05$), whereas ethidium was elevated by 4.1% ($p > 0.05$) and 19.5% ($p > 0.05$), respectively. Although not statistically significant, these initial data provided a stable trend for increased cardiac mitochondrial ROS levels with respect to BMI and suggested the use of other quantitative methods for further studies. Staining of cardiac cryosections with DHE did not require isolation of mitochondria (which could already affect the ROS signals) and hence provided less specificity but better sensitivity than HPLC measurements of superoxide formation (2-HE signal). Accordingly, oxidative fluorescence microtopography provided a more general read-out of oxidative stress but with broader application than HPLC analysis [31, 32]. The fluorescence-based analysis of DHE-stained sections revealed a significant increase in the concentration of ROS in the group of overweight patients by 36% ($p < 0.001$) and obese individuals by 27% ($p < 0.001$) (Figure 1(b)). Furthermore, by using a linear regression analysis, despite a low correlation coefficient (R^2), it was observed that an increased BMI led to increased oxidative stress levels in the myocardium of all the study patients ($R^2 = 0.112$, $p = 0.014$) (Figure 1(b)).

These results show that obese and overweight patients with CAD have increased ROS levels in cardiac tissue, which could be related to increased production (activation of sources) or decreased detoxification (impaired antioxidant defense). In order to test for the first argument (increased ROS formation), we measured the protein expression of xanthine oxidase (XO) and p47phox, a regulatory subunit of the NADPH oxidase isoform 2 (formerly known as gp91phox-dependent phagocytic NADPH oxidase). As shown in Figures 1(c) and 1(d), the expression of p47phox and XO increased by 57% ($p = 0.008$) and by 92% ($p = 0.005$), respectively, in overweight individuals. In addition, in the obese group, an enhancement of p47phox by 77% ($p < 0.001$) and XO by 34% ($p > 0.05$) was detected. It was also found that the expression of the Nox2 major subunit—p47phox—a required subunit for activation of Nox2, is increased in overweight patients and was further augmented in obese patients (Figure 1(c)). Linear regression analysis showed that the expression of the p47phox subunit increased with elevated BMI ($R^2 = 0.106$, $p = 0.018$) (Figure 1(c)).

3.2. Impact of Body Weight on the Cardiac Nitric Oxide Pathway. In many cardiovascular disease conditions, eNOS may switch from a protective enzyme to uncoupled eNOS—the type that encourages disease progression. In its coupled state, eNOS produces the vasodilator nitric oxide that is attributed to antiaggregatory and antiatherogenic properties. Uncoupled eNOS on the other hand produces superoxide anion radicals that facilitate platelet aggregation and atherosclerosis [33–36]. Obesity induced a significant decrease in eNOS expression in cardiac tissue of 22% of the patients ($p < 0.001$) compared with the normal-weight control group, whereas the overweight patients showed no difference (Figure 2(a)), suggesting decreased NO synthesis in obese patients. Likewise, the proportion of eNOS phosphorylation at the serine 1177 (Ser1177) residue, indicative of eNOS activation, showed a decreased trend in overweight patients by 18% ($p > 0.05$) and was significantly reduced in the obese group by 32% ($p = 0.022$).

The level of tetrahydrobiopterin (BH_4), which is the essential cofactor of eNOS, was found reduced under oxidative stress conditions due to peroxynitrite or other ROS-mediated oxidation to dihydrobiopterin (BH_2) [37–39]. However, BH_4 supplementation in patients with myocardial infarction, diabetes, and hypercholesterolemia improved endothelial function, a surrogate parameter of the eNOS functional state [40–42]. BH_4 levels are largely regulated by de novo synthesis of GTP-cyclohydrolase-1 (GCH-1) or by

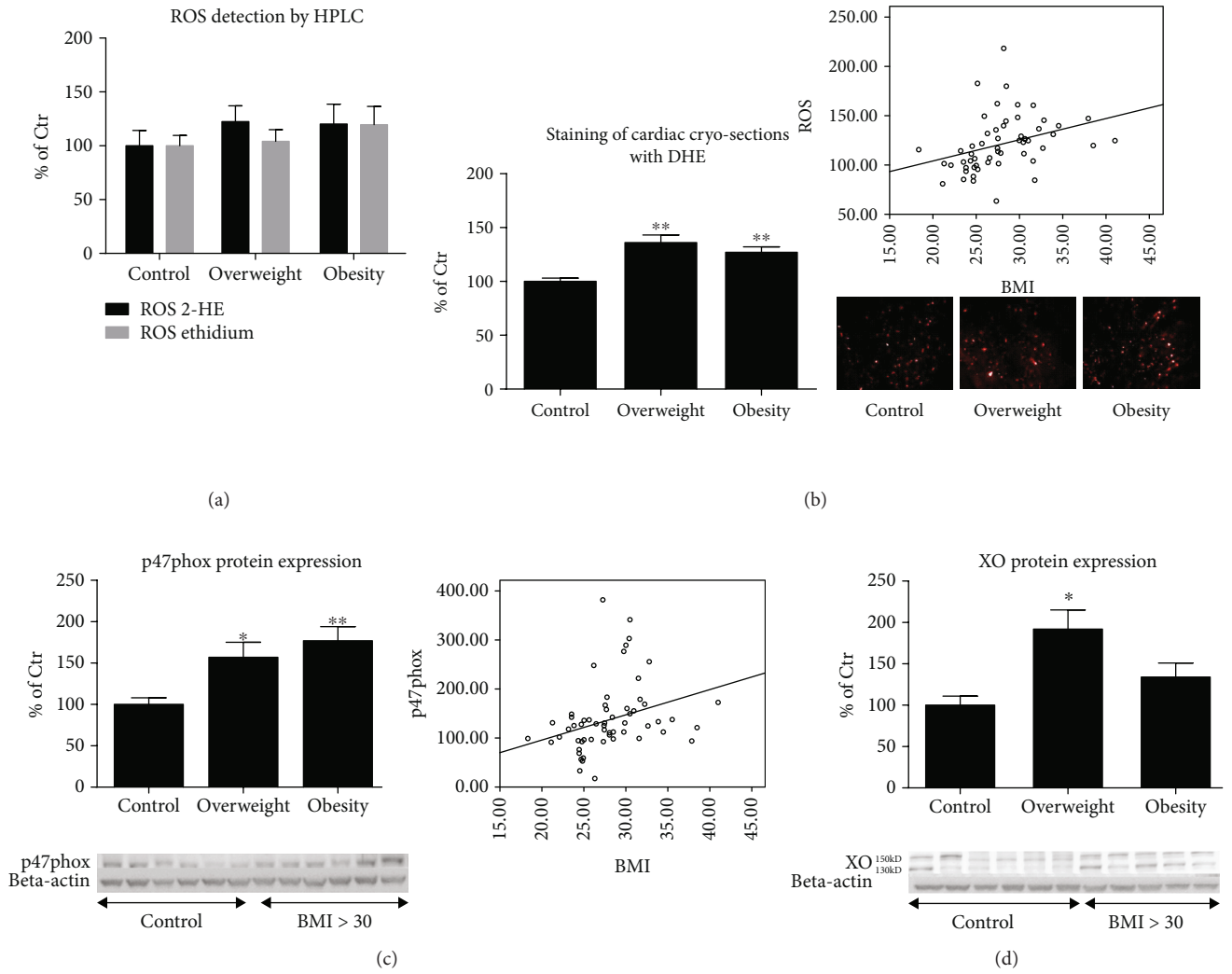

Figure 1: Oxidative stress parameters in cardiac tissue. (a) Determination of ROS formation in isolated cardiac mitochondria by HPLC-based quantification of 2-hydroxyethidium (2-HE) and ethidium. The values are shown as percentage of control (normal BMI). (b) Determination of ROS formation in cardiac tissue by oxidative dihydroethidium (DHE, 1 μM) fluorescence microtopography in cryosections. Representative DHE-stained images are shown besides the densitometric quantification. The correlation between cardiac oxidative stress and the patient's BMI is shown along the densitometric quantification ($R^2 = 0.112$, $p = 0.014$). (c) Expression of the cytosolic/regulatory p47phox subunit of Nox2 isoform in cardiac tissue was determined by western blot analysis. Original blots are shown below the densitometric quantification. The signal of p47phox was normalized to the loading control—beta-actin. The correlation between BMI and the expression of p47phox is shown along the densitometric quantification ($R^2 = 0.106$, $p = 0.018$). (d) Determination of xanthine oxidase (XO) expression in cardiac tissue was performed by western blot analysis. Original blots are shown below the densitometric quantification. The signal of XO was normalized to the loading control—beta-actin. Control: BMI < 25 kg/m^2; overweight: BMI 25–29 kg/m^2; obese: BMI > 30 kg/m^2. All data are expressed as mean ± SEM from $n = 61$ (a, b, c, d) independent measurements/patients. $^*p < 0.05$ vs. Ctr. group; $^{**}p < 0.001$ vs. Ctr. group.

"recycling" of BH_2 to BH_4 by dihydrofolate reductase (DHFR) [36]. Although no significant differences were observed among the three groups regarding the expression of GCH-1 (data not shown), the expression of DHFR decreased with increasing BMI by 26% ($p = 0.018$) in the overweight group and by 37% ($p = 0.004$) in the obese group (Figure 2(b)). This inverse correlation was supported by linear correlation analysis between DHFR expression and BMI levels ($R^2 = 0.079$, $p = 0.023$) (Figure 2(b)), supporting the hypothesis of reduced BH_4 levels causing eNOS dysfunction in cardiac tissue of obese individuals.

3.3. Impact of Body Weight on the Cardiac Antioxidant Defense System. As proposed above, increased oxidative stress may be a consequence of either increased ROS formation or impaired ROS detoxification. Although both mitochondrial (Mn-SOD, SOD2) and cytoplasmic (Cu,Zn-SOD, SOD1) superoxide dismutases represent important antioxidant enzymes, genetic deficiency of only the mitochondrial isoform is lethal. Importantly, administration of an encapsulated cytoplasmic isoform conferred protection against cardiac ischemia-reperfusion injury [43, 44]. Here, no differences in Mn-SOD expression were identified among

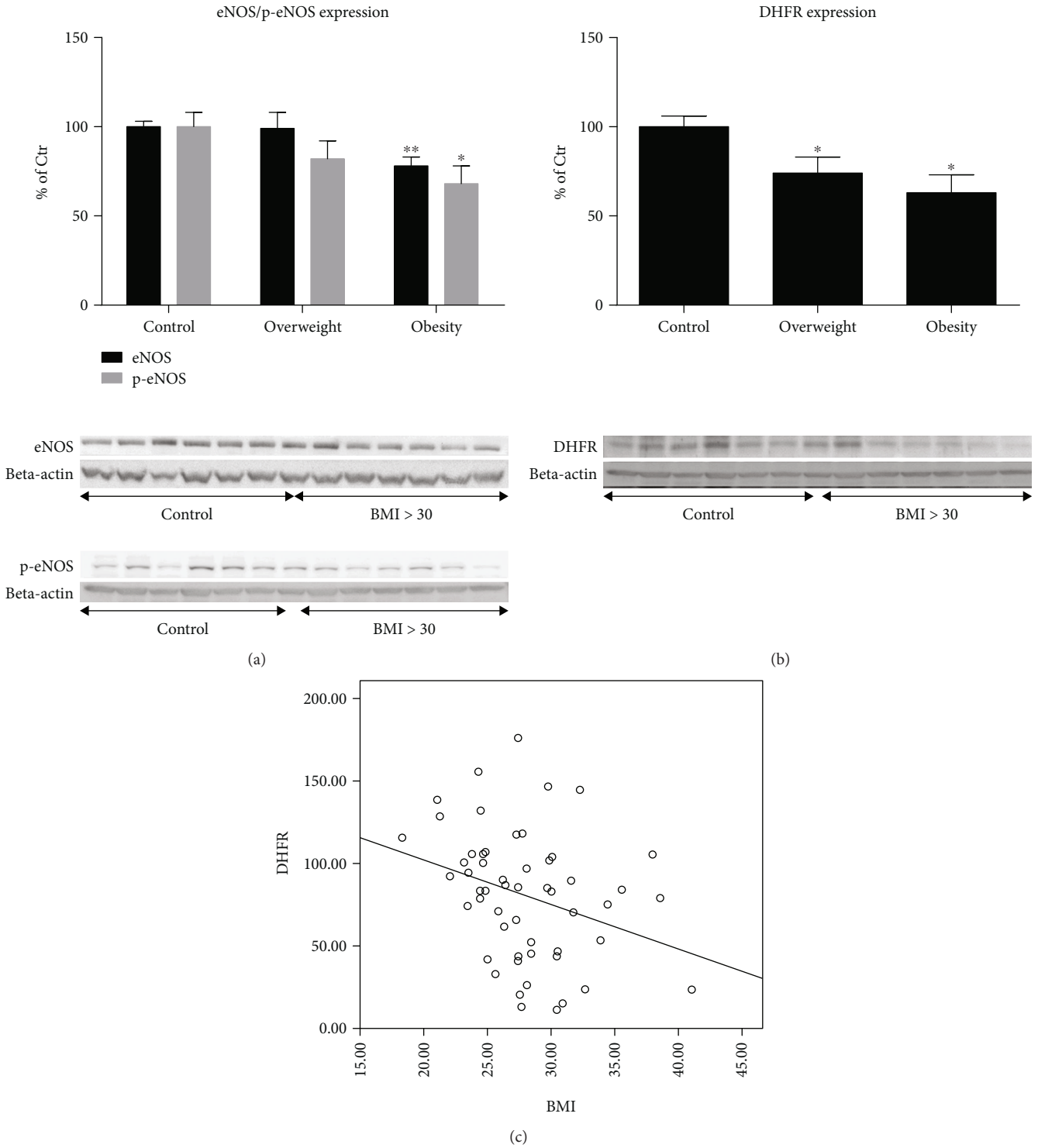

Figure 2: Expression of regulatory proteins of the vascular tone in cardiac tissue. (a) Determination of the expression of endothelial NO synthase (eNOS) and its activated form, pSer1177-eNOS, by western blot analysis. The values are shown as percentage of control (normal BMI). Original blots are shown below the densitometric quantification. The signals of eNOS/pSer1177-eNOS were normalized to the loading control—beta-actin. (b) Expression of dihydrofolate reductase (DHFR) was measured by western blot analysis. Original blots are shown below the densitometric quantification. The signal of DHFR was normalized to the loading control—beta-actin. (c) The correlation between the BMI and the expression of DHFR is shown along the densitometric quantification ($R^2 = 0.079$, $p = 0.023$). Control: BMI < 25 kg/m^2; overweight: BMI 25–29 kg/m^2; obese: BMI > 30 kg/m^2. All data are expressed as mean ± SEM from $n = 61$ (a, b, c) independent measurements/patients. $^*p < 0.05$ vs. Ctr. group; $^{**}p < 0.001$ vs. Ctr. group.

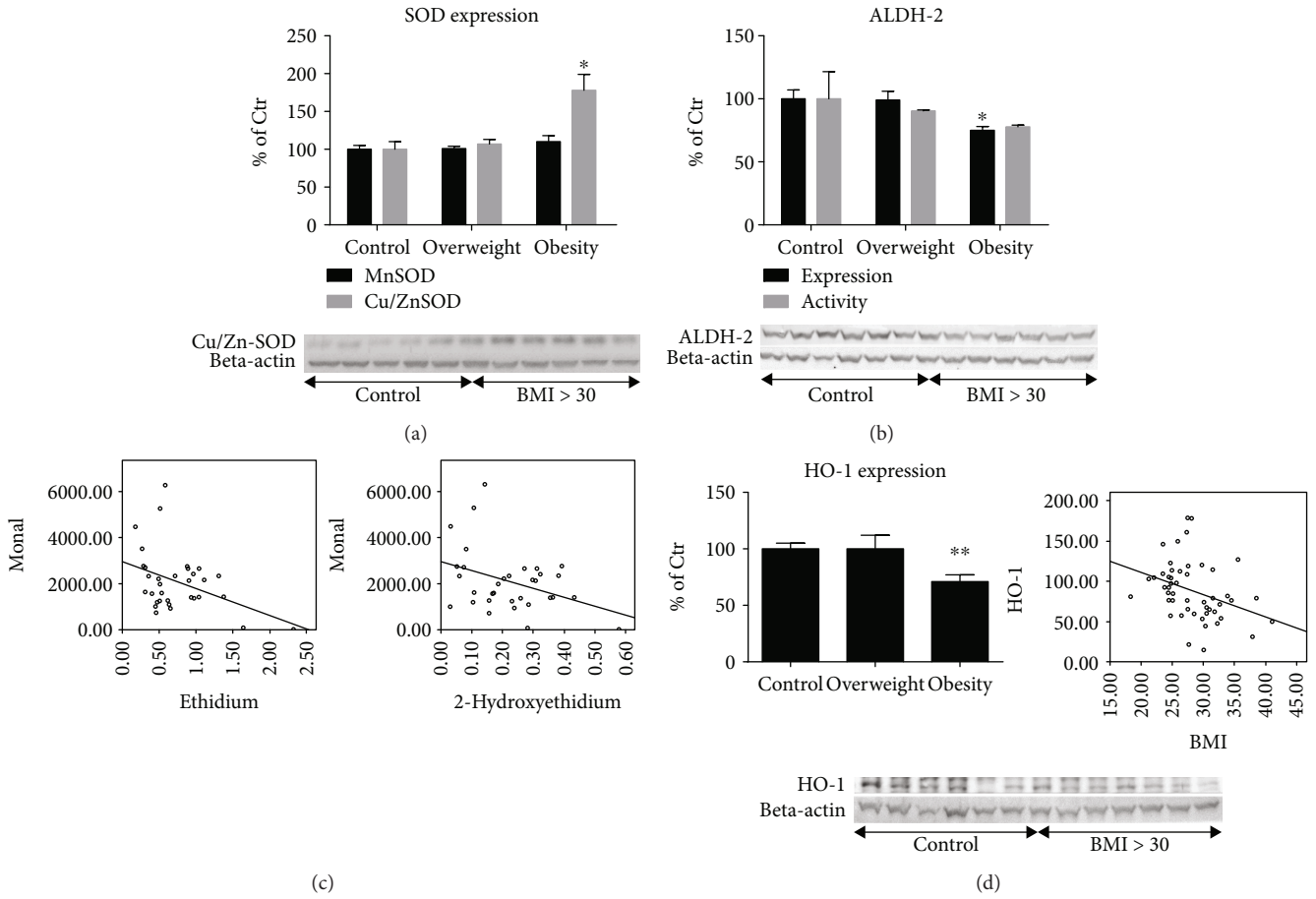

Figure 3: Expression of antioxidant proteins in cardiac tissue. (a) Expression of mitochondrial superoxide dismutase (Mn-SOD) and the cytosolic isoform (Cu,Zn-SOD) was determined by western blot analysis. The values are shown as percentage of control (normal BMI). Original blots are shown below the densitometric quantification. The signals of the SODs were normalized to the loading control—beta-actin. (b) Expression of the mitochondrial aldehyde dehydrogenase (ALDH-2) by western blot analysis. Original blots are shown below the densitometric quantification. The signal of the ALDH-2 was normalized to the loading control—beta-actin. ALDH-2 activity was determined by Monal-62 as a substrate and HPLC-based quantification. (c) Correlations between cardiac oxidative stress (2-HE and ethidium) and ALDH-2 activity (Monal-62) are shown. Ethidium ($R^2 = 0.130$, $p = 0.022$); 2-HE ($R^2 = 0.111$, $p = 0.033$). (d) Expression of heme oxygenase-1 (HO-1) by western blot analysis. Original blots are shown below the densitometric quantification. The signal of HO-1 was normalized to the loading control—beta-actin. The correlation between BMI and HO-1 is shown ($R^2 = 0.101$, $p = 0.014$). Control: BMI < 25 kg/m^2; overweight: BMI 25–29 kg/m^2; obese: BMI > 30 kg/m^2. All data are expressed as mean ± SEM from $n = 61$ (a), 61 (expression)/33 (activity) (b), and 61 (c) independent measurements/patients. $^*p < 0.05$ vs. Ctr. group; $^{**}p < 0.001$ vs. Ctr. group.

groups, but a significant increase in Cu,Zn-SOD levels by 78% ($p = 0.002$) was observed in the obese group, whereas overweight individuals showed no difference (Figure 3(a)). These observations were consistent with an at least transitory compensatory response to increased superoxide production.

The mitochondrial ALDH-2 has been reported as a major cardioprotective enzyme. Its genetic deficiency increased whereas overexpression decreased infarct size and ischemic damage in animal models of myocardial infarction [45, 46]. Expression levels of ALDH-2 decreased in a BMI-dependent manner showing a significant attenuation in the obese group by 25% ($p = 0.002$) (Figure 3(b)). In a subgroup analysis, we could show that mitochondrial ALDH-2 activity decreases in a superoxide formation rate-dependent fashion resulting in a linear correlation between ALDH-2 activity and cardiac superoxide formation ($n = 33$; $R^2 = 0.111$, $p = 0.033$) (Figure 3(c), right graph).

Heme oxygenases are antioxidant enzymatic systems that produce the free radical scavengers biliverdin and bilirubin as well as the carbon monoxide that acts as an antiatherogenic, antiaggregatory, and vasodilatory agent and the iron-storing protein ferritin, which is responsible for transmitting the stress response. Notably, the inducible isoform—heme oxygenase-1 (HO-1)—confers high cardioprotective effects [47–50]. The expression of HO-1 was significantly decreased in obese patients by 29% ($p < 0.001$) as compared to the control group with normal BMI and showed an inverse correlation with BMI (Figure 3(d)).

3.4. Impact of Body Weight on Cardiac Inflammation. VCAM-1 is an important vascular (mainly endothelial)

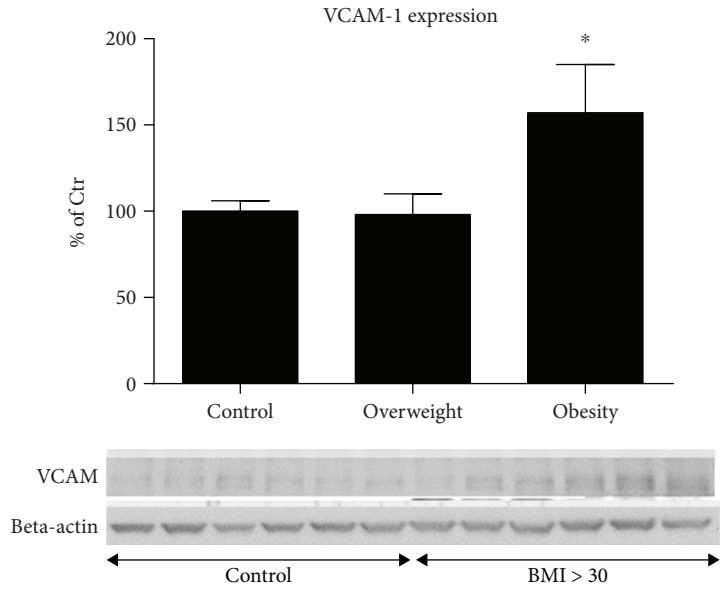

Figure 4: Marker of inflammation. Expression of vascular cell adhesion molecule-1 (VCAM-1) was determined by western blot analysis. The values are shown as percentage of control (normal BMI). Original blots are shown below the densitometric quantification. The signal of VCAM-1 was normalized to the loading control—beta-actin. Control: BMI < 25 kg/m^2; overweight: BMI 25–29 kg/m^2; obese: BMI > 30 kg/m^2. All data are expressed as mean ± SEM from $n = 61$ independent measurements/patients. $^*p < 0.05$ vs. Ctr. group

adhesion protein, which initiates the first step in the adhesion of circulating immune cells, followed by infiltration of these immune cells into adjacent tissues leading to the progression of atherosclerosis and unspecific tissue damage [51]. However, adhesion and infiltration of leukocytes are also essential for the removal of infiltrating pathogens and cell debris, thereby leading to the resolution of inflammation. VCAM-1 expression can be triggered by increased oxidative stress [52, 53] but is also controlled by other cytokines. VCAM-1 expression was increased in obese patients by 63% ($p = 0.049$), whereas no difference was seen in overweight patients (Figure 4). In accordance with higher cardiac tissue VCAM-1 expression in obese patients, the markers of the proinflammatory state, sVCAM-1 and RANTES, showed an elevated trend with increasing BMI (supplemental Figure S1).

4. Discussion

In this study of 61 overweight CAD patients, we show an increased myocardial burden of oxidative stress and decreased expression of antioxidant and cardioprotective enzymes as well as augmented markers of inflammation. These changes suggest a role of elevated BMI in the progression of heart disease mediated by oxidative stress.

4.1. Oxidative Stress Promotes Pathophysiological Pathways. Reactive oxygen species (ROS) are known to cause cardiac damage at different levels: first, apoptosis can be induced by oxidative damage and altered mitochondrial permeability in a redox-dependent manner [54]. Second, in the setting of atherosclerosis, ROS may lead to plaque erosion and thrombosis [55, 56]. Third, redox-sensitive enzymes are oxidized by ROS and functionally altered [57]. In this study, we provide evidence for ROS-dependent regulation of eNOS, XO, and ALDH-2 in the myocardium of patients with increased BMI: endothelial NO synthase (eNOS) activity is altered by redox-dependent changes in BH_4 levels [58], xanthine oxidoreductase expression by redox-dependent conversion of the xanthine dehydrogenase form to the oxidase form (reviewed in [59]), and finally ALDH-2 activity/expression by redox-dependent cysteine sulfhydryl group oxidation and altered protein degradation (reviewed in [60, 61]). Many different mechanisms (redox switches) besides BH_4 depletion were described for oxidant-driven uncoupling of eNOS, such as S-glutathionylation in the reductase domain, adverse phosphorylation by redox-sensitive kinases, disruption of the zinc-sulfur complex in the dimer binding region, and finally dysregulated formation/degradation of the eNOS inhibitor asymmetric dimethyl arginine (ADMA) (reviewed in [59]). Fourth, the vasodilator and signal molecule nitric oxide (NO) reacts with its biological and chemical antagonist superoxide to form peroxynitrite ($ONOO^-$) [62], a highly potent oxidant, also promoting the nitration and inactivation of prostacyclin synthase [63].

The decreased NO bioavailability leads to a plethora of cardiovascular complications such as increased platelet aggregation and activation, increased vascular permeability and inflammation, augmented leukocyte adhesion and infiltration into the vascular wall, progression of atherosclerosis, and plaque instability [56, 64–70]. Likewise, excess formation of peroxynitrite eliminates another important vasodilator—prostacyclin (PGI_2) [71]. Under physiological conditions, vascular tone is regulated by endothelial cells through the production of NO and PGI_2, decreasing intracellular calcium concentration in smooth muscle cells. NO and prostacyclin act synergistically. With increasing oxidative stress, however, prostacyclin synthase is nitrated by peroxynitrite at an essential tyrosine residue and thus inhibited [72], cyclooxygenase

is activated by higher peroxide tone [73], and both mechanisms lead to the accumulation of the substrate PGH_2, activation of the PGH_2/thromboxane receptor, and subsequent vasoconstriction and platelet aggregation and adhesion. This was observed in diabetes-associated atherosclerosis and coronary reperfusion damage after ischemia [74, 75]. Peroxynitrite can cause multiple oxidative damage and trigger pathophysiological events such as lipid and protein oxidation [76], endothelial dysfunction, and vascular inflammation by promoting oxidation of LDL (low-density lipoprotein) to oxLDL [56, 77].

4.2. Sources of Oxidative Stress in Cardiovascular Disease. As sources of oxidative stress, we could identify the phagocytic NADPH oxidase isoform (Nox2 and to a lesser extent Nox1) with its regulatory subunit p47phox, XO, and potentially dysregulated endothelial NO synthase (eNOS) (Figures 1 and 2). It has already been described that the XO is significantly elevated in several conditions such as in limb ischemia [78], after major surgery [79], or in CAD [80]. In the present study, being overweight was found to be a strong trigger of increased XO expression (Figure 1(d)). Accordingly, the inhibition of XO activity improved numerous parameters that are associated with cardiac disease conditions, but this effect appears to be limited to hyperuricemic patients [81]. The role of XO in various forms of ischemic and other types of tissue and vascular injury, inflammatory diseases, and chronic heart failure seems certain, whereas current clinical trials for the therapeutic effect of XO inhibition yielded rather heterogeneous results, as reported for allopurinol, which was investigated in a decisive manner by Pacher et al. [82].

NADPH oxidases are a major source of oxidative stress in the cardiovascular system and contribute, for instance, to the pathogenesis of hypertension, atherosclerosis, myocardial infarction, myocardial hypertrophy, vascular restenosis, and arrhythmia [18, 56, 83–87]. The present study showed that the expression of p47phox increased in overweight patients by approximately 60% and in obese patients by approximately 80% (Figure 1(c)). The increase in the p47phox is consistent with the increase in global cardiac oxidative stress (Figure 1(b)), whereas specific cardiac mitochondrial oxidative stress showed a rather moderate trend of increase in dependence of BMI (Figure 1(a)). The p47phox subunit is the major Nox2 (gp91phox) regulatory subunit. Its phosphorylation is mandatory for Nox2 activation [88]. Nox2-knockout mice are protected from angiotensin II-induced hypertension and endothelial dysfunction [89], from myocardial infarction-induced damage of heart tissue [90], and from cardiac hypertrophy, cardiac fibrosis, and cardiac insufficiency [91]. Silver et al. showed an increase in p47phox in endothelial cells of obese patients with BMI $> 25\,kg/m^2$ and the active form of endothelial NO synthase—p-eNOS (Ser1177) [92]. In line with our findings, the Cu,Zn-SOD expression was most likely increased as a compensatory response. The authors hypothesized increased oxidative stress in obese patients. In addition, in the human myocardium, increased Nox2 expression was found in areas of myocardial infarction [93]. Therapeutic approaches to target Nox2 or its subunits are already present [56]. A key role of Nox2 in ischemic heart disease is supported by the observation that p47phox overexpression is associated with worse outcome in myocardial infarction [94].

There was a very significant decrease in eNOS expression in obese patients compared to normal-weight control subjects, by approximately 25%. Of interest, we found no difference in the group of overweight patients (Figure 2). This result was associated with a decrease in phosphorylation at serine residue 1177 (Ser1177) (activated eNOS) of about 20% and 30% in overweight and obese patients, respectively. These results suggest both a deficiency of eNOS and a decreased/dysregulated eNOS activity (p-eNOS Ser1177) in the cardiac tissue of these patients, which may lead to not only a loss of the protective properties but also an uncoupling of eNOS and subsequent superoxide production. One possible reason for the pathogenesis of cardiomyopathy in metabolic syndrome may be based on the deficiency of functional eNOS, which has already been demonstrated in animal models [95, 96]. The excessive formation of peroxynitrite and the overall increased oxidative stress in cardiac tissue of overweight and obese patients have been demonstrated in this work, which can be interpreted as a transformation of the protective physiological properties of NO to pathophysiological properties mediated by peroxynitrite [36, 97, 98]. Among other pathways, oxidative depletion of BH_4 was demonstrated as an important trigger of eNOS dysfunction. Of note, DHFR is responsible for "recycling" BH_2 to BH_4 [99, 100]. Our results indicate, for the first time to our knowledge, a deficiency of DHFR in the cardiac tissue of patients with increasing BMI (Figure 2(c)) and suggest an impaired cardiac BH_4 metabolism in obesity. In a previous study, Denk et al. demonstrated decreased contractility of the cardiac muscle of obese patients [12], which may be explained by the impaired NO system (Figure 2), a hypothesis that is also supported by studies in animal models [101, 102].

4.3. Impact of BMI on Cardiac Antioxidant Defense Systems. An increase in the aforementioned prooxidative processes may be attributed to not only activated sources of ROS formation but also impaired antioxidant defense systems such as SOD, ALDH-2, and inducible heme oxygenase (HO-1). Although no change was observed in mitochondrial Mn-SOD (SOD-2) expression, the cytoplasmic Cu,Zn-SOD (SOD-1) was increased in obese patients (Figure 3(a)), which most likely reflects a compensatory mechanism [103, 104] in a more profound disease state. Upregulation of SOD-1 protects against endothelial dysfunction and ischemic damage [24, 105]. One of the main findings of this work is the BMI-dependent decreased expression and ROS-dependent inhibition of ALDH-2 activity in the cardiac tissue of obese individuals (Figure 3(b)). Several animal and human studies have shown that ALDH-2 is regulated/inhibited in conditions of increased oxidative stress [45, 106]. In the present study, to our best knowledge, we show for the first time that the level of ALDH-2 inhibition is directly correlated with the superoxide formation rate in the human myocardium (Figure 3(c))

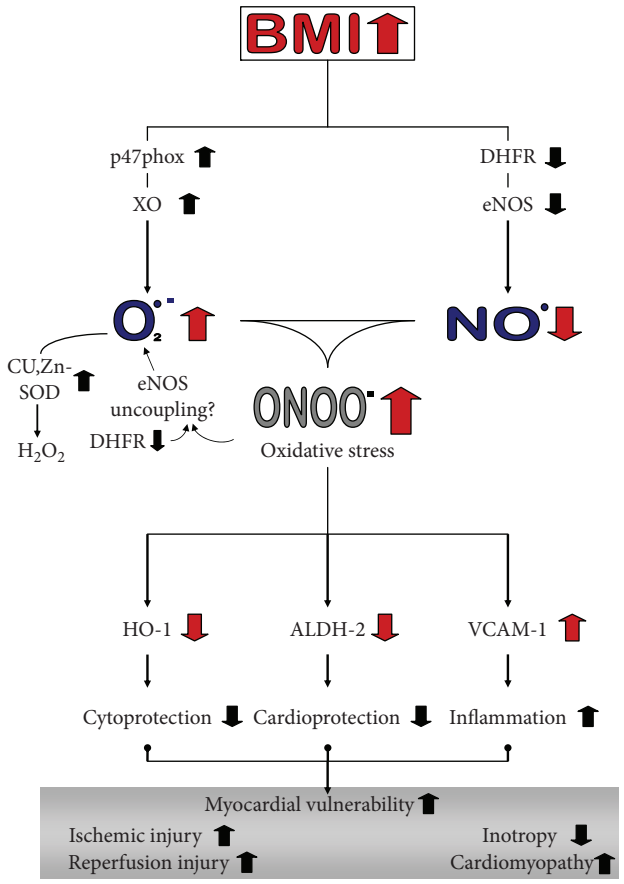

Figure 5: Schematic summarizing the major findings and providing a hypothesis on the major pathways that lead to cardiac and vascular dysfunction in obese patients.

and that its expression is negatively influenced by obesity (Figure 3(b)). In recent publications, a larger ischemic heart damage and further reduced inotropy were demonstrated in animals with reduced ALDH-2 expression [94, 99, 100]. In addition, we demonstrated that eNOS expression was reduced, which also contributes to reduced inotropy [107, 108]. Taken together, a lower antioxidant potency, increased myocardial vulnerability, especially to aldehyde stress, and a lower overall cardioprotection by the ALDH-2 enzyme in obese patients must be postulated [109, 110]. The lower expression of HO-1 in the cardiac tissue of obese patients is a further indicator for reduced antioxidant protection in the myocardium of obese patients with CAD (Figure 3(d)). A possible mechanism may be a lack of induction of HO-1 by NO or adiponectin.

4.4. Impact of BMI on the Cardiac Expression of VCAM-1 Adhesion Molecule as a Marker of Local Inflammation. The VCAM-1 protein is an endothelial adhesion molecule, which triggers adhesion of lymphocytes, monocytes, eosinophils, and basophils to the endothelial cell layer. Its expression is triggered by cytokines, and it is considered a marker of inflammation. It is assumed that VCAM-1 plays a role in the pathogenesis of cardiovascular disease, especially atherosclerosis and rheumatoid arthritis [111]. Western blotting analysis revealed an increase in VCAM-1 expression by 63% ($p = 0.049$) in the group of obese patients; however, there were no differences seen between overweight and control group patients. These observations suggest local inflammation in obesity, supported by studies that showed a positive correlation of visceral fat content with higher levels of procoagulant plasminogen activator inhibitor 1 (PAI-1) that links adipokines to "low-grade inflammation."

5. Conclusion

In summary, the myocardium of patients with CAD with increasing BMI shows increased oxidative stress and enzymatic alterations suggestive of inadequate antioxidant defense (Figure 5). We therefore suggest that the myocardium of overweight patients is more susceptible to damage caused by ischemia and reperfusion during cardiac surgery or acute coronary syndromes and to the development of cardiomyopathies.

Data Availability

Since all the data used for this article are deposited in the archive of the IZKS of the University Medical Center Mainz together with the patient personal information, a public access cannot be granted. The involved study physicians have access to the data via SPSS within the campus network and can provide raw data without patients' personal information on reasonable request.

Disclosure

The work contains parts of the thesis of Yves Gramlich. Yves Gramlich and Andreas Daiber are considered the first authors.

Conflicts of Interest

The authors declare that they have no conflicts of interest.

Authors' Contributions

Yves Gramlich and Andreas Daiber contributed equally to this study.

Acknowledgments

This study was supported by the Stiftung Mainzer Herz, the Robert Müller Stiftung, and the Center for Translational Vascular Biology (CTVB). TM is the PI of the German Center for Cardiovascular Research (DZHK) at the partner site Rhine-Main in Mainz, Germany.

Supplementary Materials

Table S1: patient inclusion and exclusion criteria. Table S2: patient characteristics. Table S3: details on used antibodies. Figure S1: ELISA for sVCAM-1 and RANTES. *(Supplementary Materials)*

References

[1] Zentral Blatt des Bundes Statistisches Bundesamt, "Todesursachenstatistik (Stand 31.07.2012)," Ed., Statistisches Bundesamt, Zweigstelle Bonn [destatis (BN)], 2011.

[2] K. F. Adams, A. Schatzkin, T. B. Harris et al., "Overweight, obesity, and mortality in a large prospective cohort of persons 50 to 71 years old," *The New England Journal of Medicine*, vol. 355, no. 8, pp. 763–778, 2006.

[3] P. T. James, N. Rigby, R. Leach, and International Obesity Task Force, "The obesity epidemic, metabolic syndrome and future prevention strategies," *European Journal of Cardiovascular Prevention and Rehabilitation*, vol. 11, no. 1, pp. 3–8, 2004.

[4] A. Agatston, "Why America is fatter and sicker than ever," *Circulation*, vol. 126, no. 1, pp. e3–e5, 2012.

[5] S. Kenchaiah, J. C. Evans, D. Levy et al., "Obesity and the risk of heart failure," *The New England Journal of Medicine*, vol. 347, no. 5, pp. 305–313, 2002.

[6] M. A. Alpert, C. R. Lambert, B. E. Terry et al., "Influence of left ventricular mass on left ventricular diastolic filling in normotensive morbid obesity," *American Heart Journal*, vol. 130, no. 5, pp. 1068–1073, 1995.

[7] M. A. Alpert, C. R. Lambert, B. E. Terry et al., "Interrelationship of left ventricular mass, systolic function and diastolic filling in normotensive morbidly obese patients," *International Journal of Obesity and Related Metabolic Disorders*, vol. 19, no. 8, pp. 550–557, 1995.

[8] M. A. Alpert, C. R. Lambert, B. E. Terry et al., "Effect of weight loss on left ventricular diastolic filling in morbid obesity," *The American Journal of Cardiology*, vol. 76, no. 16, pp. 1198–1201, 1995.

[9] C. Y. Wong, T. O'Moore-Sullivan, R. Leano, N. Byrne, E. Beller, and T. H. Marwick, "Alterations of left ventricular myocardial characteristics associated with obesity," *Circulation*, vol. 110, no. 19, pp. 3081–3087, 2004.

[10] G. F. Mureddu, G. de Simone, R. Greco, G. F. Rosato, and F. Contaldo, "Left ventricular filling in arterial hypertension. Influence of obesity and hemodynamic and structural confounders," *Hypertension*, vol. 29, no. 2, pp. 544–550, 1997.

[11] M. Chinali, G. de Simone, M. J. Roman et al., "Impact of obesity on cardiac geometry and function in a population of adolescents: the Strong Heart Study," *Journal of the American College of Cardiology*, vol. 47, no. 11, pp. 2267–2273, 2006.

[12] K. Denk, J. Albers, N. Kayhan et al., "Evidence for a negative inotropic effect of obesity in human myocardium?," *European Journal of Cardio-Thoracic Surgery*, vol. 36, no. 2, pp. 300–305, 2009.

[13] E. E. Calle, M. J. Thun, J. M. Petrelli, C. Rodriguez, and C. W. Heath Jr., "Body-mass index and mortality in a prospective cohort of U.S. adults," *The New England Journal of Medicine*, vol. 341, no. 15, pp. 1097–1105, 1999.

[14] A. S. Greenstein, K. Khavandi, S. B. Withers et al., "Local inflammation and hypoxia abolish the protective anticontractile properties of perivascular fat in obese patients," *Circulation*, vol. 119, no. 12, pp. 1661–1670, 2009.

[15] F. Perticone, R. Ceravolo, M. Candigliota et al., "Obesity and body fat distribution induce endothelial dysfunction by oxidative stress: protective effect of vitamin C," *Diabetes*, vol. 50, no. 1, pp. 159–165, 2001.

[16] S. B. Withers, C. Agabiti-Rosei, D. M. Livingstone et al., "Macrophage activation is responsible for loss of anticontractile function in inflamed perivascular fat," *Arteriosclerosis, Thrombosis, and Vascular Biology*, vol. 31, no. 4, pp. 908–913, 2011.

[17] C. Marchesi, T. Ebrahimian, O. Angulo, P. Paradis, and E. L. Schiffrin, "Endothelial nitric oxide synthase uncoupling and perivascular adipose oxidative stress and inflammation contribute to vascular dysfunction in a rodent model of metabolic syndrome," *Hypertension*, vol. 54, no. 6, pp. 1384–1392, 2009.

[18] D. Sorescu, D. Weiss, B. Lassegue et al., "Superoxide production and expression of Nox family proteins in human atherosclerosis," *Circulation*, vol. 105, no. 12, pp. 1429–1435, 2002.

[19] A. Daiber, M. Oelze, M. Coldewey et al., "Oxidative stress and mitochondrial aldehyde dehydrogenase activity: a comparison of pentaerythritol tetranitrate with other organic nitrates," *Molecular Pharmacology*, vol. 66, no. 6, pp. 1372–1382, 2004.

[20] H. Zhao, J. Joseph, H. M. Fales et al., "Detection and characterization of the product of hydroethidine and intracellular superoxide by HPLC and limitations of fluorescence," *Proceedings of the National Academy of Sciences of the United States of America*, vol. 102, no. 16, pp. 5727–5732, 2005.

[21] P. Wenzel, H. Mollnau, M. Oelze et al., "First evidence for a crosstalk between mitochondrial and NADPH oxidase-derived reactive oxygen species in nitroglycerin-triggered vascular dysfunction," *Antioxidants & Redox Signaling*, vol. 10, no. 8, pp. 1435–1448, 2008.

[22] S. Kroller-Schon, S. Steven, S. Kossmann et al., "Molecular mechanisms of the crosstalk between mitochondria and NADPH oxidase through reactive oxygen species-studies in white blood cells and in animal models," *Antioxidants & Redox Signaling*, vol. 20, no. 2, pp. 247–266, 2014.

[23] M. Beretta, A. Sottler, K. Schmidt, B. Mayer, and A. C. F. Gorren, "Partially irreversible inactivation of mitochondrial aldehyde dehydrogenase by nitroglycerin," *The Journal of Biological Chemistry*, vol. 283, no. 45, pp. 30735–30744, 2008.

[24] M. Oelze, M. Knorr, R. Schell et al., "Regulation of human mitochondrial aldehyde dehydrogenase (ALDH-2) activity by electrophiles *in vitro*," *The Journal of Biological Chemistry*, vol. 286, no. 11, pp. 8893–8900, 2011.

[25] P. Wenzel, E. Schulz, M. Oelze et al., "AT1-receptor blockade by telmisartan upregulates GTP-cyclohydrolase I and protects eNOS in diabetic rats," *Free Radical Biology & Medicine*, vol. 45, no. 5, pp. 619–626, 2008.

[26] M. Oelze, M. Knorr, S. Schuhmacher et al., "Vascular dysfunction in streptozotocin-induced experimental diabetes strictly depends on insulin deficiency," *Journal of Vascular Research*, vol. 48, no. 4, pp. 275–284, 2011.

[27] M. Oelze, A. Daiber, R. P. Brandes et al., "Nebivolol inhibits superoxide formation by NADPH oxidase and endothelial dysfunction in angiotensin II-treated rats," *Hypertension*, vol. 48, no. 4, pp. 677–684, 2006.

[28] P. Wenzel, M. Knorr, S. Kossmann et al., "Lysozyme M-positive monocytes mediate angiotensin II-induced arterial hypertension and vascular dysfunction," *Circulation*, vol. 124, no. 12, pp. 1370–1381, 2011.

[29] D. G. Altman, "Statistics in medical journals: developments in the 1980s," *Statistics in Medicine*, vol. 10, no. 12, pp. 1897–1913, 1991.

[30] A. Victor, A. Elsasser, G. Hommel, and M. Blettner, "Judging a plethora of p-values: how to contend with the problem of multiple testing – part 10 of a series on evaluation of scientific publications," *Deutsches Ärzteblatt International*, vol. 107, no. 4, pp. 50–56, 2010.

[31] B. Fink, K. Laude, L. McCann, A. Doughan, D. G. Harrison, and S. Dikalov, "Detection of intracellular superoxide formation in endothelial cells and intact tissues using dihydroethidium and an HPLC-based assay," *American Journal of Physiology. Cell Physiology*, vol. 287, no. 4, pp. C895–C902, 2004.

[32] T. Münzel, I. B. Afanas'ev, A. L. Kleschyov, and D. G. Harrison, "Detection of superoxide in vascular tissue," *Arterioscle-rosis, Thrombosis, and Vascular Biology*, vol. 22, no. 11, pp. 1761–1768, 2002.

[33] U. Forstermann, "Janus-faced role of endothelial NO synthase in vascular disease: uncoupling of oxygen reduction from NO synthesis and its pharmacological reversal," *Biological Chemistry*, vol. 387, no. 12, pp. 1521–1533, 2006.

[34] U. Hink, H. Li, H. Mollnau et al., "Mechanisms underlying endothelial dysfunction in diabetes mellitus," *Circulation Research*, vol. 88, no. 2, pp. E14–E22, 2001.

[35] H. Li and U. Forstermann, "The pharmacology of nitric oxide and nitrates," *Pharmazie in Unserer Zeit*, vol. 39, no. 5, pp. 345–350, 2010.

[36] M. J. Crabtree, A. L. Tatham, Y. Al-Wakeel et al., "Quantitative regulation of intracellular endothelial nitric-oxide synthase (eNOS) coupling by both tetrahydrobiopterin-eNOS stoichiometry and biopterin redox status: insights from cells with tet-regulated GTP cyclohydrolase I expression," *The Journal of Biological Chemistry*, vol. 284, no. 2, pp. 1136–1144, 2009.

[37] J. K. Bendall, N. J. Alp, N. Warrick et al., "Stoichiometric relationships between endothelial tetrahydrobiopterin, endothelial NO synthase (eNOS) activity, and eNOS coupling in vivo: insights from transgenic mice with endothelial-targeted GTP cyclohydrolase 1 and eNOS overexpression," *Circulation Research*, vol. 97, no. 9, pp. 864–871, 2005.

[38] S. Milstien and Z. Katusic, "Oxidation of tetrahydrobiopterin by peroxynitrite: implications for vascular endothelial function," *Biochemical and Biophysical Research Communications*, vol. 263, no. 3, pp. 681–684, 1999.

[39] E. Schulz, T. Jansen, P. Wenzel, A. Daiber, and T. Munzel, "Nitric oxide, tetrahydrobiopterin, oxidative stress, and endothelial dysfunction in hypertension," *Antioxidants & Redox Signaling*, vol. 10, no. 6, pp. 1115–1126, 2008.

[40] T. Masano, S. Kawashima, R. Toh et al., "Beneficial effects of exogenous tetrahydrobiopterin on left ventricular remodeling after myocardial infarction in rats: the possible role of oxidative stress caused by uncoupled endothelial nitric oxide synthase," *Circulation Journal*, vol. 72, no. 9, pp. 1512–1519, 2008.

[41] F. Cosentino, D. Hurlimann, C. Delli Gatti et al., "Chronic treatment with tetrahydrobiopterin reverses endothelial dysfunction and oxidative stress in hypercholesterolaemia," *Heart*, vol. 94, no. 4, pp. 487–492, 2008.

[42] T. Heitzer, K. Krohn, S. Albers, and T. Meinertz, "Tetrahydrobiopterin improves endothelium-dependent vasodilation by increasing nitric oxide activity in patients with type II diabetes mellitus," *Diabetologia*, vol. 43, no. 11, pp. 1435–1438, 2000.

[43] Y. Li, T. T. Huang, E. J. Carlson et al., "Dilated cardiomyopathy and neonatal lethality in mutant mice lacking manganese superoxide dismutase," *Nature Genetics*, vol. 11, no. 4, pp. 376–381, 1995.

[44] G. Seshadri, J. C. Sy, M. Brown et al., "The delivery of superoxide dismutase encapsulated in polyketal microparticles to rat myocardium and protection from myocardial ischemia-reperfusion injury," *Biomaterials*, vol. 31, no. 6, pp. 1372–1379, 2010.

[45] C. H. Chen, G. R. Budas, E. N. Churchill, M. H. Disatnik, T. D. Hurley, and D. Mochly-Rosen, "Activation of aldehyde dehydrogenase-2 reduces ischemic damage to the heart," *Science*, vol. 321, no. 5895, pp. 1493–1495, 2008.

[46] H. Ma, R. Guo, L. Yu, Y. Zhang, and J. Ren, "Aldehyde dehydrogenase 2 (ALDH2) rescues myocardial ischaemia/reperfusion injury: role of autophagy paradox and toxic aldehyde," *European Heart Journal*, vol. 32, no. 8, pp. 1025–1038, 2011.

[47] H. J. Duckers, M. Boehm, A. L. True et al., "Heme oxygenase-1 protects against vascular constriction and proliferation," *Nature Medicine*, vol. 7, no. 6, pp. 693–698, 2001.

[48] J. Dulak, J. Deshane, A. Jozkowicz, and A. Agarwal, "Heme oxygenase-1 and carbon monoxide in vascular pathobiology: focus on angiogenesis," *Circulation*, vol. 117, no. 2, pp. 231–241, 2008.

[49] A. L. True, M. Olive, M. Boehm et al., "Heme oxygenase-1 deficiency accelerates formation of arterial thrombosis through oxidative damage to the endothelium, which is rescued by inhaled carbon monoxide," *Circulation Research*, vol. 101, no. 9, pp. 893–901, 2007.

[50] S. F. Yet, R. Tian, M. D. Layne et al., "Cardiac-specific expression of heme oxygenase-1 protects against ischemia and reperfusion injury in transgenic mice," *Circulation Research*, vol. 89, no. 2, pp. 168–173, 2001.

[51] R. Candido, T. J. Allen, M. Lassila et al., "Irbesartan but not amlodipine suppresses diabetes-associated atherosclerosis," *Circulation*, vol. 109, no. 12, pp. 1536–1542, 2004.

[52] E. Lubos, C. E. Mahoney, J. A. Leopold, Y. Y. Zhang, J. Loscalzo, and D. E. Handy, "Glutathione peroxidase-1 modulates lipopolysaccharide-induced adhesion molecule expression in endothelial cells by altering CD14 expression," *The FASEB Journal*, vol. 24, no. 7, pp. 2525–2532, 2010.

[53] M. Oelze, S. Kroller-Schon, S. Steven et al., "Glutathione peroxidase-1 deficiency potentiates dysregulatory modifications of endothelial nitric oxide synthase and vascular dysfunction in aging," *Hypertension*, vol. 63, no. 2, pp. 390–396, 2014.

[54] F. Jiang, Y. Zhang, and G. J. Dusting, "NADPH oxidase-mediated redox signaling: roles in cellular stress response, stress tolerance, and tissue repair," *Pharmacological Reviews*, vol. 63, no. 1, pp. 218–242, 2011.

[55] E. Durand, A. Scoazec, A. Lafont et al., "In vivo induction of endothelial apoptosis leads to vessel thrombosis and endothelial denudation: a clue to the understanding of the mechanisms of thrombotic plaque erosion," *Circulation*, vol. 109, no. 21, pp. 2503–2506, 2004.

[56] J. Streeter, W. Thiel, K. Brieger, and F. J. Miller Jr, "Opportunity Nox: the future of NADPH oxidases as therapeutic targets in cardiovascular disease," *Cardiovascular Therapeutics*, vol. 31, no. 3, pp. 125–137, 2012.

[57] A. Daiber and M. Bachschmid, "Enzyme inhibition by peroxynitrite-mediated tyrosine nitration and thiol oxidation," *Current Enzyme Inhibition*, vol. 3, no. 2, pp. 103–117, 2007.

[58] U. Landmesser, S. Dikalov, S. R. Price et al., "Oxidation of tetrahydrobiopterin leads to uncoupling of endothelial cell nitric oxide synthase in hypertension," *The Journal of Clinical Investigation*, vol. 111, no. 8, pp. 1201–1209, 2003.

[59] E. Schulz, P. Wenzel, T. Munzel, and A. Daiber, "Mitochondrial redox signaling: interaction of mitochondrial reactive oxygen species with other sources of oxidative stress," *Antioxidants & Redox Signaling*, vol. 20, no. 2, pp. 308–324, 2014.

[60] A. Daiber, T. Munzel, and T. Gori, "Organic nitrates and nitrate tolerance—state of the art and future developments," *Advances in Pharmacology*, vol. 60, pp. 177–227, 2010.

[61] T. Munzel, A. Daiber, and T. Gori, "More answers to the still unresolved question of nitrate tolerance," *European Heart Journal*, vol. 34, no. 34, pp. 2666–2673, 2013.

[62] R. Kissner, T. Nauser, P. Bugnon, P. G. Lye, and W. H. Koppenol, "Formation and properties of peroxynitrite as studied by laser flash photolysis, high-pressure stopped-flow technique, and pulse radiolysis," *Chemical Research in Toxicology*, vol. 10, no. 11, pp. 1285–1292, 1997.

[63] M. H. Zou and V. Ullrich, "Peroxynitrite formed by simultaneous generation of nitric oxide and superoxide selectively inhibits bovine aortic prostacyclin synthase," *FEBS Letters*, vol. 382, no. 1-2, pp. 101–104, 1996.

[64] D. R. Riddell and J. S. Owen, "Nitric oxide and platelet aggregation," *Vitamins and Hormones*, vol. 57, pp. 25–48, 1999.

[65] F. Violi, S. Basili, C. Nigro, and P. Pignatelli, "Role of NADPH oxidase in atherosclerosis," *Future Cardiology*, vol. 5, no. 1, pp. 83–92, 2009.

[66] P. Kubes, "Nitric oxide affects microvascular permeability in the intact and inflamed vasculature," *Microcirculation*, vol. 2, no. 3, pp. 235–244, 1995.

[67] J. Hwang, A. Saha, Y. C. Boo et al., "Oscillatory shear stress stimulates endothelial production of O_2^- from $p47^{phox}$-dependent NAD(P)H oxidases, leading to monocyte adhesion," *The Journal of Biological Chemistry*, vol. 278, no. 47, pp. 47291–47298, 2003.

[68] G. P. Sorescu, H. Song, S. L. Tressel et al., "Bone morphogenic protein 4 produced in endothelial cells by oscillatory shear stress induces monocyte adhesion by stimulating reactive oxygen species production from a nox1-based NADPH oxidase," *Circulation Research*, vol. 95, no. 8, pp. 773–779, 2004.

[69] K. M. Channon, "Oxidative stress and coronary plaque stability," *Arteriosclerosis, Thrombosis, and Vascular Biology*, vol. 22, no. 11, pp. 1751-1752, 2002.

[70] E. Schulz, N. Tsilimingas, R. Rinze et al., "Functional and biochemical analysis of endothelial (dys)function and NO/cGMP signaling in human blood vessels with and without nitroglycerin pretreatment," *Circulation*, vol. 105, no. 10, pp. 1170–1175, 2002.

[71] M. Bachschmid, S. Schildknecht, and V. Ullrich, "Redox regulation of vascular prostanoid synthesis by the nitric oxide-superoxide system," *Biochemical and Biophysical Research Communications*, vol. 338, no. 1, pp. 536–542, 2005.

[72] M. Zou, C. Martin, and V. Ullrich, "Tyrosine nitration as a mechanism of selective inactivation of prostacyclin synthase by peroxynitrite," *Biological Chemistry*, vol. 378, no. 7, pp. 707–713, 1997.

[73] S. Schildknecht, M. Bachschmid, and V. Ullrich, "Peroxynitrite provides the peroxide tone for PGHS-2-dependent prostacyclin synthesis in vascular smooth muscle cells," *The FASEB Journal*, vol. 19, no. 9, pp. 1169–1171, 2005.

[74] M. H. Zou and M. Bachschmid, "Hypoxia-reoxygenation triggers coronary vasospasm in isolated bovine coronary arteries via tyrosine nitration of prostacyclin synthase," *The Journal of Experimental Medicine*, vol. 190, no. 1, pp. 135–140, 1999.

[75] M. H. Zou, C. Shi, and R. A. Cohen, "High glucose via peroxynitrite causes tyrosine nitration and inactivation of prostacyclin synthase that is associated with thromboxane/prostaglandin H_2 receptor-mediated apoptosis and adhesion molecule expression in cultured human aortic endothelial cells," *Diabetes*, vol. 51, no. 1, pp. 198–203, 2002.

[76] K. Irani, "Oxidant signaling in vascular cell growth, death, and survival: a review of the roles of reactive oxygen species in smooth muscle and endothelial cell mitogenic and apoptotic signaling," *Circulation Research*, vol. 87, no. 3, pp. 179–183, 2000.

[77] K. Daub, P. Seizer, K. Stellos et al., "Oxidized LDL-activated platelets induce vascular inflammation," *Seminars in Thrombosis and Hemostasis*, vol. 36, no. 2, pp. 146–156, 2010.

[78] S. Tan, S. Gelman, J. K. Wheat, and D. A. Parks, "Circulating xanthine oxidase in human ischemia reperfusion," *Southern Medical Journal*, vol. 88, no. 4, pp. 479–482, 1995.

[79] E. J. Pesonen, N. Linder, K. O. Raivio et al., "Circulating xanthine oxidase and neutrophil activation during human liver transplantation," *Gastroenterology*, vol. 114, no. 5, pp. 1009–1015, 1998.

[80] S. Spiekermann, U. Landmesser, S. Dikalov et al., "Electron spin resonance characterization of vascular xanthine and NAD(P)H oxidase activity in patients with coronary artery disease: relation to endothelium-dependent vasodilation," *Circulation*, vol. 107, no. 10, pp. 1383–1389, 2003.

[81] W. Doehner and U. Landmesser, "Xanthine oxidase and uric acid in cardiovascular disease: clinical impact and therapeutic options," *Seminars in Nephrology*, vol. 31, no. 5, pp. 433–440, 2011.

[82] P. Pacher, A. Nivorozhkin, and C. Szabo, "Therapeutic effects of xanthine oxidase inhibitors: renaissance half a century after the discovery of allopurinol," *Pharmacological Reviews*, vol. 58, no. 1, pp. 87–114, 2006.

[83] S. C. Dudley Jr., N. E. Hoch, L. A. McCann et al., "Atrial fibrillation increases production of superoxide by the left atrium and left atrial appendage: role of the NADPH and xanthine oxidases," *Circulation*, vol. 112, no. 9, pp. 1266–1273, 2005.

[84] K. Szocs, B. Lassegue, D. Sorescu et al., "Upregulation of Nox-based NAD(P)H oxidases in restenosis after carotid injury," *Arteriosclerosis, Thrombosis, and Vascular Biology*, vol. 22, no. 1, pp. 21–27, 2002.

[85] C. Heymes, J. K. Bendall, P. Ratajczak et al., "Increased myocardial NADPH oxidase activity in human heart failure," *Journal of the American College of Cardiology*, vol. 41, no. 12, pp. 2164–2171, 2003.

[86] D. Sorescu and K. K. Griendling, "Reactive oxygen species, mitochondria, and NAD(P)H oxidases in the development and progression of heart failure," *Congestive Heart Failure*, vol. 8, no. 3, pp. 132–140, 2002.

[87] M. Sedeek, R. L. Hebert, C. R. Kennedy, K. D. Burns, and R. M. Touyz, "Molecular mechanisms of hypertension: role of Nox family NADPH oxidases," *Current Opinion in Nephrology and Hypertension*, vol. 18, no. 2, pp. 122–127, 2009.

[88] J. El-Benna, P. M.-C. Dang, and M.-A. Gougerot-Pocidalo, "Priming of the neutrophil NADPH oxidase activation: role of p47phox phosphorylation and NOX2 mobilization to the plasma membrane," *Seminars in Immunopathology*, vol. 30, no. 3, pp. 279–289, 2008.

[89] O. Jung, J. G. Schreiber, H. Geiger, T. Pedrazzini, R. Busse, and R. P. Brandes, "gp91phox-containing NADPH oxidase mediates endothelial dysfunction in renovascular hypertension," *Circulation*, vol. 109, no. 14, pp. 1795–1801, 2004.

[90] C. Doerries, K. Grote, D. Hilfiker-Kleiner et al., "Critical role of the NAD(P)H oxidase subunit p47^{phox} for left ventricular remodeling/dysfunction and survival after myocardial infarction," *Circulation Research*, vol. 100, no. 6, pp. 894–903, 2007.

[91] J. K. Bendall, A. C. Cave, C. Heymes, N. Gall, and A. M. Shah, "Pivotal role of a gp91^{phox}-containing NADPH oxidase in angiotensin II-induced cardiac hypertrophy in mice," *Circulation*, vol. 105, no. 3, pp. 293–296, 2002.

[92] A. E. Silver, S. D. Beske, D. D. Christou et al., "Overweight and obese humans demonstrate increased vascular endothelial NAD(P)H oxidase-p47^{phox} expression and evidence of endothelial oxidative stress," *Circulation*, vol. 115, no. 5, pp. 627–637, 2007.

[93] P. A. Krijnen, C. Meischl, C. E. Hack et al., "Increased Nox2 expression in human cardiomyocytes after acute myocardial infarction," *Journal of Clinical Pathology*, vol. 56, no. 3, pp. 194–199, 2003.

[94] E. Nisoli, E. Clementi, M. O. Carruba, and S. Moncada, "Defective mitochondrial biogenesis: a hallmark of the high cardiovascular risk in the metabolic syndrome?," *Circulation Research*, vol. 100, no. 6, pp. 795–806, 2007.

[95] A. Daiber, D. Frein, D. Namgaladze, and V. Ullrich, "Oxidation and nitrosation in the nitrogen monoxide/superoxide system," *The Journal of Biological Chemistry*, vol. 277, no. 14, pp. 11882–11888, 2002.

[96] A. Daiber and T. Münzel, *Pentaerithyltetrananitrat*, Steinkopff Darmstadt, 2006.

[97] C. Antoniades, C. Shirodaria, M. Crabtree et al., "Altered plasma versus vascular biopterins in human atherosclerosis reveal relationships between endothelial nitric oxide synthase coupling, endothelial function, and inflammation," *Circulation*, vol. 116, no. 24, pp. 2851–2859, 2007.

[98] T. Sugiyama, B. D. Levy, and T. Michel, "Tetrahydrobiopterin recycling, a key determinant of endothelial nitric-oxide synthase-dependent signaling pathways in cultured vascular endothelial cells," *The Journal of Biological Chemistry*, vol. 284, no. 19, pp. 12691–12700, 2009.

[99] E. A. Ashley, C. E. Sears, S. M. Bryant, H. C. Watkins, and B. Casadei, "Cardiac nitric oxide synthase 1 regulates basal and β-adrenergic contractility in murine ventricular myocytes," *Circulation*, vol. 105, no. 25, pp. 3011–3016, 2002.

[100] M. G. V. Petroff, S. H. Kim, S. Pepe et al., "Endogenous nitric oxide mechanisms mediate the stretch dependence of Ca^{2+} release in cardiomyocytes," *Nature Cell Biology*, vol. 3, no. 10, pp. 867–873, 2001.

[101] H. Azumi, N. Inoue, Y. Ohashi et al., "Superoxide generation in directional coronary atherectomy specimens of patients with angina pectoris: important role of NAD(P)H oxidase," *Arteriosclerosis, Thrombosis, and Vascular Biology*, vol. 22, no. 11, pp. 1838–1844, 2002.

[102] S. Kobayashi, N. Inoue, H. Azumi et al., "Expressional changes of the vascular antioxidant system in atherosclerotic coronary arteries," *Journal of Atherosclerosis and Thrombosis*, vol. 9, no. 4, pp. 184–190, 2002.

[103] H. Kamii, I. Kato, H. Kinouchi et al., "Amelioration of vasospasm after subarachnoid hemorrhage in transgenic mice overexpressing CuZn-superoxide dismutase," *Stroke*, vol. 30, no. 4, pp. 867–872, 1999.

[104] J. Q. Liu, I. N. Zelko, and R. J. Folz, "Reoxygenation-induced constriction in murine coronary arteries: the role of endothelial NADPH oxidase (gp91^{phox}) and intracellular superoxide," *Journal of Biological Chemistry*, vol. 279, no. 23, pp. 24493–24497, 2004.

[105] U. Hink, A. Daiber, N. Kayhan et al., "Oxidative inhibition of the mitochondrial aldehyde dehydrogenase promotes nitroglycerin tolerance in human blood vessels," *Journal of the American College of Cardiology*, vol. 50, no. 23, pp. 2226–2232, 2007.

[106] J. Liao, A. Sun, Y. Xie et al., "Aldehyde dehydrogenase-2 deficiency aggravates cardiac dysfunction elicited by endoplasmic reticulum stress induction," *Molecular Medicine*, vol. 18, no. 5, p. 1, 2012.

[107] D. R. Petersen and J. A. Doorn, "Reactions of 4-hydroxynonenal with proteins and cellular targets," *Free Radical Biology & Medicine*, vol. 37, no. 7, pp. 937–945, 2004.

[108] G. R. Budas, M. H. Disatnik, and D. Mochly-Rosen, "Aldehyde dehydrogenase 2 in cardiac protection: a new therapeutic target?," *Trends in Cardiovascular Medicine*, vol. 19, no. 5, pp. 158–164, 2009.

[109] A. L'Abbate, D. Neglia, C. Vecoli et al., "Beneficial effect of heme oxygenase-1 expression on myocardial ischemia-reperfusion involves an increase in adiponectin in mildly diabetic rats," *American Journal of Physiology-Heart and Circulatory Physiology*, vol. 293, no. 6, pp. H3532–H3541, 2007.

[110] M. Li, D. H. Kim, P. L. Tsenovoy et al., "Treatment of obese diabetic mice with a heme oxygenase inducer reduces visceral and subcutaneous adiposity, increases adiponectin levels, and improves insulin sensitivity and glucose tolerance," *Diabetes*, vol. 57, no. 6, pp. 1526–1535, 2008.

[111] P. H. Dessein, B. I. Joffe, and S. Singh, "Biomarkers of endothelial dysfunction, cardiovascular risk factors and atherosclerosis in rheumatoid arthritis," *Arthritis Research & Therapy*, vol. 7, no. 3, pp. R634–R643, 2005.

Hindawi
Oxidative Medicine and Cellular Longevity
Volume 2018, Article ID 5407482, 12 pages
https://doi.org/10.1155/2018/5407482

Research Article

Curcumin Modulates DNA Methyltransferase Functions in a Cellular Model of Diabetic Retinopathy

Andrea Maugeri,[1] Maria Grazia Mazzone,[2] Francesco Giuliano,[2] Manlio Vinciguerra,[3] Guido Basile,[4] Martina Barchitta,[1] and Antonella Agodi[1]

[1]*Department of Medical and Surgical Sciences and Advanced Technologies "GF Ingrassia", University of Catania, Via S. Sofia 87, Catania 95123, Italy*
[2]*Research and Development Department, SIFI SpA, Via Ercole Patti 36, Catania 95025, Italy*
[3]*International Clinical Research Center, St. Anne's University Hospital, Brno, Czech Republic*
[4]*Department of General Surgery and Medical-Surgical Specialties, University of Catania, Via Plebiscito 628, Catania 95124, Italy*

Correspondence should be addressed to Manlio Vinciguerra; manlio.vinciguerra@fnusa.cz and Antonella Agodi; agodia@unict.it

Received 2 April 2018; Accepted 5 June 2018; Published 2 July 2018

Academic Editor: Ewa Stachowska

Hyperglycaemia-induced oxidative stress appears to be involved in the aetiology of diabetic retinopathy (DR), a major public health issue, via altering DNA methylation process. We investigated the effect of hyperglycaemia on retinal DNA methyltransferase (DNMT) expression in diabetic mice, using Gene Expression Omnibus datasets. We also evaluated the effect of curcumin both on high glucose-induced reactive oxygen species (ROS) production and altered DNMT functions, in a cellular model of DR. We observed that three months of hyperglycaemia, in insulin-deficient $Ins2^{Akita}$ mice, decrease DNMT1 and DNMT3a expression levels. In retinal pigment epithelium (RPE) cells, we also demonstrated that high glucose-induced ROS production precedes upregulation of DNMT expression and activity, suggesting that changes in DNMT function could be mediated by oxidative stress via a potential dual effect. The early effect results in decreased DNMT activity, accompanied by the highest ROS production, while long-term oxidative stress increases DNMT activity and DNMT1 expression. Interestingly, treatment with 25 μM curcumin for 6 hours restores ROS production, as well as DNMT functions, altered by the exposure of RPE to acute and chronic high glucose concentration. Our study suggests that curcumin may represent an effective antioxidant compound against DR, via restoring oxidative stress and DNMT functions, though further studies are recommended.

1. Introduction

The growing incidence of diabetes and longer life span in the aging population point towards an increase in patients with diabetic retinopathy (DR), a diabetes-related microvascular complication which represents a major public health issue as one of the leading causes of blindness in elderly adults [1]. Clinically, DR can be classified into nonproliferative and proliferative: the first is characterized by macular oedema, while the second one may manifest as proliferative retinal neovascularization [2]. The incidence of DR appears to be higher in patients suffering from type 1 than in those with type 2 diabetes [3]. However, regardless of the type of diabetes, both hyperglycaemia and hyperglycaemia-induced oxidative stress have been identified as the major contributing factors [4, 5]. Moreover, it has been demonstrated that DR progression continues even if normal glycaemic control is restored, suggesting that the harmful effect depends on both the duration and the severity of hyperglycaemic insult [6]. Oxidative stress has been shown to alter histone modifications and DNA methylation [7], which have been further recognized as potential epigenetic mechanisms involved in the pathophysiology of DR [8–11]. The methylation process of DNA is carried out by DNA methyltransferases (DNMTs), a family comprising 5 members, of which only DNMT1, DNMT3a, and DNMT3b are catalytically active. DNMT1 is

described as the maintenance methyltransferase, while DNMT3A and DNMT3B are de novo methyltransferases [12]. In mammals, methylation almost exclusively occurs at short DNA sequences, termed CpG islands, which typically contain around 5–10 CpGs per 100 bp, and up to 80% of CpG islands is localized in noncoding regions that mainly contribute to the global methylation status [12]. There are different types of repetitive sequences scattered throughout the genome (e.g., satellite repeat, short interspersed nuclear element, and long interspersed nuclear element-1 (LINE-1)). LINE-1 sequences, accounting for ≈18% of human genome, are widely used as a surrogate marker of global DNA methylation [13–16].

The effects of curcumin, a natural phenol from the rhizome of *Curcuma longa*, have been determined in animal models and in vitro systems [17]. Recent literature reports the wound healing properties of curcumin indicating the capability to accelerate the wound healing process [18]. Particularly, the anti-inflammatory and antioxidant potentials of curcumin enhance the healing process quite effectively in diabetic rats [19]. Several lines of evidence have shown that curcumin significantly decreases lipid peroxidation, increases intracellular antioxidant amount, regulates antioxidant enzymes, and scavenges hyperglycaemia-induced ROS production [20, 21]. Particularly, treatment with curcumin reduced ROS production both in retinal pigment epithelium (RPE) cells [22] and in the retina of diabetic rats [23]. However, the relying antioxidant activity of curcumin on epigenetic mechanisms has not been completely elucidated.

The present study investigated the effect of hyperglycaemia and high glucose-induced oxidative stress on retinal DNMT activity and expression, as well as on LINE-1 methylation levels. To achieve this objective, we compared the expression levels of DNMTs in the retina of diabetic and nondiabetic mice, using the Gene Expression Omnibus (GEO) datasets. In RPE cells, we analysed the time-related effect of high glucose condition on ROS production and DNMT activity and expression. Finally, we evaluated whether the antioxidant properties of curcumin may restore high glucose-induced changes of DNMT function in RPE cells.

2. Materials and Methods

2.1. Microarray Data. Microarray datasets were retrieved and downloaded from the Gene Expression Omnibus (GEO) database (http://www.ncbi.nlm.nih.gov/geo) of the National Center for Biotechnology Information (NCBI), using the keyword "diabetic retinopathy." The GSE12610 dataset included expression microarray profiling data derived from the whole retina of adult CD1 streptozotocin- (STZ-) induced diabetic mice (3-week and 5-week) and age-matched controls. Mice with glucose levels above 250 mg/dL were considered diabetic from the date of the last injection. To get adequate amounts of RNA, four retinas (2 animals) for each group were pooled. Total RNA was extracted and processed for being hybridized on the GPL1261 platform of Affymetrix Mouse Genome 430 2.0 Array (Affymetrix Inc., Santa Clara, CA, USA). The GSE19122 dataset compared expression microarray profiling data derived from the whole retina of eight C57BL/6J STZ-induced diabetic mice and nine insulin-deficient $Ins2^{Akita}$ mice after 3 months of hyperglycaemia, with those derived from eight controls. Total RNA was extracted and processed for being hybridized on the GPL6885 platform of Illumina MouseRef-8 v2.0 expression Beadchip (Illumina Inc., San Diego, USA) [24]. The dataset GSE55389 included expression microarray profiling data derived from the whole retina of four 8-week-old db/db diabetic mice and four age-matched lean nondiabetic controls. Total RNA was extracted and processed for being hybridized on the GPL6246 platform of Affymetrix Mouse Gene 1.0 ST Array (Affymetrix Inc., Santa Clara, CA, USA) [25]. Due to skewed distribution, for each dataset, raw data of DNMT1, DNMT3a, and DNMT3b were extracted and signal values from the selected genes were log-transformed and normalized using the MeV free software online. The difference in log-transformed DNMT expression levels between diabetic mice and controls was compared using Student's t-test and reported as the absolute mean difference (MD).

2.2. Cell Culture. The human retinal pigment epithelial cells (ARPE-19) were purchased from the American Type Culture Collection (Manassas, VA) and maintained in Dulbecco's Modified Eagle's medium (DMEM) supplemented with 10% foetal bovine serum (FBS; Gibco BRL), 100 U/mL of penicillin and 100 lg/mL of streptomycin (Gibco BRL). Cells maintained at the following glucose conditions were used:

(i) Cells maintained at 5.5 mM glucose for 3 weeks (normal glucose (NG) condition)

(ii) Cells maintained at 25 mM glucose for 3 weeks (chronic high glucose (HG) condition)

(iii) Cells maintained at 5.5 mM glucose for 3 weeks and then transferred to 25 mM glucose medium for 24 hours (Acute HG condition)

Normal glucose condition (5.5 mM) corresponded to the fasting plasma glucose level of diabetes-free subjects, while high glucose condition (25 mM) reflected 2 h after-meal plasma glucose level in diabetic patients [26–28]. To rule out the potential effect of hyperosmotic stress, cells maintained in 25 mM mannitol medium were used as osmotic control. Cells between 6 and 10 passages were used in all experiments and incubated at 37°C and 5% CO2. The medium was changed every 48 hours. A flow-chart of in vitro experiments was reported in Figure S1.

2.3. Curcumin Treatment. The effect of curcumin on ROS production, DNMT activity and expression, and LINE-1 methylation was evaluated in ARPE-19 cells. In brief, cells were maintained either at 5.5 mM or at 25 mM glucose concentrations or maintained at 5.5 mM glucose and then transferred to 25 mM glucose medium. After 24 hours, cells were exposed to 25 μM curcumin (Sigma Aldrich, St. Louis, MO) for 6 hours, and then processed to further analyses.

2.4. Determination of Cell Viability. To evaluate the effect of curcumin on cell viability, the Thiazolyl blue tetrazolium bromide (MTT) assay was performed. Cells, maintained either in normal or in high glucose conditions, were seeded at a density of 2.0×10^4 cells/well in a 96-well plate. Cells were then exposed to increasing concentrations (1–50 μM) of curcumin for 6 h. To determine the time-dependent effect of curcumin treatment on cell viability, cells were also exposed to 25 μM curcumin for 1 to 24 hours. MTT (1.6 mg/mL) was added to the cells in each well, followed by a further incubation at 37°C for 4 h. After removing the solution, cells were resuspended in 100 μL of dimethyl sulfoxide (DMSO). The optical density was read at 540 nm, and the background was subtracted at 670 nm. Cell viability (%) was reported as (OD of the treated samples/OD of the control) × 100.

2.5. Determination of Reactive Oxygen Species (ROS). The intracellular ROS level was determined using the Abcam cellular ROS detection assay kit (Abcam plc, Cambridge, UK). The redox-sensitive fluoroprobe 2′,7′ –dichlorofluorescin diacetate (DCFDA) is a fluorogenic dye that measures hydroxyl, peroxyl, and other reactive oxygen species (ROS) activity within the cell. After diffusion into the cell, DCFDA is deacetylated by cellular esterases to a nonfluorescent compound, which is later oxidized by ROS into 2′,7′-dichlorofluorescein (DCF). DCF is a highly fluorescent compound which can be detected by fluorescence spectroscopy with maximum excitation and emission spectra of 495 nm and 529 nm, respectively. Briefly, ARPE-19 cells were seeded at a density of 2.0×10^4 cells/well in a dark, clear bottom 96-well microplate. After removing the media, cells were rinsed with 100 μL/well of 1x buffer and stained by adding 100 μL/well of DCFDA solution. Cells were incubated with DCFDA solution for 45 minutes at 37°C in the dark. After removing DCFDA solution, 100 μL/well of 1x buffer was added and fluorescence was immediately measured (Ex/Em = 485/535 nm).

2.6. Nuclear Protein Extraction. Nuclear proteins were extracted from ARPE-19 cells using the Nuclear Extraction Kit (Abcam plc, Cambridge, UK). In brief, cells were grown to 70–80% confluency and removed by trypsinization following standard protocols. Cell pellets (2×10^6 cells) were resuspended in 200 μL of preextraction buffer and incubated on ice for 10 minutes. After centrifugation, nuclear pellet was resuspended in 400 μL of extraction buffer and incubated on ice for 15 minutes, with vortexing every 3 minutes. Finally, the suspension was centrifuged for 10 minutes at 14,000 rpm at 4°C; the supernatant was transferred into a new microcentrifuge vial to measure the protein concentration of the nuclear extract. Nuclear protein quantification was performed by the Qubit fluorometer (Invitrogen) using the Qubit Protein Assay Kit.

2.7. DNMT Activity Quantification. Quantification of DNMT activity was performed using the colorimetric DNMT Activity Quantification Kit (Abcam plc, Cambridge, UK), suitable for measuring total DNMT activity according to the manufacturer's instructions. In brief, 7.5 ng of nuclear extracts was diluted in 50 μL/well of reaction solution. The 96-well plate, including blank and positive control, was covered and incubated at 37°C for 120 min. After removing the reaction solution, each well was washed with 150 μL of wash buffer for three times, and 50 μL/well of the diluted capture antibody was added. The plate was covered with an aluminium foil and incubated at room temperature for 60 min. After removing the capture antibody, each well was rinsed with 150 μL of the wash buffer for three times, and 50 μL/well of the diluted detection antibody was added. The plate was covered with an aluminium foil and incubated at room temperature for 30 min. After the detection antibody was removed, each well was rinsed with 150 μL of the wash buffer for four times, and 50 μL/well of the enhancer solution was added. The plate was covered with an aluminium foil and incubated at room temperature for 30 min. After removing the enhancer solution, each well was rinsed with 150 μL of the wash buffer for five times, and 100 μL/well of the developer solution was added. The plate was covered with an aluminium foil and incubated at room temperature for 10 min, away from direct light. When the positive control turned to medium blue, 100 μL/well of stop solution was added to stop enzyme reaction. Absorbance was read on a microplate reader within 2 to 10 min at 450 nm with an optional reference wavelength of 655 nm. DNMT activity was reported as the percentage of control.

2.8. Quantitative Real-Time Polymerase Chain Reaction (qPCR). Total cellular RNA was extracted using Trizol® Reagent (Invitrogen, Carlsbad, CA, USA), and RNA was reverse transcribed to single-stranded cDNA using the SuperScript III Reverse Transcriptase (Applied Biosystems, Foster City, CA, USA) according to the manufacturer's protocols. mRNA levels were determined by qPCR with TaqMan Gene Expression Assays (Life Technologies, Monza, MB) using the 7300 Real-Time PCR System (Applied Biosystems, Foster City, CA, USA). Specific primers were used to detect DNMT1 (assay number Hs00945875_m1), DNMT3a (Hs01027162_m1), and DNMT3b (Hs00171876_m1). Threshold cycle values in each sample were used to calculate the number of cell equivalents in the test samples. The data were normalized to the values for GAPDH expression (Hs02758991_g1).

2.9. LINE-1 Methylation Analysis. DNA was extracted using the DNeasy Blood and Tissue kit and quantified using the Qubit dsDNA HS (High Sensitivity) Assay Kit according to the manufacturer's protocols. The methylation analysis of the LINE-1 promoter (GeneBank accession number X58075) was investigated by pyrosequencing-based methylation analysis, using the PyroMark Q24 instrument (Qiagen), after DNA bisulfite conversion. Bisulfite treatment of 20 μg of DNA extracted from each sample was completed using the Epitect Bisulfite kit (Qiagen), and the converted DNA was eluted with 20 μL elution buffer. The bisulfite-modified DNA was stored at −80°C until used.

A reaction volume of 25 mL was amplified by polymerase chain reaction (PCR), using the PyroMark PCR Kit (Qiagen).

According to the manufacturer's instructions, each reaction mixture contained 1.5 μL of bisulfite-converted DNA, 12.5 μL of PyroMark PCR Master Mix 2X, containing HotStart Taq DNA Polymerase, 2.5 μL of CoralLoad Concentrate 10X, and 2 μL of the forward primer (5′-TTTTGAGTTAG GTGTGGGATATA-3′) and the reverse-biotinylated primer (5′-biotin-AAAATCAAAAAATTCCCTTTC-3′) (0.2 μM for each) [29, 30]. HotStart PCR cycling conditions were 1 cycle at 95°C for 15 min; 40 cycles at 94°C for 30 s, 50°C for 30 s, and 72°C for 30 s; and a final extension at 72°C for 10 min. Electrophoresis of the PCR products was performed on a 2% Seakem Agarose (Lonza, ME, USA). Gels were stained with GelRed (Biotium Inc., Hayward, CA, USA) in order to visualize the amplified DNA fragment of 290 bps.

The biotinylated PCR product was purified and made single stranded to act as a template using the Pyrosequencing Vacuum Prep Tool (Biotage Inc., Charlottesville, VA, USA). The biotinylated single-stranded product was annealed to the pyrosequencing primer (5′ AGTTAGGTGTGGGATATAG T-3′) and then subjected to sequencing using an automatically generated nucleotide dispensation order for sequences to be analysed corresponding to each reaction. The pyrograms were analysed using allele quantification mode to determine the proportion of cytosine/thymine and, hence, methylated and unmethylated cytosines at the targeted position(s). The degree of methylation was evaluated at three specific cytosine followed by guanine (CpG) methylation sites, as well as the average percent methylation of the three CpG sites.

2.10. Statistical Analysis. All experiments were performed in triplicate for three times. Results were reported as the MD or the fold change of control. Differences were assessed by one-way-repeated measure analysis of variance (ANOVA), followed by the Bonferroni post hoc test for multiple comparisons or by Student's *t*-test for comparison of two groups. All the analyses were conducted using GraphPad version 6.0 with a significance level of 0.05.

3. Results

3.1. Analysis of DNMT Expression Using GEO Datasets. Differences in the expression levels of DNMT1, DNMT3a, and DNMT3b, between diabetic mice and controls at different time points, were evaluated in three distinct GEO datasets. Since DR incidence is higher in type 1 diabetes patients [3], we firstly analysed microarray data of type 1 diabetes mouse models. No significant difference was revealed by analysing the GSE12610 dataset, which compared adult CD1 STZ-induced diabetic mice, after 3 weeks and 5 weeks from induction, to nondiabetic mice (Figure 1(a)). The GSE19122 dataset reported microarray data of two type I diabetes mouse models, after 3 months of hyperglycaemia, and nondiabetic controls. Data analysis revealed that insulin-deficient $Ins2^{Akita}$ mice, but not STZ-induced diabetic mice, showed lower DNMT1 ($MD = -0.28$, $p < 0.001$) and DNMT3a ($MD = -0.31$, $p < 0.001$) expression levels compared to nondiabetic controls (Figures 1(b) and 1c). We also analysed the GSE55389 dataset, which compared 8-week-old db/db type 2 diabetic mice to nondiabetic controls. However, no significant difference in the expression levels of DNMT1, DNMT3a, and DNMT3b was reported (Figure 1(d)).

3.2. High Glucose-Induced Oxidative Stress Precedes Upregulation of DNMT Expression/Activity in RPE Cells. One of the common features of both type 1 and 2 diabetes is hyperglycaemia-induced oxidative stress in the retina [4, 5]. Hence, we evaluated the time-dependent effect of high glucose on ROS production in ARPE-19 cells, seeded in 6-well plates and maintained either in normal (5.5 mM) or in high glucose (25 mM) condition for 5 days. Under normal glucose condition, ROS production remained stable with increasing values after 96 hours, probably due to cell confluency. Under high glucose condition, ROS production immediately increased after 2 hours, maintaining stable high levels from 2 to 24 hours and then slightly decreased. At each time point, ROS production was higher in cells maintained at high glucose compared to normal glucose condition (Figure 2(a)).

Since the analysis of GEO datasets suggested a possible time-related effect of hyperglycaemia on DNMT expression levels, we performed a time-course analysis of DNMT activity and expression in ARPE-19 cells maintained either in normal or in high glucose condition for 5 days. DNMT activity remained stable under normal glucose condition, whereas it showed a negative peak at 24 hours and a positive peak at 120 hours under high glucose condition (Figure 2(b)). Particularly, significant differences between normal and high glucose conditions were revealed after 24 ($MD = -35.44$, $p < 0.05$) and 120 hours ($MD = 61.93$, $p < 0.001$). This result was partially confirmed by time-course analysis of DNMT1 expression (Figure 2(c)). After 48 hours, DNMT1 expression level increased in cells under high glucose condition ($FC = 1.25$ at 72 hours, $FC = 2.21$ at 96 hours, and $FC = 2.33$ at 120 hours) but not in those under normal glucose condition. No significant difference and time-related effect were reported for DNMT3a and DNMT3b expression levels (data not shown). Overall, results from time-course analysis demonstrated that high glucose-induced oxidative stress precedes the upregulation of DNMT expression and activity, suggesting that high glucose-induced changes in DNMT function could be mediated by oxidative stress.

3.3. Effect of Curcumin on Viability and ROS Production in RPE Cells. Consistently with previous studies [20–22], we aimed to evaluate the antioxidant effect of curcumin on high glucose-induced oxidative stress in RPE cells. Firstly, we determined cytotoxicity of curcumin in ARPE-19 cells, grown in a 96-well plate and then exposed to various concentrations of curcumin (1–50 μM) for 6 hours or to 25 μM curcumin for various durations of exposure. No significant cytotoxic effect was observed with 1–25 μM curcumin, while treatment with 50 μM curcumin for 6 h resulted in 39% decrease in cell viability ($p < 0.01$) (Figure 3(a)). Moreover,

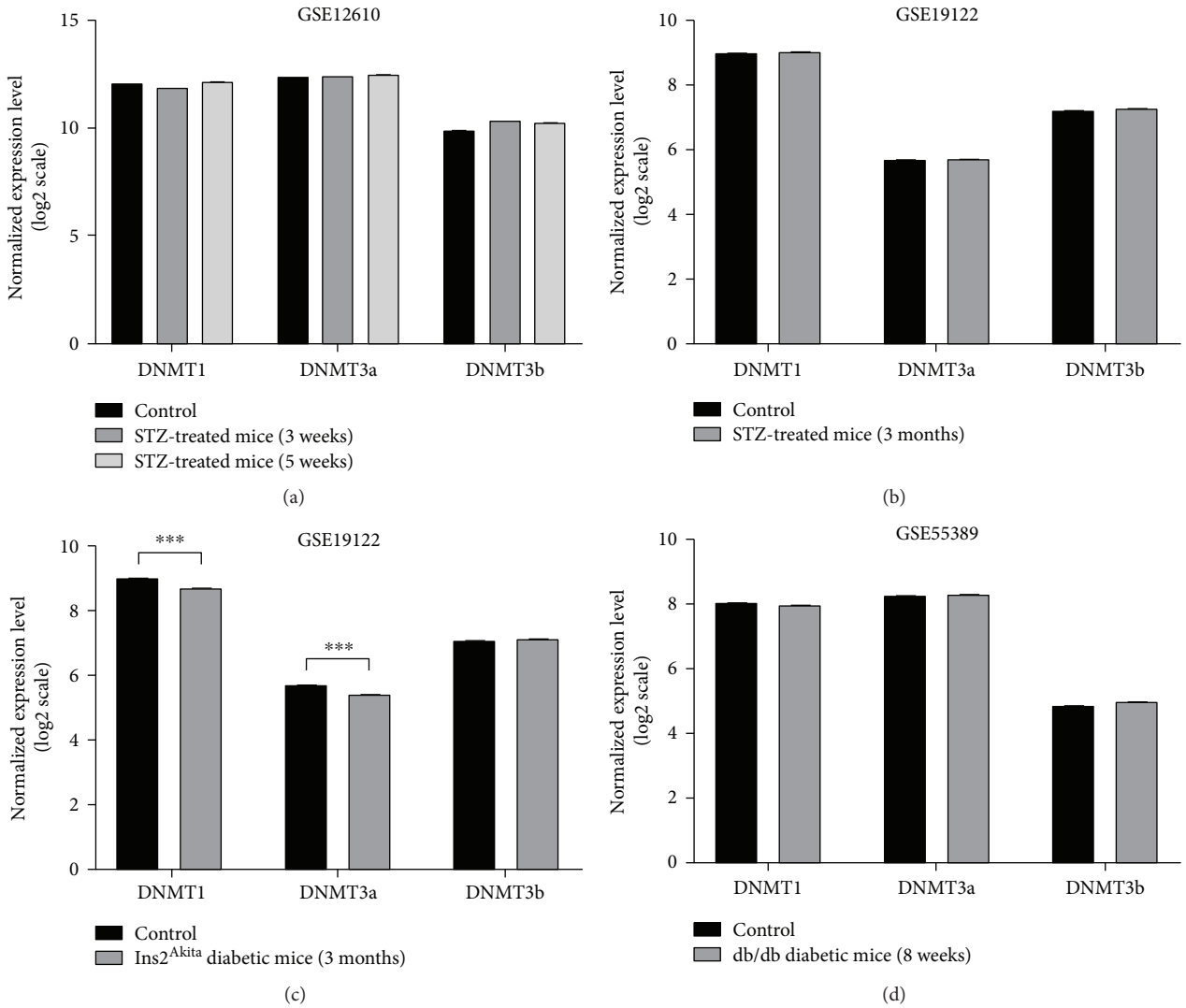

Figure 1: Comparison of DNMT expression using GEO datasets of microarray profiling in mouse models of diabetic retinopathy. (a) Comparison of retinal DNMT expression between adult CD1 streptozotocin- (STZ-) induced diabetic mice (3-week and 5-week) and age-matched controls (4 retinas for each group were pooled) using the GSE12610 dataset. (b) Comparison of retinal DNMT expression between eight C57BL/6J STZ-induced diabetic mice, after 3 months of hyperglycaemia, and eight controls, using the GSE19122 dataset. (c) Comparison of retinal DNMT expression between nine insulin-deficient $Ins2^{Akita}$ mice, after 3 months of hyperglycaemia, and eight controls, using the GSE19122 dataset. (d) Comparison of retinal DNMT expression between four 8-week-old db/db diabetic mice and four age-matched lean nondiabetic controls, using the GSE55389 dataset. $^{***}p < 0.001$.

treatment with 25 μM curcumin for up to 12 hours had no significant effect on cell viability. However, cell viability was reduced by 22% ($p = 0.179$) and 36% ($p < 0.01$) of the untreated controls after 25 μM exposure for 12 and 24 h, respectively (Figure 3(b)). To avoid potential cytotoxicity, treatment with 25 μM curcumin for 6 hours was chosen for further experiments. The effect of curcumin on ROS production was evaluated in ARPE-19 cells maintained at normal glucose or exposed to acute and chronic high glucose condition. Similar to time-course analysis, exposure to acute and chronic high glucose condition increased the intracellular ROS levels compared to normal glucose ($p < 0.05$ and $p < 0.01$, resp.). However, ROS production was restored by treatment with 25 μM curcumin for 6 hours in both cells under acute and chronic high glucose condition (Figure 4(a)).

3.4. Curcumin Restores Basal Levels of DNMT Activity and Expression in RPE Cells upon Hyperglycaemic Conditions. We also evaluated the effect of curcumin on DNMT activity and expression. Compared to cells at normal glucose concentration, we confirmed a 35% decrease in DNMT activity under acute high glucose condition ($p < 0.05$); in contrast, chronic high glucose exposure led to 70% increase in DNMT activity. However, DNMT activity was restored by treatment with 25 μM curcumin for 6 hours in both conditions (Figure 4(b)). With regard to DNMT1 expression level, chronic high glucose exposure up-

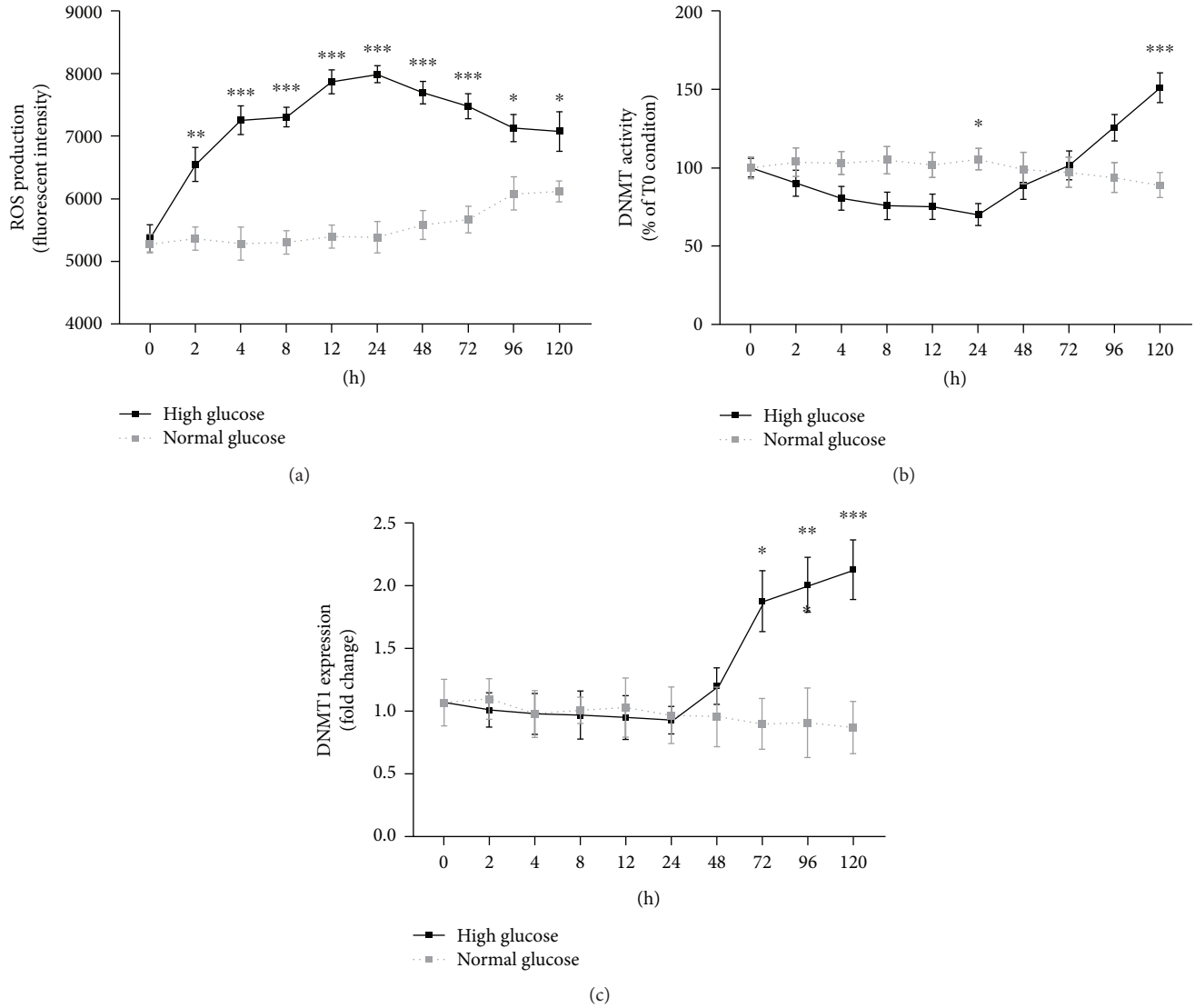

Figure 2: Time-dependent effects of high glucose in ARPE-19 cells. (a) Time-course analysis of ROS production in ARPE-19 cells maintained under normal and high glucose conditions. (b) Time-course analysis of total DNMT activity in ARPE-19 cells maintained under normal and high glucose conditions. (c) Time-course analysis of DNMT1 expression in ARPE-19 cells maintained under normal and high glucose conditions. $^{*}p < 0.05$; $^{**}p < 0.01$; $^{***}p < 0.001$.

regulated mRNA expression levels compared to cells at normal glucose concentration (FC = 2.01; $p < 0.05$). However, consistent with results on DNMT activity, treatment with 25 μM curcumin for 6 hours restored DNMT1 expression level (Figure 4(c)). No significant effect of high glucose and curcumin was reported for DNMT3a and DNMT3b expression levels (Figures 4(d) and 4(e)).

3.5. LINE-1 Methylation Analysis. The effect of high glucose exposure and/or curcumin treatment on LINE-1 methylation, a surrogate marker of global DNA methylation, was evaluated using the bisulfite-converted DNA. Consistent with the higher expression level of the maintenance DNMT1, exposure of ARPE-19 cells to acute or chronic high glucose condition did not affect LINE-1 methylation levels. Similarly, no significant effect of treatment with 25 μM curcumin for 6 hours on LINE-1 methylation levels was reported (Figure 4(f)).

4. Discussion

Emerging evidence suggests that pathogenesis of diabetes-related microvascular complications relies on a complex gene-environment interaction [31]. Epigenetic changes, such as DNA methylation, histone modifications, and miRNA regulation, contribute to the dysregulation of signalling pathways (i.e., oxidative stress, inflammation, apoptosis, and aging), modulating the expression of several key genes in diabetes mellitus [32, 33]. The elucidation of epigenetic changes involved in microvascular complications could improve our knowledge of pathophysiology and therapeutic management of these diseases, an important

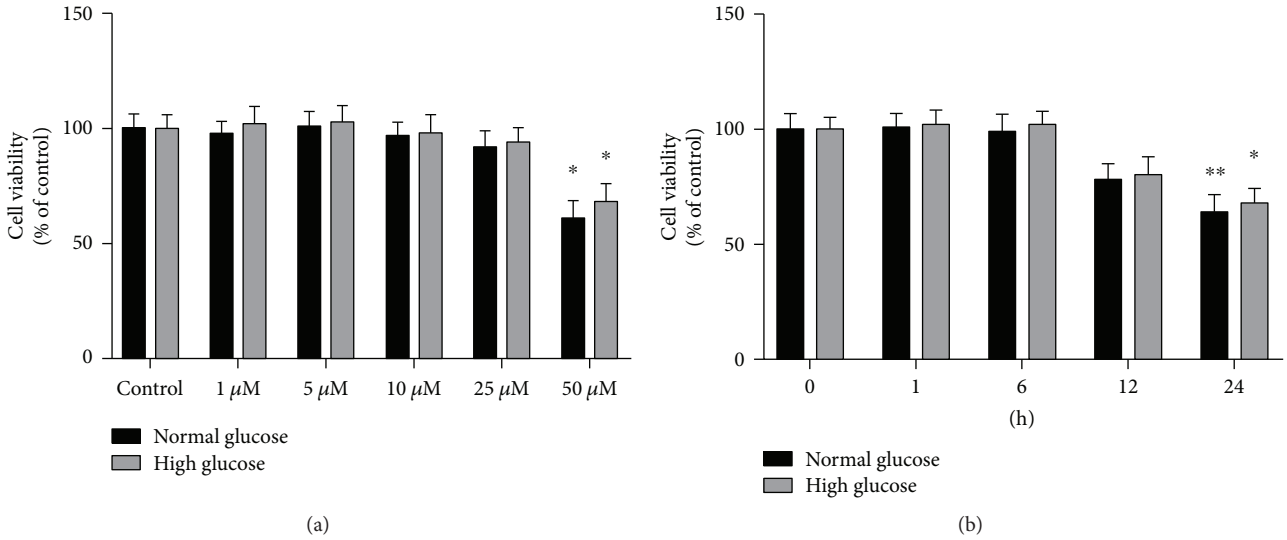

Figure 3: Effect of curcumin on viability of ARPE-19 cells. (a) Thiazolyl blue tetrazolium bromide (MTT) assay performed on ARPE-19 cells, maintained either in normal or in high glucose conditions, and then exposed to increasing concentrations (1–50 μM) of curcumin for 6 h. (b) MTT assay performed on ARPE-19 cells, maintained either in normal or in high glucose conditions, and then exposed to 25 μM curcumin for 1 to 24 hours. $^{*}p < 0.05$; $^{**}p < 0.01$.

public health issue. The role of DNA methylation in vascular complications of diabetes has been recently reviewed [34]. Several lines of evidence described distinct methylation patterns in diabetes-associated cardiovascular complications [35–38], suggesting that high glucose-induced oxidative stress is an important mediator [39, 40]. Moreover, *in vitro* and epidemiological studies reported that altered promoter methylation led to the dysregulation of several genes in diabetic nephropathy [41–43].

In diabetic retinopathy, differential DNA methylation of genes involved in the natural killer cell-mediated cytotoxicity pathway was described [44]. Moreover, retinal endothelial cells exposed to high glucose concentration showed increased mitochondrial DNA methylation [8] and an imbalance between methylcytosine and hydroxyl methylation of *Matrix metalloproteinase-9* gene [45], impairing mitochondrial integrity and functions. However, in spite of substantial findings suggesting that hyperglycaemia might affect DNA methylation in the retina, the limited knowledge about the effect of high glucose in RPE is needed to be explored.

In this study, we first evaluated whether differences in the retinal DNMT expression levels existed between diabetic and nondiabetic mice, using microarray data of three distinct GEO datasets. Since DR incidence is higher in patients suffering from type 1 diabetes [3], we firstly analysed microarray data of type 1 diabetes mouse models. Data analysis did not reveal dysregulation of DNMT expression levels in 3-week, 5-week, and 3-month STZ-induced diabetic mice. Similarly, inconclusive results have been recognized analysing DNMT expression level of 8-week-old db/db diabetic mice, a genetic mouse model of type 2 diabetes. By contrast, three months of hyperglycaemia in insulin-deficient $Ins2^{Akita}$ mice resulted in the downregulation of DNMT1 and DNMT3a expression. The $Ins2^{Akita}$ mouse, harbouring a missense mutation in the *Insulin 2* gene, is a model for type 1 diabetes [46]. However, a previous study reported that nonobese $Ins2^{Akita}$ mice also developed type 2 diabetes phenotypes, such as peripheral and hepatic insulin resistance and cardiac remodelling, suggesting long-term intermediate complications between type 1 and type 2 diabetes [47].

Regardless of the type of diabetes, hyperglycaemia-induced oxidative stress in the retina is one of the common features of DR pathogenesis [4, 5]. When we evaluated the time-dependent effect of high glucose in ARPE-19 cells, ROS production immediately increased after 2 hours of exposure, maintaining stable high levels from 2 to 24 hours, and then slightly decreased. Particularly, at each time point, ROS production was higher in cells maintained at high glucose compared to normal glucose condition.

Previous studies suggested that high glucose-induced oxidative stress might modulate epigenetic changes involved in the pathophysiology of DR [4, 8–11, 45, 48]. This substantial evidence, together with findings from GEO dataset analysis, prompted us to determine the effect of high glucose on DNMT function, taking into account the duration of insult. In ARPE-19 cells maintained at different glucose conditions, we demonstrated the time-related effect of high glucose exposure on DNMT activity, as shown by the time-course analysis, with a negative peak after 24 hours and a positive peak after 120 hours. Consistently, the high glucose-induced effect on DNMT expression was evident after 48 hours from the insult, with the upregulation of DNMT1. By contrast, we did not observe dysregulation of DNMT3a and DNMT3b expression.

Since DNMT1 is responsible for maintenance of DNA methylation on hemimethylated DNA [12], we also evaluated the effect of high glucose exposure on global DNA methylation, using LINE-1 methylation level as a surrogate marker. Consistent with higher DNMT1 expression, we did not observe differences in LINE-1 methylation levels between

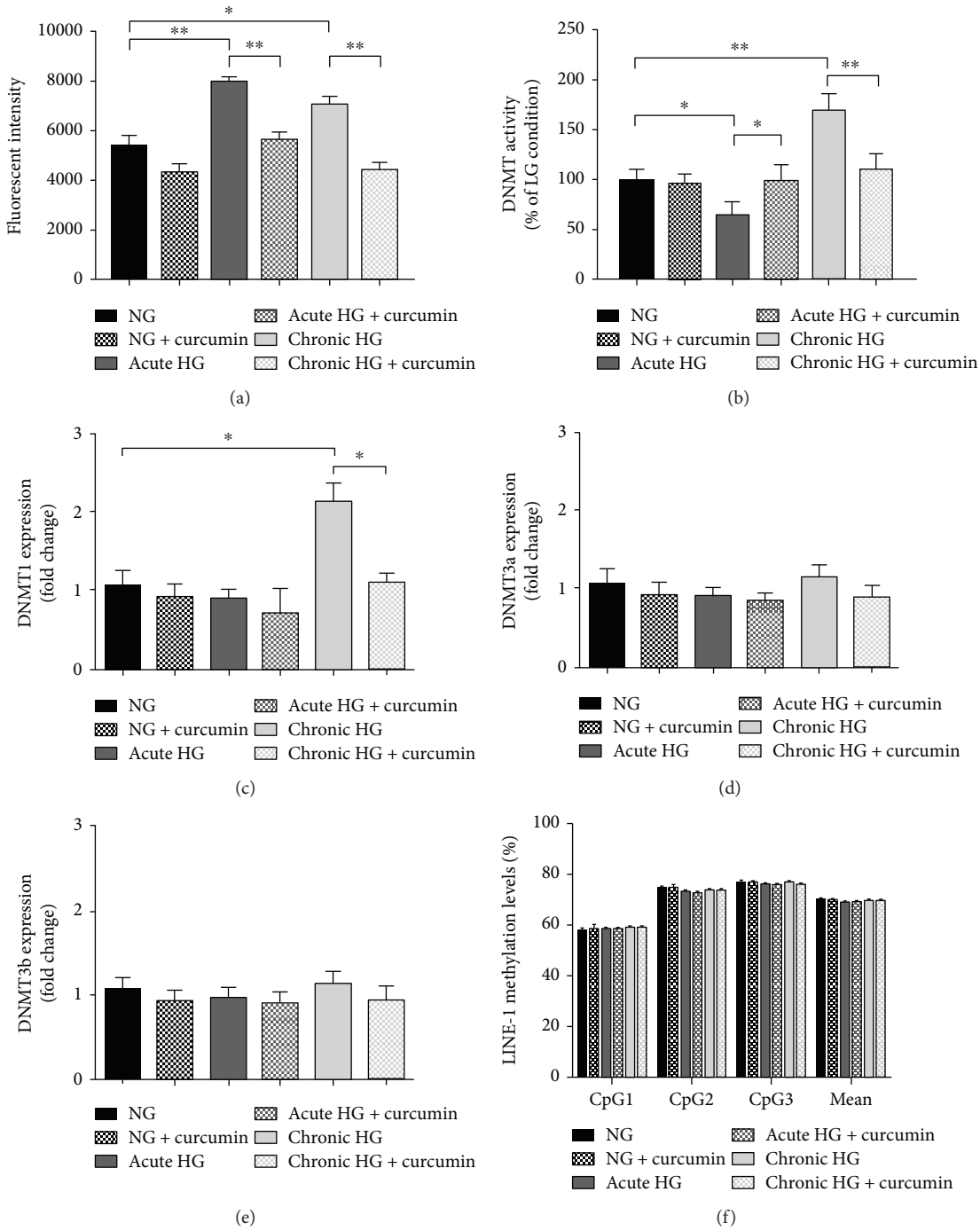

Figure 4: Effects of curcumin on ROS production and DNMT function in ARPE-19 cells. (a) Comparison of ROS production in ARPE-19 cells, maintained either in normal or in high glucose conditions (acute and chronic exposure), and then exposed to 25 μM curcumin for 6 hours. (b) Comparison of total DNMT activity in ARPE-19 cells, maintained either in normal or in high glucose conditions (acute and chronic exposure), and then exposed to 25 μM curcumin for 6 hours. (c–e) Comparison of DNMT expression in ARPE-19 cells, maintained either in normal or in high glucose conditions (acute and chronic exposure), and then exposed to 25 μM curcumin for 6 hours. (f) Comparison of LINE-1 methylation level in ARPE-19 cells, maintained either in normal or in high glucose conditions (acute and chronic exposure), and then exposed to 25 μM curcumin for 6 hours. $^{*}p < 0.05$; $^{**}p < 0.01$.

cells maintained at normal glucose concentration and those exposed to acute or chronic high glucose condition. However, the potential effects on other repetitive sequences and/or on specific promoter regions cannot be completely excluded.

Our data were in line with previous studies which demonstrated that hyperglycaemia significantly increased both DNMT activity and DNMT1 expression in retinal endothelial cells [8, 45, 49]. These changes persisted even

when the glucose level is normalized, indicating that DNA methylation is probably involved in the metabolic memory of DR [11, 49–51].

This study, to our knowledge, is the first to demonstrate that high glucose-induced oxidative stress precedes the upregulation of DNMT expression and activity in RPE, suggesting that changes in DNMT function could be mediated by oxidative stress via a potential dual effect. The early effect results in decreasing DNMT activity, accompanied by the highest ROS production, while long-term oxidative stress increases DNMT activity and DNMT1 expression. It is plausible that ROS production is involved in the activation of redox-sensitive enzymes, accelerating the reaction of DNA methylation via deprotonating the cytosine molecule [52]. On the other side, it has also been demonstrated that inhibition of DNMTs, using the DNMT inhibitor RG108 (RG), protected RPE from detrimental effects of oxidative stress by the modulation of antioxidant enzyme gene expression [53]. Although the temporal relationship between high glucose-induced oxidative stress and changes in DNMT function appears evident, further *in vitro* and *in vivo* studies, using antioxidants and DNMT inhibitors, are recommended to better clarify molecular pathways involved in this mechanism.

Curcumin is considered, especially for its antioxidant properties, an interesting phytochemical candidate for the treatment of hyper-inflammatory wounds such as chronic diabetic wounds. Since it has been demonstrated that topical curcumin treatment of the wounds of diabetic rats showed enhanced angiogenesis [54], it will be interesting to evaluate the efficacy of topical curcumin on human diabetic wounds [55]. Extensive researches have increase the disease set for which curcumin may be valuable, and the identification of molecular targets will help future research in the development of curcumin as an important therapeutic agent [56]. In the present study, we also investigated whether antioxidant properties of curcumin might restore the high glucose-induced changes in RPE cells. Growing body of evidence demonstrated the pleiotropic effect of curcumin on several signalling pathways, via modulating the expression and activation of cellular regulatory systems, such as NFκB, AKT, growth factors, and Nrf2 transcription factor [57–64]. Consistent with previous works [65, 66], we observed that treatment with 25 μM curcumin for up to 12 hours had no significant effect on cell viability. Interestingly, we demonstrated that curcumin treatment for 6 hours reduced ROS production associated with acute and chronic exposure to high glucose concentration. In turn, the normalization of intracellular ROS levels restored the DNMT activity and DNMT1 expression. These results suggest that the antioxidant properties of curcumin might exert a beneficial effect on high glucose-induced changes in DNMT function. In line with this evidence, a previous work also demonstrated that curcumin downregulated the oxidative stress-induced expression of miR-302, an inhibitor of DNMT1 [65]. However, further studies are needed to explore if curcumin modulates DNMT function via an antioxidant effect or if it reduces oxidative stress acting on DNMT inhibition.

One of the main weaknesses of our study is that it is not evident if curcumin mainly acts as an antioxidant or DNMT inhibitor. Since curcumin treatment restored both ROS production and DNMT functions, further experiments should evaluate whether the effect of curcumin depends on the oxidative and/or DNMT pathways. Moreover, inconclusive evidence from in vivo studies exists. While we did not reveal the dysregulation of DNMT expression using microarray data of short-term type 1 diabetes mouse models, three months of hyperglycaemia in insulin-deficient $Ins2^{Akita}$ mice resulted in the downregulation of DNMT1 and DNMT3a expression. As reported, the $Ins2^{Akita}$ mouse is a model for type 1 diabetes, which also developed type 2 diabetes phenotypes. Overall, these findings suggest the long-term intermediate effect of type 1 and type 2 diabetes on DNA methylation, but they also point out the need for additional in vivo studies. Finally, we observed that treatment with 25 μM curcumin (≈9.2 μg/mL) for up to 12 hours had no significant effect on cell viability, which was consistent with previous in vitro studies [65, 66]. In addition, a previous clinical trial found that daily high-dose curcumin consumption—up to 3.6 g—was not associated with toxicity and adverse outcomes [67]. However, pharmacokinetic studies of oral Curcuma extracts in rats showed poor absorption, rapid metabolism, and elimination, which in turn suggest a low oral bioavailability [68, 69]. On the other hand, it is well established that curcumin passes through the blood-brain barrier, and dietary supplementation (≈0.2% in diet) was found to be effective against retinal degeneration in an in vivo model of light-induced retinal degeneration [70, 71]. Accordingly, further studies should be encouraged to evaluate how much diet-supplemented curcumin reaches the human retina.

5. Conclusions

For the first time, we demonstrated that high glucose-induced ROS production precedes the upregulation of DNMT expression and activity in RPE, suggesting that changes in DNMT function could be mediated by oxidative stress. Curcumin may represent an effective antioxidant compound to restore DNMT expression and function. However, further *in vitro* and *in vivo* studies and well-designed epidemiological studies are recommended to better clarify whether curcumin mainly acts as an antioxidant or a DNMT inhibitor.

Data Availability

The data used to support the findings of this study are available from the co-corresponding authors upon request.

Conflicts of Interest

Maria Grazia Mazzone and Francesco Giuliano are employees of SIFI SpA. The other authors declare no conflict of interest.

Acknowledgments

Manlio Vinciguerra is supported by the European Social Fund and European Regional Development Fund Project MAGNET (no. CZ.02.1.01/0.0/0.0/15_003/0000492). Andrea Maugeri, Martina Barchitta, and Antonella Agodi are supported by the Department of Medical and Surgical Sciences and Advanced Technologies "GF Ingrassia", Università di Catania (Piano triennale di sviluppo delle attività di ricerca scientifica del dipartimento—2016-18).

Supplementary Materials

Figure S1: flow chart of in vitro experiments. *(Supplementary Materials)*

References

[1] S. R. Flaxman, R. R. A. Bourne, S. Resnikoff et al., "Global causes of blindness and distance vision impairment 1990-2020: a systematic review and meta-analysis," *The Lancet Global Health*, vol. 5, no. 12, pp. e1221–e1234, 2017.

[2] N. Congdon, Y. Zheng, and M. He, "The worldwide epidemic of diabetic retinopathy," *Indian Journal of Ophthalmology*, vol. 60, no. 5, pp. 428–431, 2012.

[3] J. W. Yau, S. L. Rogers, R. Kawasaki et al., "Global prevalence and major risk factors of diabetic retinopathy," *Diabetes Care*, vol. 35, no. 3, pp. 556–564, 2012.

[4] S. A. Madsen-Bouterse and R. A. Kowluru, "Oxidative stress and diabetic retinopathy: pathophysiological mechanisms and treatment perspectives," *Reviews in Endocrine & Metabolic Disorders*, vol. 9, no. 4, pp. 315–327, 2008.

[5] J. M. Santos, G. Mohammad, Q. Zhong, and R. A. Kowluru, "Diabetic retinopathy, superoxide damage and antioxidants," *Current Pharmaceutical Biotechnology*, vol. 12, no. 3, pp. 352–361, 2011.

[6] L. P. Aiello and DCCT/EDIC Research Group, "Diabetic retinopathy and other ocular findings in the diabetes control and complications trial/epidemiology of diabetes interventions and complications study," *Diabetes Care*, vol. 37, no. 1, pp. 17–23, 2014.

[7] R. A. Kowluru, J. M. Santos, and M. Mishra, "Epigenetic modifications and diabetic retinopathy," *BioMed Research International*, vol. 2013, Article ID 635284, 9 pages, 2013.

[8] M. Mishra and R. A. Kowluru, "Epigenetic modification of mitochondrial DNA in the development of diabetic retinopathy," *Investigative Ophthalmology & Visual Science*, vol. 56, no. 9, pp. 5133–5142, 2015.

[9] H. R. Pelzel, C. L. Schlamp, M. Waclawski, M. K. Shaw, and R. W. Nickells, "Silencing of Fem1cR3 gene expression in the DBA/2J mouse precedes retinal ganglion cell death and is associated with histone deacetylase activity," *Investigative Ophthalmology & Visual Science*, vol. 53, no. 3, pp. 1428–1435, 2012.

[10] Q. Zhong and R. A. Kowluru, "Epigenetic changes in mitochondrial superoxide dismutase in the retina and the development of diabetic retinopathy," *Diabetes*, vol. 60, no. 4, pp. 1304–1313, 2011.

[11] Q. Zhong and R. A. Kowluru, "Epigenetic modification of Sod2 in the development of diabetic retinopathy and in the metabolic memory: role of histone methylation," *Investigative Ophthalmology & Visual Science*, vol. 54, no. 1, pp. 244–250, 2013.

[12] G. Auclair and M. Weber, "Mechanisms of DNA methylation and demethylation in mammals," *Biochimie*, vol. 94, no. 11, pp. 2202–11, 2012.

[13] M. Barchitta, A. Quattrocchi, A. Maugeri, M. Vinciguerra, and A. Agodi, "LINE-1 hypomethylation in blood and tissue samples as an epigenetic marker for cancer risk: a systematic review and meta-analysis," *PLoS One*, vol. 9, no. 10, article e109478, 2014.

[14] P. E. Carreira, S. R. Richardson, and G. J. Faulkner, "L1 retrotransposons, cancer stem cells and oncogenesis," *The FEBS Journal*, vol. 281, no. 1, pp. 63–73, 2014.

[15] S. Fabris, D. Ronchetti, L. Agnelli et al., "Transcriptional features of multiple myeloma patients with chromosome 1q gain," *Leukemia*, vol. 21, no. 5, pp. 1113–1116, 2007.

[16] N. Rodić and K. H. Burns, "Long interspersed element-1 (LINE-1): passenger or driver in human neoplasms?," *PLoS Genetics*, vol. 9, no. 3, article e1003402, 2013.

[17] A. Amalraj, A. Pius, S. Gopi, and S. Gopi, "Biological activities of curcuminoids, other biomolecules from turmeric and their derivatives - a review," *Journal of Traditional and Complementary Medicine*, vol. 7, no. 2, pp. 205–233, 2017.

[18] D. Akbik, M. Ghadiri, W. Chrzanowski, and R. Rohanizadeh, "Curcumin as a wound healing agent," *Life Sciences*, vol. 116, no. 1, pp. 1–7, 2014.

[19] Y. Zhang, S. A. McClain, H.-M. Lee et al., "A novel chemically modified curcumin "normalizes" wound-healing in rats with experimentally induced type I diabetes: initial studies," *Journal of Diabetes Research*, vol. 2016, Article ID 5782904, 11 pages, 2016.

[20] J. Epstein, I. R. Sanderson, and T. T. Macdonald, "Curcumin as a therapeutic agent: the evidence from in vitro, animal and human studies," *The British Journal of Nutrition*, vol. 103, no. 11, pp. 1545–1557, 2010.

[21] T. Osawa and Y. Kato, "Protective role of antioxidative food factors in oxidative stress caused by hyperglycemia," *Annals of the New York Academy of Sciences*, vol. 1043, no. 1, pp. 440–451, 2005.

[22] J. M. Woo, D. Y. Shin, S. J. Lee et al., "Curcumin protects retinal pigment epithelial cells against oxidative stress via induction of heme oxygenase-1 expression and reduction of reactive oxygen," *Molecular Vision*, vol. 18, pp. 901–908, 2012.

[23] R. A. Kowluru and M. Kanwar, "Effects of curcumin on retinal oxidative stress and inflammation in diabetes," *Nutrition & Metabolism*, vol. 4, no. 1, p. 8, 2007.

[24] W. M. Freeman, G. V. Bixler, R. M. Brucklacher et al., "Transcriptomic comparison of the retina in two mouse models of diabetes," *Journal of Ocular Biology, Diseases, and Informatics*, vol. 2, no. 4, pp. 202–213, 2009.

[25] P. Bogdanov, L. Corraliza, J. A. Villena et al., "The db/db mouse: a useful model for the study of diabetic retinal neurodegeneration," *PLoS One*, vol. 9, no. 5, article e97302, 2014.

[26] H. Candiloros, S. Muller, N. Zeghari, M. Donner, P. Drouin, and O. Ziegler, "Decreased erythrocyte membrane fluidity in poorly controlled IDDM. Influence of ketone bodies," *Diabetes Care*, vol. 18, no. 4, pp. 549–551, 1995.

[27] Y. H. Chen, H. C. Chou, S. T. Lin, Y. W. Chen, Y. W. Lo, and H. L. Chan, "Effect of high glucose on secreted proteome in cultured retinal pigmented epithelium cells: its possible

relevance to clinical diabetic retinopathy," *Journal of Proteomics*, vol. 77, pp. 111–128, 2012.

[28] X. Jouven, R. N. Lemaître, T. D. Rea, N. Sotoodehnia, J. P. Empana, and D. S. Siscovick, "Diabetes, glucose level, and risk of sudden cardiac death," *European Heart Journal*, vol. 26, no. 20, pp. 2142–2147, 2005.

[29] A. Agodi, M. Barchitta, A. Quattrocchi et al., "Low fruit consumption and folate deficiency are associated with LINE-1 hypomethylation in women of a cancer-free population," *Genes & Nutrition*, vol. 10, no. 5, p. 480, 2015.

[30] M. Barchitta, A. Quattrocchi, A. Maugeri et al., "LINE-1 hypermethylation in white blood cell DNA is associated with high-grade cervical intraepithelial neoplasia," *BMC Cancer*, vol. 17, no. 1, p. 601, 2017.

[31] M. Khullar, B. S. Cheema, and S. K. Raut, "Emerging evidence of epigenetic modifications in vascular complication of diabetes," *Frontiers in Endocrinology*, vol. 8, 2017.

[32] E. R. Gilbert and D. Liu, "Epigenetics: the missing link to understanding β-cell dysfunction in the pathogenesis of type 2 diabetes," *Epigenetics*, vol. 7, no. 8, pp. 841–852, 2012.

[33] C. Ling and L. Groop, "Epigenetics: a molecular link between environmental factors and type 2 diabetes," *Diabetes*, vol. 58, no. 12, pp. 2718–2725, 2009.

[34] J. Zheng, J. Cheng, Q. Zhang, and X. Xiao, "Novel insights into DNA methylation and its critical implications in diabetic vascular complications," *Bioscience Reports*, vol. 37, no. 2, p. BSR20160611, 2017.

[35] A. El-Osta, D. Brasacchio, D. Yao et al., "Transient high glucose causes persistent epigenetic changes and altered gene expression during subsequent normoglycemia," *The Journal of Experimental Medicine*, vol. 205, no. 10, pp. 2409–2417, 2008.

[36] M. Movassagh, M.-K. Choy, M. Goddard, M. R. Bennett, T. A. Down, and R. S.-Y. Foo, "Differential DNA methylation correlates with differential expression of angiogenic factors in human heart failure," *PLoS One*, vol. 5, no. 1, article e8564, 2010.

[37] H. Mönkemann, A. S. De Vriese, H. J. Blom et al., "Early molecular events in the development of the diabetic cardiomyopathy," *Amino Acids*, vol. 23, no. 1–3, pp. 331–336, 2002.

[38] L. Pirola, A. Balcerczyk, R. W. Tothill et al., "Genome-wide analysis distinguishes hyperglycemia regulated epigenetic signatures of primary vascular cells," *Genome Research*, vol. 21, no. 10, pp. 1601–1615, 2011.

[39] Z. Z. Liu, X. Z. Zhao, X. S. Zhang, and M. Zhang, "Promoter DNA demethylation of Keap1 gene in diabetic cardiomyopathy," *International Journal of Clinical and Experimental Pathology*, vol. 7, no. 12, pp. 8756–8762, 2014.

[40] J. Zhong, G. Agha, and A. A. Baccarelli, "The role of DNA methylation in cardiovascular risk and disease: methodological aspects, study design, and data analysis for epidemiological studies," *Circulation Research*, vol. 118, no. 1, pp. 119–131, 2016.

[41] C. G. Bell, A. E. Teschendorff, V. K. Rakyan, A. P. Maxwell, S. Beck, and D. A. Savage, "Genome-wide DNA methylation analysis for diabetic nephropathy in type 1 diabetes mellitus," *BMC Medical Genomics*, vol. 3, no. 1, article 33, 2010.

[42] R. Peng, H. Liu, H. Peng et al., "Promoter hypermethylation of let-7a-3 is relevant to Its down-expression in diabetic nephropathy by targeting UHRF1," *Gene*, vol. 570, no. 1, pp. 57–63, 2015.

[43] C. Sapienza, J. Lee, J. Powell et al., "DNA methylation profiling identifies epigenetic differences between diabetes patients with ESRD and diabetes patients without nephropathy," *Epigenetics*, vol. 6, no. 1, pp. 20–28, 2011.

[44] E. Agardh, A. Lundstig, A. Perfilyev et al., "Genome-wide analysis of DNA methylation in subjects with type 1 diabetes identifies epigenetic modifications associated with proliferative diabetic retinopathy," *BMC Medicine*, vol. 13, no. 1, article 182, 2015.

[45] R. A. Kowluru and Y. Shan, "Role of oxidative stress in epigenetic modification of MMP-9 promoter in the development of diabetic retinopathy," *Graefe's Archive for Clinical and Experimental Ophthalmology*, vol. 255, no. 5, pp. 955–962, 2017.

[46] J. Wang, T. Takeuchi, S. Tanaka et al., "A mutation in the insulin 2 gene induces diabetes with severe pancreatic beta-cell dysfunction in the Mody mouse," *The Journal of Clinical Investigation*, vol. 103, no. 1, pp. 27–37, 1999.

[47] E. G. Hong, D. Y. Jung, H. J. Ko et al., "Nonobese, insulin-deficient Ins2Akita mice develop type 2 diabetes phenotypes including insulin resistance and cardiac remodeling," *American Journal of Physiology Endocrinology and Metabolism*, vol. 293, no. 6, pp. E1687–E1696, 2007.

[48] R. A. Kowluru, A. Kowluru, M. Mishra, and B. Kumar, "Oxidative stress and epigenetic modifications in the pathogenesis of diabetic retinopathy," *Progress in Retinal and Eye Research*, vol. 48, pp. 40–61, 2015.

[49] S. Tewari, Q. Zhong, J. M. Santos, and R. A. Kowluru, "Mitochondria DNA replication and DNA methylation in the metabolic memory associated with continued progression of diabetic retinopathy," *Investigative Ophthalmology & Visual Science*, vol. 53, no. 8, pp. 4881–4888, 2012.

[50] M. Mishra and R. A. Kowluru, "The role of DNA methylation in the metabolic memory phenomenon associated with the continued progression of diabetic retinopathy," *Investigative Ophthalmology & Visual Science*, vol. 57, no. 13, pp. 5748–5757, 2016.

[51] A. S. Olsen, M. P. Sarras, A. Leontovich, and R. V. Intine, "Heritable transmission of diabetic metabolic memory in zebrafish correlates with DNA hypomethylation and aberrant gene expression," *Diabetes*, vol. 61, no. 2, pp. 485–491, 2012.

[52] I. Afanas'ev, "New nucleophilic mechanisms of ros-dependent epigenetic modifications: comparison of aging and cancer," *Aging and Disease*, vol. 5, no. 1, pp. 52–62, 2014.

[53] P. Tokarz, K. Kaarniranta, and J. Blasiak, "Inhibition of DNA methyltransferase or histone deacetylase protects retinal pigment epithelial cells from DNA damage induced by oxidative stress by the stimulation of antioxidant enzymes," *European Journal of Pharmacology*, vol. 776, pp. 167–175, 2016.

[54] V. Kant, A. Gopal, D. Kumar et al., "Curcumin-induced angiogenesis hastens wound healing in diabetic rats," *The Journal of Surgical Research*, vol. 193, no. 2, pp. 978–988, 2015.

[55] A. Shah and S. Amini-Nik, "The role of phytochemicals in the inflammatory phase of wound healing," *International Journal of Molecular Sciences*, vol. 18, no. 5, 2017.

[56] R. L. Thangapazham, S. Sharad, and R. K. Maheshwari, "Phytochemicals in wound healing," *Advances in Wound Care*, vol. 5, no. 5, pp. 230–241, 2016.

[57] Y. Abe, S. Hashimoto, and T. Horie, "Curcumin inhibition of inflammatory cytokine production by human peripheral blood

monocytes and alveolar macrophages," *Pharmacological Research*, vol. 39, no. 1, pp. 41–47, 1999.

[58] E. Balogun, M. Hoque, P. Gong et al., "Curcumin activates the haem oxygenase-1 gene via regulation of Nrf2 and the antioxidant-responsive element," *The Biochemical Journal*, vol. 371, no. 3, pp. 887–895, 2003.

[59] M. T. Huang, T. Lysz, T. Ferraro, T. F. Abidi, J. D. Laskin, and A. H. Conney, "Inhibitory effects of curcumin on in vitro lipoxygenase and cyclooxygenase activities in mouse epidermis," *Cancer Research*, vol. 51, no. 3, pp. 813–819, 1991.

[60] A. C. Reddy and B. R. Lokesh, "Studies on spice principles as antioxidants in the inhibition of lipid peroxidation of rat liver microsomes," *Molecular and Cellular Biochemistry*, vol. 111, no. 1-2, pp. 117–124, 1992.

[61] G. Scapagnini, C. Colombrita, M. Amadio et al., "Curcumin activates defensive genes and protects neurons against oxidative stress," *Antioxidants & Redox Signaling*, vol. 8, no. 3-4, pp. 395–403, 2006.

[62] S. Singh and B. B. Aggarwal, "Activation of transcription factor NF-kappa B is suppressed by curcumin (diferuloylmethane) [corrected]," *The Journal of Biological Chemistry*, vol. 270, no. 42, pp. 24995–25000, 1995.

[63] M. Susan and M. N. Rao, "Induction of glutathione S-transferase activity by curcumin in mice," *Arzneimittel-Forschung*, vol. 42, no. 7, pp. 962–964, 1992.

[64] J. H. Woo, Y. H. Kim, Y. J. Choi et al., "Molecular mechanisms of curcumin-induced cytotoxicity: induction of apoptosis through generation of reactive oxygen species, down-regulation of Bcl-XL and IAP, the release of cytochrome c and inhibition of Akt," *Carcinogenesis*, vol. 24, no. 7, pp. 1199–1208, 2003.

[65] J. C. Howell, E. Chun, A. N. Farrell et al., "Global microRNA expression profiling: curcumin (diferuloylmethane) alters oxidative stress-responsive microRNAs in human ARPE-19 cells," *Molecular Vision*, vol. 19, pp. 544–560, 2013.

[66] V. Pittalà, A. Fidilio, F. Lazzara et al., "Effects of novel nitric oxide-releasing molecules against oxidative stress on retinal pigmented epithelial cells," *Oxidative Medicine and Cellular Longevity*, vol. 2017, Article ID 1420892, 11 pages, 2017.

[67] R. A. Sharma, S. A. Euden, S. L. Platton et al., "Phase I clinical trial of oral curcumin: biomarkers of systemic activity and compliance," *Clinical Cancer Research*, vol. 10, no. 20, pp. 6847–6854, 2004.

[68] V. Ravindranath and N. Chandrasekhara, "Absorption and tissue distribution of curcumin in rats," *Toxicology*, vol. 16, no. 3, pp. 259–265, 1980.

[69] V. Ravindranath and N. Chandrasekhara, "Metabolism of curcumin–studies with [3H] curcumin," *Toxicology*, vol. 22, no. 4, pp. 337–344, 1981.

[70] M. N. A. Mandal, J. M. R. Patlolla, L. Zheng et al., "Curcumin protects retinal cells from light-and oxidant stress-induced cell death," *Free Radical Biology & Medicine*, vol. 46, no. 5, pp. 672–679, 2009.

[71] P. Suryanarayana, M. Saraswat, T. Mrudula, T. P. Krishna, K. Krishnaswamy, and G. B. Reddy, "Curcumin and turmeric delay streptozotocin-induced diabetic cataract in rats," *Investigative Ophthalmology & Visual Science*, vol. 46, no. 6, p. 2092, 2005.

Hindawi
Oxidative Medicine and Cellular Longevity
Volume 2018, Article ID 2151429, 11 pages
https://doi.org/10.1155/2018/2151429

Research Article

Changes of Plasma FABP4, CRP, Leptin, and Chemerin Levels in relation to Different Dietary Patterns and Duodenal-Jejunal Omega Switch Surgery in Sprague–Dawley Rats

Dominika Stygar[1], **Elżbieta Chełmecka**[2], **Tomasz Sawczyn**[1], **Bronisława Skrzep-Poloczek**[1], **Jakub Poloczek**[3] and **Konrad Wojciech Karcz**[4]

[1]*Department of Physiology, School of Medicine with Dentistry Division in Zabrze, Medical University of Silesia, Katowice, Poland*
[2]*Department of Statistics, Department of Instrumental Analysis, School of Pharmacy with the Division of Laboratory Medicine in Sosnowiec, Medical University of Silesia, Katowice, Poland*
[3]*Department of Rehabilitation, 3rd Specialist Hospital, Rybnik, Poland*
[4]*Clinic of General, Visceral, Transplantation and Vascular Surgery, Hospital of the Ludwig Maximilian University, Munich, Germany*

Correspondence should be addressed to Dominika Stygar; dstygar@gmail.com

Received 28 January 2018; Accepted 4 April 2018; Published 22 April 2018

Academic Editor: Ana B. Crujeiras

Background. Pathophysiological links between inflammation, obesity, and adipokines can be used for the treatment of metabolic dysregulation. *Aims*. To examine the influence of duodenal-jejunal omega switch surgery in combination with different diet patterns on plasma concentrations of fatty acid-binding protein 4 (FABP4), C-reactive protein (CRP), leptin, and chemerin. *Methods*. After 8 weeks on a high-fat diet (HF) or control diet (CD), rats underwent surgery. Duodenal-jejunal omega switch (DJOS) with an exclusion of one-third of intestinal length and SHAM surgery were performed. For the next 8 weeks, 50% of DJOS/SHAM animals were kept on the same diet as before (HF/DJOS/HF, HF/SHAM/HF, CD/DJOS/CD, and CD/SHAM/CD), and 50% had a changed diet (HF/DJOS/CD, HF/SHAM/CD, CD/DJOS/HF, and CD/SHAM/HF). FABP4, CRP, leptin, and chemerin were assessed using ELISA kits. *Results*. FABP4: significant differences between DJOS and SHAM were observed in animals maintained on CD/CD; CRP: varied between DJOS and SHAM groups maintained on HF/HF, CD/CD, and CD/HF; leptin and chemerin levels: DJOS lowered leptin and chemerin plasma levels versus SHAM, while HF/HF, CD/HF, and HF/CD significantly increased leptin and chemerin plasma levels when compared to CD/CD. *Conclusions*. The beneficial effect of DJOS surgery is stronger than proinflammatory conditions caused by an HF obesogenic diet.

1. Introduction

Systematic energy surplus with "unhealthy dietary patterns" is known to be a strong driver in the development of obesity, for which a chronic low-grade inflammatory condition called metabolically triggered inflammation, metainflammation, or parainflammation is characteristic [1, 2]. The condition of chronic inflammation if occurs in metabolically involved organs, like liver and adipose tissue, plays a main role in the development of chronic metabolic diseases, such as diabetes, and fatty liver disease [2]. Adipose tissue, aside from controlling fat mass and nutrient homeostasis, realises an inflammatory cytokine, which regulates metabolic homeostasis and the immune response. Fatty acid-binding proteins (FAPBs) are intracellular proteins known to facilitate lipid-mediated processes in cells [3]. So far, 9 types of FAPBs have been described and named in relation to the organ/tissue expression [4]. FABP4, expressed by adipocytes and macrophages, plays a key role in regulating systemic metabolism. It is an important mediator of inflammatory processes and metabolic syndrome [1]. The low-grade systemic inflammation is as well characterised by C-reactive protein (CRP).

CRP is produced in the liver on the binding of proinflammatory cytokines and is associated with obesity [5]. Leptin is an adipose-derived cytokine, which shows appetite-suppressant acting mediated through hypothalamic signaling. Leptin-resistant conditions, characteristic for obesity, lead to a loss of hypothalamus control of appetite and feeding behavior, exacerbating the already excessive body weight gain [6]. Leptin stimulates the gene expression of proinflammatory cytokines such as tumor necrosis factor alpha (TNF-α), interleukin 1 (IL-1), and interleukin (IL-6), improves phagocytosis by regulating oxidative stress, and acts on immune cells [7–11]. Chemerin, also called retinoic acid receptor responder 2 or tazarotene-induced gene 2, has been found to be highly expressed in adipose tissue. Plasma total chemerin concentrations are positively associated with obesity, metabolic syndrome, and inflammation [12]. Chemerin merges obesity with inflammation inactivating the orphan G-protein coupled receptor chemokine-like receptor 1 (CMKLR1, ChemR23) which is characteristic for cells of the innate immune system [12–15]. Bariatric surgery is one of the most efficient treatments for long-term weight loss and its long-term maintenance [16]. A systematic review of long-term follow-ups after bariatric surgery shows that this is one of the most efficient treatments of obesity, which helps to reduce body weight by up to 60% during the first two years after surgery, and gives about a 38% reduction of comorbidities in studied individuals [17]. Duodenal-jejunal omega switch (DJOS) is a type of bariatric surgery, with proximal loop duodeno-enterostomy, which bypasses the foregut (foregut theory), and allows for direct hindgut stimulation (hindgut theory) [18, 19]. The advantage of DJOS is a bypass-like procedure, where the pylorus of the patients is saved. This modification prevents patients from symptoms characteristic for postgastrectomy conditions such as dumping, diarrhoea, and dyspepsia [20, 21]. DJOS is a relatively new technique, thus an animal model, for exploring the physiological long-term effects of this procedure, is still needed [20, 22].

A pathophysiological link between dietary patterns, obesity, inflammation, and adipokines can be used as a potential target in therapeutic strategies for treatment of metabolic dysregulation like obesity, insulin resistance, and T2DM. Thus, the aim of the study was to measure the impact of DJOS surgery in combination with different types of dietary patterns on FABP4, leptin, chemerin, and CRP plasma levels. In this study, we decided to use an HF diet in order to induce obesity as a model close to human behaviour for the investigation of the underlying mechanisms mediating metabolic benefits of DJOS, measured by the plasma levels of selected adipokines. The experimental design of this study also includes the observations that not all patients after surgery follow the nutritional recommendations [23, 24]. Many physiological and psychological factors influence postoperative differences in weight-related outcomes, but it is known that weight regain occurs in up to 20% of patients after the surgery [25–27]. Thus, the selected study groups differ in terms of diet used before and after surgery. We assumed that after a bariatric operation, one might switch from a regular diet to an HF and from an HF to a regular diet. Then, we assessed the effect of duodenal-jejunal omega switch surgery in combination with CD, and an HF diet, before and after surgery, on the plasma levels of selected adipokines.

2. Materials and Methods

2.1. Animals and Diets. This individual study is based on experimental design applied and described in an earlier work by Stygar et al. [28]. Seven-week-old, male Sprague–Dawley rats (Charles River Laboratories Inc., Wilmington, MA) were kept in 12 h light-dark cycles at 22°C and 40–60% humidity. Environmental enrichment was provided, and all rats had free access to water and food. The composition of control diet (CD) was (Provimi Kliba AG, Kaiseraugst, Switzerland) 24% protein, 4.9% fat, 7% crude ashes, 4.7% crude fiber, lysine (13.6 g/kg), calcium (12 g/kg), methionine (4.5 g/kg), and phosphorus (8.3 g/kg). The animals from the control group were kept on CD for the period of two months, before and after surgery. Obesity was induced by keeping the animals on a high-fat diet (HF; 23.0 kJ/g; 59% fat, 27% carbohydrate, and 14% protein (EF RAT [E15744] Ssniff Spezialdiäten GmbH, Soest, Germany)) for the period of two months before and after surgery. All rats fasted overnight before surgery.

3. Experimental Design

After one week of acclimatisation, the animals were assigned to the experimental dietary patterns HF groups ($n = 28$) and CD ($n = 28$). The total duration of the experiment was 16 weeks. The animals were kept on selected diets for the period of 8 weeks before and 8 weeks after the DJOS and SHAM surgery. The first part of the protocol, before the surgery, included 8 weeks of maintenance of animals on selected diets. After this time, both groups (CD and HF) were divided into two subgroups, which underwent different types of surgery: 50% of rats underwent DJOS (14 animals) and 50% underwent SHAM surgery, which is a control type of surgery (14 animals, Figure 1(a)).

In the second part of the experiment, after the surgery, 50% of DJOS/SHAM animals were kept on the same diet as before (HF/DJOS/HF, HF/SHAM/HF, CD/DJOS/CD, and CD/SHAM/CD), and 50% had changed the diet (HF/DJOS/CD, HF/SHAM/CD, CD/DJOS/HF, and CD/SHAM/HF; Figure 1(a)). The "3Rs" for the ethical treatment of animals was followed in the study [29]. In the HF/SHAM/CD subgroup, 6 out of 7 rats survived till the end of the experiment, while in the rest of subgroups, the survival was 100%.

4. Experimental Procedures

A DJOS was performed according to Karcz et al. methodology [22], described in the aforementioned study [28]. To perform DJOS, the animals were anaesthetized with 2% isoflurane (AbbVie Deutschland GmbH & Co. KG, Ludwigshafen, Germany) and oxygen flow at 2 l/min under spontaneous breathing. Analgesia with xylazine (5 mg/kg, ip; Xylapan, Vetoquinol Biovet, Poland) and antibiotic

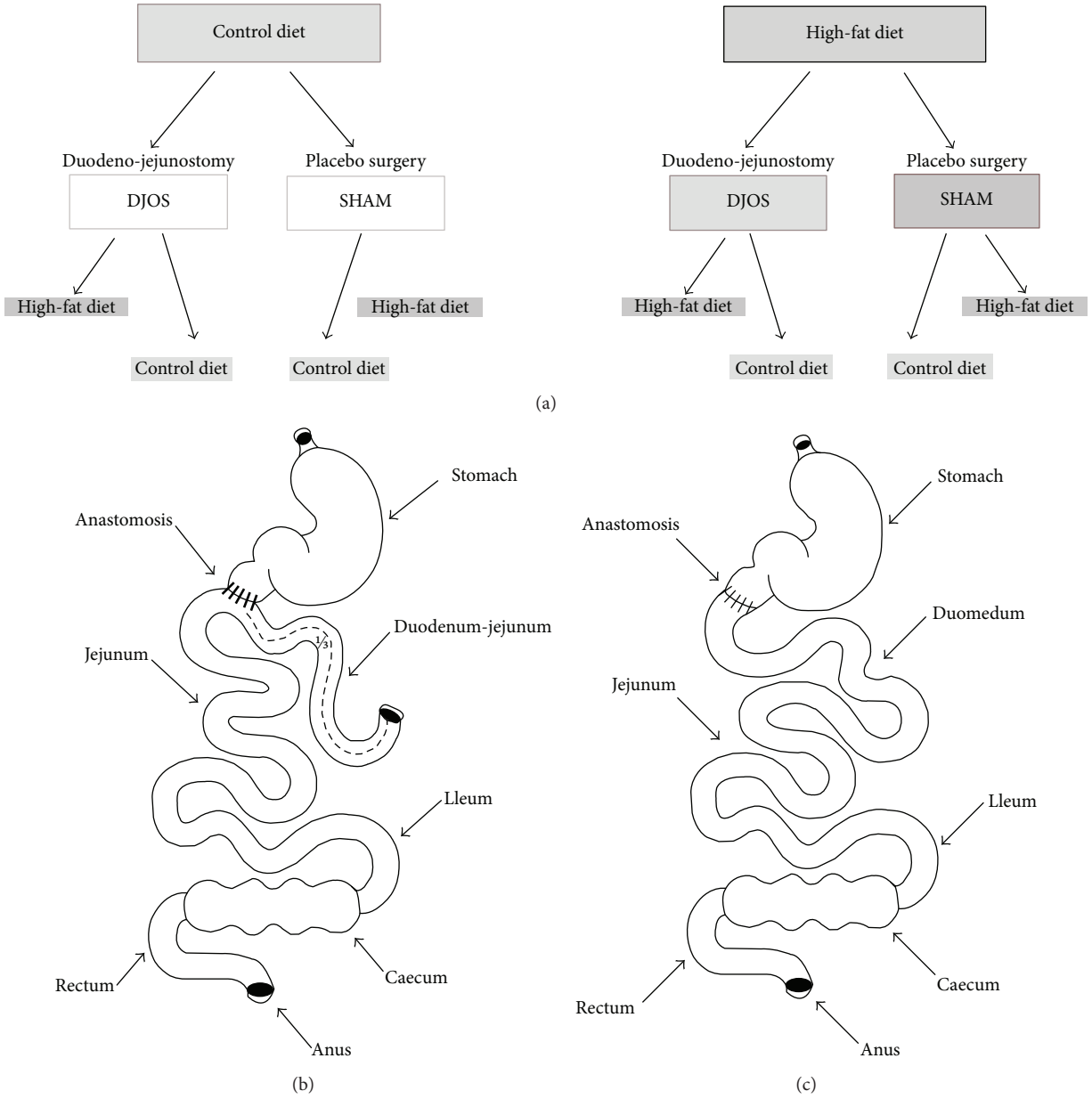

Figure 1: (a) Scheme of experimental groups. (b) Schematic illustration of DJOS. (c) SHAM surgery.

prophylaxis with gentamicin were applied. In order to gain abdominal access, a midline incision of 3-4 cm was performed, and the total length of the small intestine was determined (Figure 1(b)). The stomach was separated from the duodenum at the point just below the pylorus, and the position of anastomosis was defined at 1/3 of the total small bowel length. The jejunum was anastomosed via end-to-side duodeno-enterostomy in order to restore the physiological conduit of the food passage, excluding the duodenum and parts of the small intestine. The remaining duodenal stump was closed using PDS 6/0 (Ethicon). Mesenteric openings were closed with PDS 6/0 (Ethicon).

In the SHAM-operated animals, reanastomosis of the gastrointestinal tract was performed at the corresponding sites where enterotomies were performed for the duodenojejunostomy, thereby maintaining continuity of the food passage through the bowel (Figure 1(c)). For DJOS and SHAM protocols, postoperative analgesia was performed using carprofen (4 mg/kg, sc; Rimadyl, Pfizer, Switzerland) for 3 consecutive days after the surgery.

4.1. Tissue Collection and Assay Identification. At the end of the 8th week after surgery, corresponding to the 16th week of the experiment, blood samples for adipokines and CRP measurements were collected from the abdominal aorta, using tubes containing 10 μl EDTA (Sigma-Aldrich, St. Louis, MO). After centrifugation at 4000 rpm for 10 minutes at 4°C, plasma samples were collected, snap-frozen in liquid

nitrogen, and stored at −80°C until analyses were performed. Adipokines, including FABP4, leptin, chemerin, and CRP, were assessed in duplicate by using sandwich ELISA kits (Cloud-Clone Corp., Katy, TX). All experimental procedures were approved by the Ethical Committee for Animal Experimentation (58/2014).

5. Statistical Analysis

Statistical analysis was performed using STATISTICA 12.5 PL (StatSoft, Cracow, Poland). Statistical significance was set at a p value below 0.05. All tests were two-tailed. Interval data were expressed as mean value ± standard deviation in the case of normal distribution, or as median/lower–upper quartile range in the case of data with skewed or nonnormal distribution. Distribution of variables was evaluated by the Shapiro-Wilk test and the quantile-quantile plot. The homogeneity of variances was assessed by the Levene test. For comparison of data, the two-way parametric ANOVA and post hoc contrast analysis or nonparametric Kruskal-Wallis test or Mann–Whitney U test were used. In case of skewed data distribution, logarithmic transformation was performed before analysis.

6. Results

The results of body weight change after DJOS and SHAM surgery in all experimental groups were previously presented by Stygar et al. [28]. Plasma concentrations of FABP4, CRP, leptin, and chemerin in DJOS and SHAM-operated groups after long-term maintenance on HF and CD and mixed HF/CD and CD/HF eating patterns are shown in Table 1.

Table 2 presents results of multiple comparisons in contrast analysis of DJOS and SHAM-operated groups in relation to diet used before and after surgery. Column one presents a comparison between DJOS and SHAM surgery associated with different diets, column two shows comparisons between dietary groups of DJOS operated animals, and column three presents comparisons between dietary groups of SHAM-operated animals.

6.1. Plasma Concentrations of FABP4. The type of diet strongly influenced the FABP4 plasma levels both in animals from the DJOS and SHAM groups. Significant differences between DJOS and SHAM groups were observed only in animals maintained on CD diet before and after the surgery ($p < 0.01$; Figure 2, Tables 1 and 2).

In animals after DJOS, approximately two times lower plasma level of FABP4 was observed in the CD/CD group compared with the HF/HF, HF/CD, and CD/HF groups ($p < 0.001$; Figure 2, Tables 1 and 2).

In the control groups, plasma concentrations of FABP4 in rats subjected to HF diet before and after the surgery (HF/HF) were significantly higher than those in the groups maintained on CD before the surgery (CD/HF $p < 0.05$ and CD/CD $p < 0.001$; Figure 2, Tables 1 and 2). In addition, the change from HF to CD diet significantly increased FABP4 level than the change from CD to HF and CD/CD groups ($p < 0.01$ and $p < 0.001$, resp.; Figure 2, Tables 1 and 2).

6.2. Plasma Concentrations of CRP. The CRP concentrations were consistently lower after DJOS compared with SHAM surgery regardless of dietary pattern. CRP plasma concentrations varied between DJOS and SHAM groups maintained on HF diet before and after the surgery ($p < 0.001$), CD diet ($p < 0.05$), and mixed CD/HF diet ($p < 0.01$; Figure 3, Tables 1 and 2).

For both types of surgery, the values of CRP did not differ between selected experimental groups (Tables 1 and 2).

6.3. Plasma Concentrations of Leptin. DJOS surgery significantly lowered the leptin plasma level in comparison to SHAM surgery despite the type of diet applied before and after surgery ($p < 0.001$ for all; Figure 4, Tables 1 and 2).

HF diet significantly increased leptin level when compared to the CD/CD group in DJOS-operated animals ($p < 0.001$; Figure 4, Table 2). The maintenance of animals on different types of diet before and after surgery increased the leptin plasma level but did not reduce the positive effect of DJOS. The CD/HF and HF/CD diets significantly increased leptin plasma levels when compared to the CD/CD group ($p < 0.001$, resp.; Figure 4, Table 2).

Also in the SHAM-operated animals, the HF diet significantly increased the leptin level in comparison to the control group ($p < 0.001$, resp.; Figure 4, Table 2).

6.4. Plasma Concentrations of Chemerin. DJOS surgery significantly lowered the chemerin plasma levels when compared to SHAM surgery for all analysed groups, except CD/HF ($p < 0.001$, 0.01, and 0.01, resp.; Figure 5, Tables 1 and 2).

After DJOS surgery, the highest level of chemerin was observed in the HF/HF group in comparison with all other analysed diet combinations, and it was significantly higher when compared to the CD/CD group ($p < 0.001$; Figure 5, Table 2). The lowest level of chemerin was detected for the CD/CD group, and this value was significantly different from all other groups ($p < 0.001$, 0.01, and 0.001, resp.; Figure 5, Table 2).

The type of food given to animals before and after SHAM surgery influenced the chemerin plasma level in SHAM-operated animals. The HF/HF diet changed the chemerin plasma profile in comparison with all other analysed groups ($p < 0.001$, resp.; Figure 5, Table 2). Also, in group CD/CD, the chemerin plasma level was significantly lower when compared to HF/CD groups ($p < 0.01$; Figure 5, Table 2).

7. Discussion

Patients with severe obesity need to adopt new dietary patterns after metabolic surgery in order to achieve long-term results. Our understanding of the effect of bariatric surgery on the systematic metabolism is still incomplete. It is not possible to distinguish between the physiological effects of dietary changes, reduced food consumption, and the direct effects of metabolic surgery per se [30].

Our present study shows the influence of dietary patterns applied before and after DJOS and SHAM surgery on the

Table 1: FABP4, CRP, leptin, and chemerin plasma levels 8 weeks after DJOS (1st column) and SHAM (2nd column) surgery, subjected to 16 weeks of different dietary patterns and intergroup comparison between DJOS and SHAM study groups (3rd column) using descriptive statistics and results of two-way analysis of variance.

Parameter	DJOS				SHAM				*p* ANOVA		
	HF/HF	HF/CD	CD/HF	CD/CD	HF/HF	HF/CD	CD/HF	CD/CD	Group	Op.	Int.
FABP4 (ng/ml)	393.0 ± 46.3	391.8 ± 51.6	397.7 ± 42.1	210.4 ± 66.3	407.1 ± 50.0	428.7 ± 48.1	348.0 ± 31.0	293.4 ± 46.5	**<0.001**	0.133	**<0.05**
CRP (ng/ml)	17.3 (12.2–19.5)	19.4 (18.9–0.4)	11.6 (5.6–14.3)	1.5 (1.1–6.6)	31.9 (31.7–32.2)	27.3 (12.3–28.6)	60.2 (58.8–61.0)	11.0 (2.0–15.6)		**<0.001**	
Leptin (ng/ml)	12.8 ± 3.4	10.4 ± 2.7	10.8 ± 2.6	3.8 ± 0.6	18.3 ± 1.2	17.0 ± 1.6	16.3 ± 2.4	8.3 ± 2.4	**<0.001**	**<0.001**	0.697
Chemerin (ng/ml)	20.6 ± 6.8	15.5 ± 4.1	16.9 ± 4.2	7.8 ± 1.4	35.8 ± 6.7	23.3 ± 2.3	20.1 ± 4.3	15.2 ± 3.5	**<0.001**	**<0.001**	**<0.05**

Statistical significance was set at a $p < 0.05$. FABP4: fatty acid-binding protein 4; CRP: C-reactive protein; DJOS: duodenal-jejunal omega switch surgery; HF: high-fat diet; CD: control diet; HF/HF, CD/HF, HF/CD, CD/CD: type of diet 8 weeks before/8 weeks after surgery; Op.: operation type; Int.: interaction between group and operation type; mean ± standard deviation or median (lower–upper quartile).

Table 2: Multiple comparisons in contrast analysis. Column 1: intergroup comparisons between HF/HF, CD/HF, HF/CD, and CD/CD groups DJOS versus SHAM. Column 2: intragroup comparisons between HF/HF, CD/HF, HF/CD, and CD/CD groups after DJOS surgery. Column 3: intragroup comparisons between HF/HF, CD/HF, HF/CD, and CD/CD groups after SHAM surgery.

Post hoc	Column 1: DJOS versus SHAM				Column 2: DJOS						Column 3: SHAM					
	1: HF/HF	2: HF/CD	3: CD/HF	4: CD/CD	1 versus 2	1 versus 3	1 versus 4	2 versus 3	2 versus 4	3 versus 4	1 versus 2	1 versus 3	1 versus 4	2 versus 3	2 versus 4	3 versus 4
FABP4 (ng/ml)	0.609	0.199	0.086	**<0.01**	0.964	0.864	**<0.001**	0.835	**<0.001**	**<0.001**	0.448	**<0.05**	**<0.001**	**<0.01**	**<0.001**	0.052
CRP (ng/ml)	**<0.001**	0.394	**<0.01**	**<0.05**	—	—	—	—	—	—	—	—	—	—	—	—
Leptin (ng/ml)	**<0.001**	**<0.001**	**<0.001**	**<0.001**	0.061	0.114	**<0.001**	0.763	**<0.001**	**<0.001**	0.288	0.111	**<0.001**	0.600	**<0.001**	**<0.001**
Chemerin (ng/ml)	**<0.001**	**<0.01**	0.236	**<0.01**	0.052	0.152	**<0.001**	0.605	**<0.01**	**<0.001**	**<0.001**	**<0.001**	**<0.001**	**0.225**	**<0.01**	0.063

Post hoc analysis, statistical significance was set at $p < 0.05$. FABP4: fatty acid-binding protein 4; CRP: C-reactive protein; DJOS: duodenal-jejunal omega switch surgery; HF: high-fat diet; CD: control diet; HF/HF, CD/HF, HF/CD, CD/CD: type of diet 8 weeks before/8 weeks after surgery.

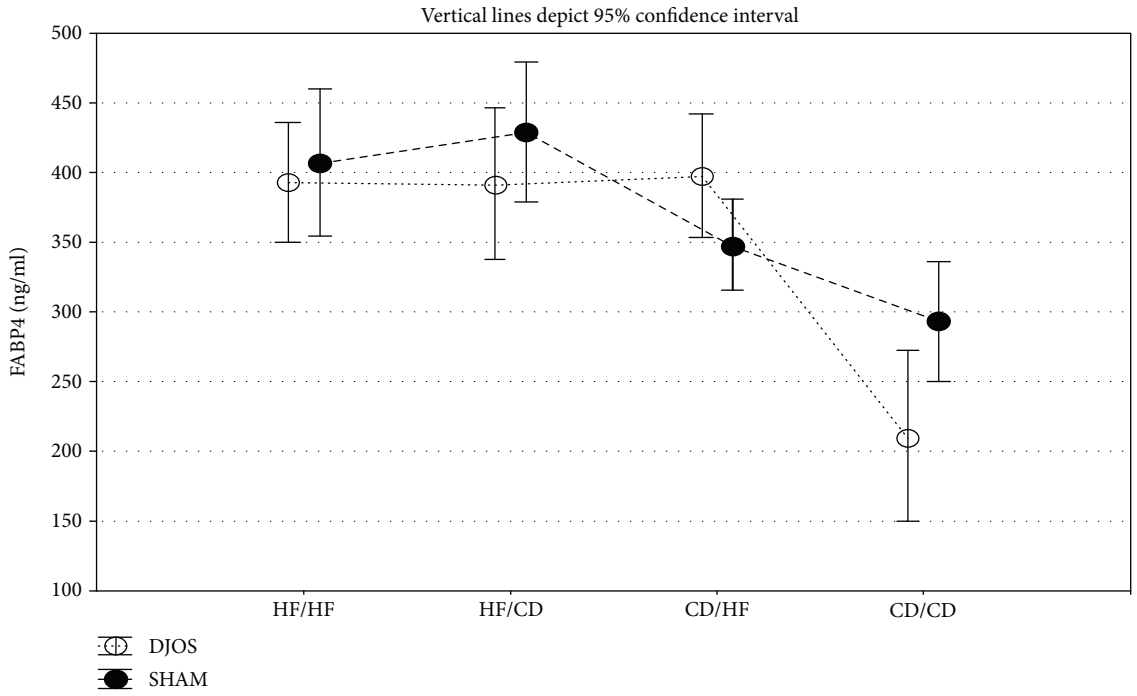

Figure 2: Mean values of FABP4 (ng/ml) plasma levels in four groups subjected to different dietary patterns, according to the DJOS and SHAM operation type. Statistical significance was set at $p < 0.05$. Vertical lines depict 95% confidence interval. DJOS: duodenal-jejunal omega switch surgery; HF: high-fat diet; CD: control diet; HF/HF, CD/HF, HF/CD, CD/CD: type of diet 8 weeks before/8 weeks after surgery.

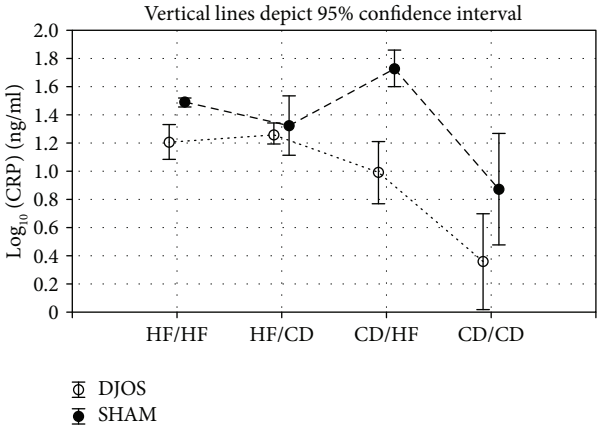

Figure 3: Mean values of CRP (ng/ml) plasma levels in four groups of different dietary patterns, according to the DJOS and SHAM operation type. Statistical significance was set at $p < 0.05$. Vertical lines depict 95% confidence interval. DJOS: duodenal-jejunal omega switch surgery; HF: high-fat diet; CD: control diet; HF/HF, CD/HF, HF/CD, CD/CD: type of diet 8 weeks before/8 weeks after surgery.

plasma FABP4 concentration. Despite the type of surgery, in FABP4, the plasma levels were influenced by the type of dietary pattern (HF and/or CD diet). HF led to the increase in FABP4 plasma concentration, reducing the positive effect of DJOS. FABP4 is characteristic for adipose tissue and macrophages, where it regulates adipocyte fatty-acid uptake and lipogenesis, and also influences cholesterol accumulation. It also delivers lipids to nuclear receptors, stimulating nuclear transcriptional patterns. In macrophages, FABP4 is known to modulate inflammatory responses by the connection to systemic inflammation and the immune system [4, 31, 32]. The elevated plasma FABP4 level is a negative prognostic factor, correlated with metabolic syndrome, insulin resistance (calculated as HOMA-IR), and mortality of patients with advanced hepatic cirrhosis and sepsis [31, 33]. Witczak et al. observed significant changes in free plasma FABP4 concentrations with time, after biliopancreatic diversion surgery. The highest level of FABP4 was observed after the 1-month follow-up and might be related to increased lipolysis after the surgery [34]. Some studies show inconsistency regarding FABP4 plasma concentrations in patients after weight loss, which may be interpreted as a normalisation of FABP4 plasma level [34–36]. In our previous study, we did not observe significant weight loss in rats maintained on an HF diet after DJOS surgery [28]. As we demonstrate here, the HF diet before and/or after both DJOS and control, SHAM surgery led to an increase in FABP4 concentration in reference to the control diet. We believe that an HF dietary pattern increases the fatty acid metabolism and is connected with upregulated FABP4 expression and secretion from the adipose tissue.

Obesity and an HF diet are associated with low-grade chronic inflammation in many tissues, which is confirmed by increased plasma concentrations of CRP, tumor necrosis factor α (TNF-α), and interleukins [5, 37]. Bariatric and metabolic surgery shows a positive impact on the reduction of inflammatory biomarkers in several tissues, for example, adipose tissue [3]. CRP, primarily produced in the liver, is known to be upregulated under conditions of obesity,

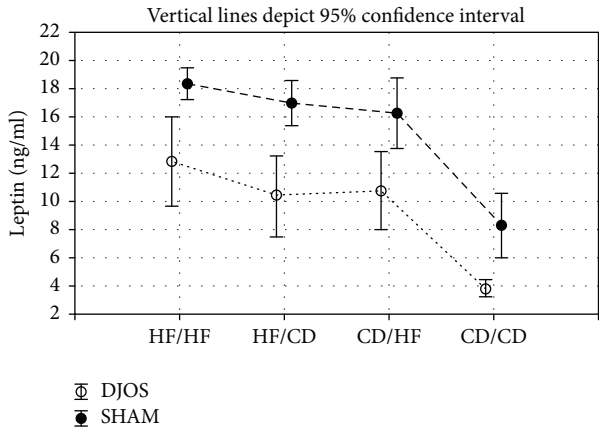

Figure 4: Mean values of leptin (ng/ml) plasma levels in four groups of different dietary patterns, according to the DJOS and SHAM operation type. Statistical significance was set at $p < 0.05$. Vertical lines depict 95% confidence interval. DJOS: duodenal-jejunal omega switch surgery; HF: high-fat diet; CD: control diet; HF/HF, CD/HF, HF/CD, CD/CD: type of diet 8 weeks before/8 weeks after surgery.

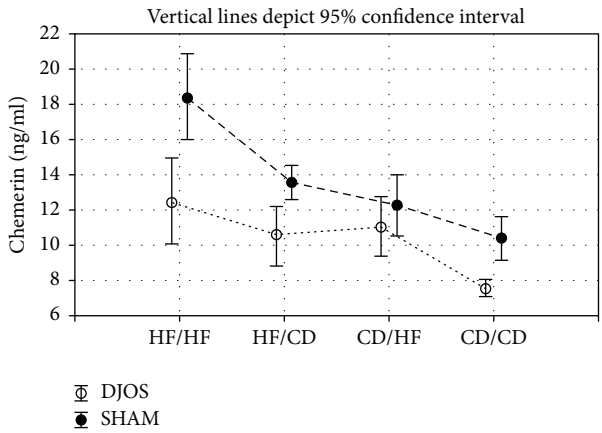

Figure 5: Mean values of chemerin (ng/ml) plasma levels in four groups of different dietary patterns, according to the DJOS and SHAM operation type. Statistical significance was set at $p < 0.05$. Vertical lines depict 95% confidence interval. DJOS: duodenal-jejunal omega switch surgery; HF: high-fat diet; CD: control diet; HF/HF, CD/HF, HF/CD, CD/CD: type of diet 8 weeks before/8 weeks after surgery.

regardless of age, sex, or ethnicity of subjects studied [5]. As a marker of inflammation, plasma concentration of CRP shows a strong and long-lasting decrease after bariatric surgery [38–40]. In the present study, we combined metabolic surgery with a regular and proinflammatory atherogenic diet. After 16 weeks of experimental dietary patterns, DJOS had a strong reductive influence on the CRP plasma level, despite the type of diet used in the experiment, including the HF/HF dietary pattern. A change of the diet from CD to HF after surgery significantly increased CRP plasma levels in SHAM-operated animals when compared to DJOS. The CRP concentrations were consistently lower in DJOS than in SHAM-operated groups, which may be interpreted as a modulation of inflammatory processes even in the conditions of an atherogenic diet. The reduction of plasma CRP was postulated to be associated with weight loss. In the human studies, Selvin et al. observed that for every 1 kg loss of weight in adults, the mean decrease in CRP plasma concentration was 0.13 mg/l, which is probably associated with reduced hypertrophy of adipocytes and lipid storage in adipose tissue [41, 42]. Although, we observed reduced CRP plasma levels after DJOS surgery. Moreover, intragroup-related analyses showed high variations in plasma CRP levels, which resulted in the lack of significant changes between the analysed groups. We hypothesize that it can be explained by the individual responses of the animals. Similar effects were observed in severely obese patients, where their gene polymorphisms were suggested to explain the interindividual variability in circulating CRP [43]. We suggest that a decline in CRP levels may be associated not only with body mass reduction but also with metabolic changes in physiologic profiles of subcutaneous adipose tissue and visceral adipose tissue, lowered adipose inflammation, decreased proinflammatory adipokine production, and lower insulin resistance induced by bariatric surgery [3].

The impaired cross-talk between the endocrine activity of adipose tissue and other insulin-dependent organs is characteristic for obesity and metabolic syndrome [44]. Leptin is the main factor involved in the regulation of energy status, stimulating satiety by metabolic communication between adipose tissue and CNS. This proinflammatory adipokine acts in the early phase of obesity-related inflammation, stimulates proinflammatory immune responses, and plays an important role in energy-deficient states, such as fasting, diet, or exercise-induced amenorrhea and lipoatrophy [3, 45]. To the best of our knowledge, this is the first study that presents the effects of DJOS surgery in combination with different dietary patterns on plasma leptin concentration. DJOS showed a significant impact on leptin plasma levels regardless of the diet applied before and after surgery. We observed a strong effect of DJOS on the leptin plasma levels in all experimental groups when compared to SHAM groups. The lowest level of leptin was observed in the CD/CD dietary pattern in both DJOS and SHAM groups. The highest levels of leptin were detected in conditions of proinflammatory HF/HF dietary intervention before and after surgery. What is interesting is that a change of the diet, in groups where HF was combined with CD, also led to increased serum leptin levels. As previously reported, bariatric surgery-induced weight loss was associated with a positive effect on the endocrine activity of adipose tissue and plasma leptin levels, which decreases independently of the type of surgery performed: Roux-en-Y gastric bypass (RYGB) or laparoscopic sleeve gastrectomy [46]. After RYGB, leptin (protein and mRNA) decreased in patients with diabetes mellitus and dyslipidemia [47]. As an appetite-related hormone, leptin may play an important role in weight regain after obesity therapy. Human studies show significant reduction in leptin blood concentrations in patients who lost at least 5% of body mass using a hypocaloric diet (restriction of 30% of the subject's total energy expenditure) but also a more significant regain of body weight 6 months after the hypocaloric diet in

patients who have a higher baseline of fasting leptin levels [48]. In the present study, we demonstrated that HF dietary patterns introduced before or/and after surgery lead to metabolic disturbances, reversing the effects of DJOS and increasing leptin plasma concentration in relation to the control group.

In rodents, chemerin plasma levels were significantly increased in the conditions of dyslipidemia and diminished after fasting [49]. In humans, elevated serum/plasma levels of chemerin are correlated with body fat, glucose, lipid metabolism, and inflammation which is connected with the fact that this adipokine plays a role in the pathophysiology of obesity and metabolic syndrome [50]. Animals fed HF diet showed to be less responsive to chemerin and its physiological actions, such as the regulation of adipogenesis in mature adipocytes, through the activation of chemokine-like receptor 1 (CMKLR1) [51]. Changes in plasma levels of chemerin were reported after biliopancreatic diversion with duodenal switch, which may be associated with improved insulin resistance and resolution from hyperlipidemia [52]. Moreover, changes in plasma chemerin levels have been reported to be time-related and might be a consequence of an improved metabolic phenotype and reduced serum insulin levels. Studying the effects of surgery in relation to eating patterns, a similar trend in leptin and chemerin plasma levels was observed, when comparing the DJOS and SHAM types of surgery. Independently of dietary interventions, there were significantly lower chemerin plasma concentrations after DJOS surgery than in SHAM-operated animals. In addition, we demonstrated that the proinflammatory HF dietary pattern used before or/and after surgery led to an increase in chemerin plasma levels in comparison to CD/CD groups, but did not reduce beneficial effects of DJOS.

8. Conclusions

It is concluded that DJOS surgery has a decreasing impact on systemic levels of proinflammatory adipokines and CRP. The beneficial effect of DJOS is strongly deteriorated by an HF diet, in most of the studied combinations, before and/or after surgery. Nevertheless, the beneficial effect of DJOS surgery is stronger than proinflammatory conditions caused by an HF obesogenic diet.

Ethical Approval

All applicable institutional and/or national guidelines for the care and use of animals were followed. All animal experimental protocols were approved by the Local Ethics Committee, Poland.

Conflicts of Interest

The authors declare that they have no conflict of interest.

Authors' Contributions

Dominika Stygar and Konrad Wojciech Karcz conceived the idea of the experiment. Dominika Stygar, Bronisława Skrzep-Poloczek, and Tomasz Sawczyn maintained the animals. Dominika Stygar and Jakub Poloczek conducted the surgery. Elżbieta Chełmecka and Dominika Stygar performed the statistical analysis of the data. Dominika Stygar and Bronisława Skrzep-Poloczek carried out overall analysis. Dominika Stygar wrote the manuscript. All authors have approved the final version of the manuscript. This work was performed in cooperation between Ludwig Maximilian University of Munich, Germany, and University of Silesia in Katowice, Poland.

Acknowledgments

The authors would like to thank Violetta Kapuśniak, PhD, VMD, and Edyta Bieńko, VMD, for the veterinary assistance. The authors would like to express their special gratitude to Anna Dulska for the illustration and graphic design. The authors would like to express their special gratitude to Mr. Scott Richards for scientific English language correction. This work was funded by Medical University of Silesia, Poland.

References

[1] G. S. Hotamisligil, "Inflammation and metabolic disorders," *Nature*, vol. 444, no. 7121, pp. 860–867, 2006.

[2] G. S. Hotamisligil and E. Erbay, "Nutrient sensing and inflammation in metabolic diseases," *Nature Reviews, Immunology*, vol. 8, no. 12, pp. 923–934, 2008.

[3] H. Freitag, "Genetic variation of fatty acid oxidation and obesity, a literature review," *International Journal of Biomedical Sciences*, vol. 12, no. 1, pp. 1–8, 2016.

[4] I. Graupera, M. Coll, E. Pose et al., "Adipocyte fatty-acid binding protein is overexpressed in cirrhosis and correlates with clinical outcomes," *Scientific Reports*, vol. 7, no. 1, p. 1829, 2017.

[5] J. Choi, L. Joseph, and L. Pilote, "Obesity and C-reactive protein in various populations: a systematic review and meta-analysis," *Obesity Reviews*, vol. 14, no. 3, pp. 232–244, 2013.

[6] M. F. Gregor and G. S. Hotamisligil, "Inflammatory mechanisms in obesity," *Annual Review of Immunology*, vol. 29, no. 1, pp. 415–445, 2011.

[7] G. Paz-Filho, C. Mastronardi, C. B. Franco, K. B. Wang, M. L. Wong, and J. Licinio, "Leptin: molecular mechanisms, systemic pro-inflammatory effects, and clinical implications," *Arquivos Brasileiros de Endocrinologia & Metabologia*, vol. 56, no. 9, pp. 597–607, 2012.

[8] J. Conde, M. Scotece, R. Gómez et al., "Adipokines: biofactors from white adipose tissue. A complex hub among inflammation, metabolism, and immunity," *BioFactors*, vol. 37, no. 6, pp. 413–420, 2011.

[9] A. Batra, B. Okur, R. Glauben et al., "Leptin: a critical regulator of $CD4^+$ T-cell polarization *in vitro* and *in vivo*," *Endocrinology*, vol. 151, no. 1, pp. 56–62, 2010.

[10] S. Rafail, K. Ritis, K. Schaefer et al., "Leptin induces the expression of functional tissue factor in human neutrophils and peripheral blood mononuclear cells through JAK2-dependent mechanisms and TNFα involvement," *Thrombosis Research*, vol. 122, no. 3, pp. 366–375, 2008.

[11] A. B. Crujeiras, M. C. Carreira, B. Cabia, S. Andrade, M. Amil, and F. F. Casanueva, "Leptin resistance in obesity: an epigenetic landscape," *Life Sciences*, vol. 140, pp. 57–63, 2015.

[12] J. Weigert, M. Neumeier, J. Wanninger et al., "Systemic chemerin is related to inflammation rather than obesity in type 2 diabetes," *Clinical Endocrinology*, vol. 72, no. 3, pp. 342–348, 2010.

[13] S. G. Roh, S. H. Song, K. C. Choi et al., "Chemerin—a new adipokine that modulates adipogenesis via its own receptor," *Biochemical and Biophysical Research Communications*, vol. 362, no. 4, pp. 1013–1018, 2007.

[14] V. Wittamer, B. Bondue, A. Guillabert, G. Vassart, M. Parmentier, and D. Communi, "Neutrophil-mediated maturation of chemerin: a link between innate and adaptive immunity," *The Journal of Immunology*, vol. 175, no. 1, pp. 487–493, 2005.

[15] V. Wittamer, J. D. Franssen, M. Vulcano et al., "Specific recruitment of antigen-presenting cells by chemerin, a novel processed ligand from human inflammatory fluids," *Journal of Experimental Medicine*, vol. 198, no. 7, pp. 977–985, 2003.

[16] A. D. Miras and C. W. le Roux, "Mechanisms underlying weight loss after bariatric surgery," *Nature Reviews. Gastroenterology & Hepatology*, vol. 10, no. 10, pp. 575–584, 2013.

[17] N. Puzziferri, T. B. Roshek III, H. G. Mayo, R. Gallagher, S. H. Belle, and E. H. Livingston, "Long-term follow-up after bariatric surgery: a systematic review," *Journal of the American Medical Association*, vol. 312, no. 9, pp. 934–942, 2014.

[18] M. A. Nauck, "Unraveling the science of incretin biology," *The American Journal of Medicine*, vol. 122, no. 6, pp. S3–S10, 2009.

[19] F. Rubino and M. Gagner, "Potential of surgery for curing type 2 diabetes mellitus," *Annals of Surgery*, vol. 236, no. 5, pp. 554–559, 2002.

[20] J. M. Grueneberger, I. Karcz-Socha, G. Marjanovic et al., "Pylorus preserving loop duodeno-enterostomy with sleeve gastrectomy - preliminary results," *BMC Surgery*, vol. 14, no. 1, p. 20, 2014.

[21] L. W. Traverso and W. P. Longmire Jr, "Preservation of the pylorus in pancreaticoduodenectomy," *Surgery, Gynecology & Obstetrics*, vol. 146, no. 6, pp. 959–962, 1978.

[22] W. K. Karcz, S. Kuesters, G. Marjanovic, and J. M. Grueneberger, "Duodeno-enteral omega switches – more physiological techniques in metabolic surgery," *Videosurgery and Other Miniinvasive Techniques*, vol. 8, no. 4, pp. 273–279, 2013.

[23] L. K. Johnson, L. F. Andersen, D. Hofsø et al., "Dietary changes in obese patients undergoing gastric bypass or lifestyle intervention: a clinical trial," *British Journal of Nutrition*, vol. 110, no. 1, pp. 127–134, 2013.

[24] V. Moizé, A. Andreu, L. Flores et al., "Long-term dietary intake and nutritional deficiencies following sleeve gastrectomy or Roux-En-Y gastric bypass in a mediterranean population," *Journal of the Academy of Nutrition and Dietetics*, vol. 113, no. 3, pp. 400–410, 2013.

[25] M. D. Kofman, M. R. Lent, and C. Swencionis, "Maladaptive eating patterns, quality of life, and weight outcomes following gastric bypass: results of an internet survey," *Obesity*, vol. 18, no. 10, pp. 1938–1943, 2010.

[26] R. H. Freire, M. C. Borges, J. I. Alvarez-Leite, and M. I. T. D. Correia, "Food quality, physical activity, and nutritional follow-up as determinant of weight regain after Roux-en-Y gastric bypass," *Nutrition*, vol. 28, no. 1, pp. 53–58, 2012.

[27] B. K. Abu Dayyeh, D. B. Lautz, and C. C. Thompson, "Gastrojejunal stoma diameter predicts weight regain after Roux-en-Y gastric bypass," *Clinical Gastroenterology and Hepatology*, vol. 9, no. 3, pp. 228–233, 2011.

[28] D. Stygar, T. Sawczyn, B. Skrzep-Poloczek et al., "The effects of duodenojejunal omega switch in combination with high-fat diet and control diet on incretins, body weight, and glucose tolerance in Sprague-Dawley rats," *Obesity Surgery*, vol. 28, no. 3, pp. 748–759, 2018.

[29] W. M. S. Russell and R. L. Burch, *The Principles of Humane Experimental Technique the Principles of Humane Experimental Technique*, Methuen Co., LTD, London, UK, 1959.

[30] H. Frikke-Schmidt, R. W. O'Rourke, C. N. Lumeng, D. A. Sandoval, and R. J. Seeley, "Does bariatric surgery improve adipose tissue function?," *Obesity Reviews*, vol. 17, no. 9, pp. 795–809, 2016.

[31] M. Furuhashi and G. S. Hotamisligil, "Fatty acid-binding proteins: role in metabolic diseases and potential as drug targets," *Nature Reviews Drug Discovery*, vol. 7, no. 6, pp. 489–503, 2008.

[32] J. Storch and A. E. Thumser, "Tissue-specific functions in the fatty acid-binding protein family," *Journal of Biological Chemistry*, vol. 285, no. 43, pp. 32679–32683, 2010.

[33] C. L. Huang, Y. W. Wu, A. R. Hsieh, Y. H. Hung, W. J. Chen, and W. S. Yang, "Serum adipocyte fatty acid-binding protein levels in patients with critical illness are associated with insulin resistance and predict mortality," *Critical Care*, vol. 17, no. 1, article R22, 2013.

[34] J. K. Witczak, T. Min, S. L. Prior, J. W. Stephens, P. E. James, and A. Rees, "Bariatric surgery is accompanied by changes in extracellular vesicle-associated and plasma fatty acid binding protein 4," *Obesity Surgery*, vol. 28, no. 3, pp. 767–774, 2018.

[35] D. Stejskal, M. Karpisek, and J. Bronsky, "Serum adipocyte-fatty acid binding protein discriminates patients with permanent and temporary body weight loss," *Journal of Clinical Laboratory Analysis*, vol. 22, no. 5, pp. 380–382, 2008.

[36] K. Comerford, W. Buchan, and S. Karakas, "The effects of weight loss on FABP4 and RBP4 in obese women with metabolic syndrome," *Hormone and Metabolic Research*, vol. 46, no. 3, pp. 224–231, 2014.

[37] T. P. Ludvigsen, R. K. Kirk, B. Ø. Christoffersen et al., "Göttingen minipig model of diet-induced atherosclerosis: influence of mild streptozotocin-induced diabetes on lesion severity and markers of inflammation evaluated in obese, obese and diabetic, and lean control animals," *Journal of Translational Medicine*, vol. 13, no. 1, p. 312, 2015.

[38] M. M. O. Lima, J. C. Pareja, S. M. Alegre et al., "Visceral fat resection in humans: effect on insulin sensitivity, beta-cell function, adipokines, and inflammatory markers," *Obesity*, vol. 21, no. 3, pp. E182–E189, 2013.

[39] E. Sdralis, M. Argentou, N. Mead, I. Kehagias, T. Alexandridis, and F. Kalfarentzos, "A prospective randomized study comparing patients with morbid obesity submitted to sleeve gastrectomy with or without omentectomy," *Obesity Surgery*, vol. 23, no. 7, pp. 965–971, 2013.

[40] D. Kardassis, M. Schönander, L. Sjöström, and K. Karason, "Carotid artery remodelling in relation to body fat distribution, inflammation and sustained weight loss in obesity," *Journal of Internal Medicine*, vol. 275, no. 5, pp. 534–543, 2014.

[41] E. Selvin, N. P. Paynter, and T. P. Erlinger, "The effect of weight loss on C-reactive protein: a systematic review," *Archives of Internal Medicine*, vol. 167, no. 1, pp. 31–39, 2007.

[42] L. K. Forsythe, J. M. W. Wallace, and M. B. E. Livingstone, "Obesity and inflammation: the effects of weight loss," *Nutrition Research Reviews*, vol. 21, no. 2, pp. 117–133, 2008.

[43] G. Faucher, F. Guénard, L. Bouchard et al., "Genetic contribution to C-reactive protein levels in severe obesity," *Molecular Genetics and Metabolism*, vol. 105, no. 3, pp. 494–501, 2012.

[44] S. Lehr, S. Hartwig, and H. Sell, "Adipokines: a treasure trove for the discovery of biomarkers for metabolic disorders," *Proteomics Clinical Applications*, vol. 6, no. 1-2, pp. 91–101, 2012.

[45] A. La Cava, C. Alviggi, and G. Matarese, "Unraveling the multiple roles of leptin in inflammation and autoimmunity," *Journal of Molecular Medicine*, vol. 82, no. 1, pp. 4–11, 2004.

[46] X. Terra, T. Auguet, E. Guiu-Jurado et al., "Long-term changes in leptin, chemerin and ghrelin levels following different bariatric surgery procedures: Roux-en-Y gastric bypass and sleeve gastrectomy," *Obesity Surgery*, vol. 23, no. 11, pp. 1790–1798, 2013.

[47] R. Ferrer, E. Pardina, J. Rossell et al., "Decreased lipases and fatty acid and glycerol transporter could explain reduced fat in diabetic morbidly obese," *Obesity*, vol. 22, no. 11, pp. 2379–2387, 2014.

[48] A. B. Crujeiras, E. Goyenechea, I. Abete et al., "Weight regain after a diet-induced loss is predicted by higher baseline leptin and lower ghrelin plasma levels," *The Journal of Clinical Endocrinology & Metabolism*, vol. 95, no. 11, pp. 5037–5044, 2010.

[49] E. T. Wargent, M. S. Zaibi, J. F. O'Dowd et al., "Evidence from studies in rodents and in isolated adipocytes that agonists of the chemerin receptor CMKLR1 may be beneficial in the treatment of type 2 diabetes," *PeerJ*, vol. 3, article e753, 2015.

[50] M. C. Ernst and C. J. Sinal, "Chemerin: at the crossroads of inflammation and obesity," *Trends in Endocrinology & Metabolism*, vol. 21, no. 11, pp. 660–667, 2010.

[51] C. Huang, M. Wang, L. Ren et al., "CMKLR1 deficiency influences glucose tolerance and thermogenesis in mice on high fat diet," *Biochemical and Biophysical Research Communications*, vol. 473, no. 2, pp. 435–441, 2016.

[52] S. D. Parlee, Y. Wang, P. Poirier et al., "Biliopancreatic diversion with duodenal switch modifies plasma chemerin in early and late post-operative periods," *Obesity*, vol. 23, no. 6, pp. 1201–1208, 2015.